Stochastic Dynamics of Cooperation under Different Learning Rules

António Medeiros Fernandes

Thesis to obtain the Master of Science Degree in

Engineering Physics

Supervisor(s): Prof. Francisco João Duarte Cordeiro Correia dos Santos
Prof. José Luís Rodrigues Júlio Martins

Examination Committee

Chairperson: Prof. Carlos Manuel Dos Santos Rodrigues da Cruz
Supervisor: Prof. Francisco João Duarte Cordeiro Correia dos Santos
Member of the Committee: Prof. Jorge Miguel Ramos Domingues Ferreira Vieira
Prof. Elias Fernández Domingos

July 2021

Dedicated to my family.

Acknowledgments

Firstly, I owe my gratitude to all the ones who have made this project possible, who gave me motivation, inspiration and support, and because of whom I could finally finish this journey.

Especially, I would like thank to Professor Francisco C. Santos, my adviser, that for the past few months tirelessly supported, inspired and helped me, in many ways, giving me many opportunities from which I've learned so much. Not only he introduced me to these wide and exciting branches of Evolutionary Game Theory and Complex Networks, but also encouraged me to overcome my limits and innovate, not to fear trying something new. I would also like to thank Professor José Luis Martins for all his support within MEFT.

I would like to thank all my closest friends, Bernardo, Luís, Morim, Ana e Vanessa, who were always there to support and help me, with a lot of patience and dedication. To Ana Paula, I thank all the love, dedication, support, friendship, and the humongous patience to deal with my crazy ideas, and to be by my side, regardless of the 8000 km that set us apart.

Finally, I owe my deepest thanks to my family, to my father, my mother and all my brothers, Filipa, José and Miguel, for always giving me the best conditions to work, for pushing me and giving me all the motivation I needed to not give up, for being very kind and patient with me, and, above all, for giving me all your love and dedication, never letting me feel alone.

To all, thank you.

Resumo

Compreender o enigma da cooperação na Natureza foi declarado um dos grandes desafios do século. A seleção natural, sendo o principal motor da evolução das espécies, promove a sobrevivência dos mais aptos, porém interações cooperativas prevalecem nos sistemas vivos. As relações entre indivíduos, seja como processos diádicos ou coletivos, são usualmente modeladas por jogos sociais, que se baseiam nas recompensas relativas das estratégias. No entanto, estas interações podem nem sempre ser impulsionadas por uma agenda egoísta, como maximização do fitness ou tomada de decisões racionais. Nesta tese, analisamos diferentes regras de revisão de estratégia, que podem ocorrer em sistemas sociais, recorrendo à análise de processos de Markov em larga escala. Primeiramente, começamos por descrever analiticamente a dinâmica estocástica da população decorrente de processos de atualização síncronos e assíncronos. Concluímos um impacto quase insignificante emergente desta distinção. Seguidamente, descrevemos a dinâmica da cooperação emergente da interação de diferentes paradigmas de revisão de estratégia: aprendizagem social (base), conformidade e pensamento contrafactual. Mostramos que a conformidade cria uma dinâmica biestável, independentemente dos dilemas que analisamos. Esse resultado só se altera quando aumentam os níveis de heterogeneidade da população. O pensamento contrafactual, por si, embora promova a cooperação em toda a população, falha em promover a cooperação entre aqueles que também aprendem por esta heurística. Além disso, mostramos que, embora uma ligeira prevalência de indivíduos recorrendo ao raciocínio contrafactual seja suficiente para modificar a dinâmica natural de cada dilema, será necessária uma quantidade significativa de agentes movidos pela conformidade para criar um impacto análogo.

Palavras-chave: Emergência de Cooperação, Teoria Evolutiva dos Jogos, Conformidade, Pensamento Contrafactual, Processos Síncronos

Abstract

Understanding the conundrum of cooperative action in nature has been declared one of the century's grand challenges. Natural selection is the main engine of the evolution of species and promotes the survival of the fittest, yet cooperative interactions prevail in living systems. Interactions between individuals, either as dyadic or collective processes, are commonly modelled through the lens of game theory, based on relative strategies payoffs. However, these interactions may not always be driven by a selfish agenda such as fitness maximization or rational decision making. In this thesis, we analyze different strategy revision rules that may take place in social systems resorting to the analysis of large-scale Markov processes. Firstly, we start by describing analytically the stochastic population dynamics arising from synchronous and asynchronous update processes. We conclude a nearly negligible impact emerge from this distinction. Secondly, we describe the cooperation dynamics emerging from the interplay of different strategy revision paradigms: social learning (our baseline), conformity and counterfactual thinking. We show that conformity creates bistable dynamics irrespectively of the various dilemmas we analyzed. This outcome is only altered whenever one increases the heterogeneity levels of the population. Counterfactual thinking, in turn, while fostering cooperation in the entire population, fails to promote cooperation among those that also learn through counterfactual reasoning. Moreover, we show that, whereas a slight prevalence of individuals resorting to counterfactual thinking is enough to modify the dynamical nature of each dilemma, a fair amount of conformity-driven agents will be required to create an analogous impact.

Keywords: Emergence of cooperation, Evolutionary Game Theory, Conformity, Counterfactual Thinking, Synchronous Processes

Contents

List of Tables

List of Figures

Nomenclature

Games Configurations

b	Received benefit
c	Public good contribution
F	Enhancement factor
M	Threshold
N	Group's size
P	Punishment
R	Reward
r	Risk of future losses
S	Sucker's Payoff
T	Temptation

Populations Configurations

$[C]$	Conformity
$[CT]$	Counterfactual Thinking
$\beta^{[L]}$	Intensity of learning rule L
$\boldsymbol{i}$	Population configuration
$\delta^{[L]}$	Probability of individuals following learning rule L
$\mathcal{L}$	Set of available learning rules
$\mathcal{S}$	Set of available strategies
μ	Mutation Probability
C	Cooperation
D	Defection

$f_S^{[L]}$	Fitness of strategy S for learning rule L
h	Homophily
$i_S^{[L]}$	Number of individuals following strategy S and with learning rule L
k	Number of cooperators (in simpler cases)
n_r	Number of revisions
SL	Social Learning
$x_S^{[L]}$	Fraction of individuals following strategy S and with learning rule L
Z	Population size
$Z^{[L]}$	Size of sub-population of learning rule L

Dynamics Tools

$\bar{s}$	Stationary distribution
$\mathcal{T}$	Transition Matrix
$\mathcal{T}^n$	n-th transition probability
∇	Multi-dimensional gradient of selection
$G^{[L]}$	Gradient of selection for learning rule L
$p^{[L]}_{S_A \to S_B}$	Switching probability for interaction $S_A \to S_B$, for learning rule L
$T_v^{[L]}$	Transition probability of variation v, for learning rule L

Dynamics Evaluation

η_G	Group Achievement
ϕ_i	Fixation probability for i cooperators
τ_j	Unconditional fixation time
τ_j^S	Conditional fixation time for absorbing state S
EFC	Expected Fraction of Cooperation
EFC_L	Expected Fraction of Cooperation for learning rule L

List of Acronyms

CRD	Collective Risk Dilemma
EGT	Evolutionary Game Theory
GT	Game Theory
HG	Harmony Game
NPD	N-person Prisoners Dilemma
NSG	N-person Snowdrift Game
NSH	N-person Stag-Hunt Game
PD	Prisoner's Dilemma
PGG	Public Good Games
SG	Snowdrift Game
SH	Stag-Hunt Game
ToM	Theory of Mind

Chapter 1

Introduction

> *"The only thing that will redeem mankind is cooperation."*
>
> — Bertrand Russel, in *Human Society in Ethics and Politics* (1954)

1.1 Motivation

In this world of selfish individuals, when should we expect cooperation to emerge? This problematic of cooperation has been widely studied and yet it is still one of the biggest mysteries about animal behaviour [1]. In fact, the understanding of cooperative behavior in societies has been declared as one of the grand scientific challenges of the 21st century and has been intriguing the scientific community in various areas such as sociology, biology, mathematics, physics and even computer science [2, 3].

In 1859, on his famous book *On the Origin of Species*, Charles Darwin has laid down the foundations of what has come to be the most commonly accepted theory of the evolution of species. In his book, he brilliantly introduced and popularized the concept of natural selection as one of the fundamental key mechanisms of evolution, which was very surprising in light they were done in the absence of any genetics knowledge. In fact, the idea of hereditary genetic mutation, as the main cause of diversity among organisms (species differentiation), came only long after Darwin's genius insights. This way, and as it is also a fundamental engine in the evolution of species, genetic mutation becomes the second building block of evolution, next to natural selection.

Following the definition of survival as the continuous will to live, it is natural that individuals will focus mainly on extending their life expectancy, in order to maximize the probability of propagation of their genes along future generations. From a Darwinist perspective, this survival of individuals is highly dependent on their adaptability to the demands of the environment and it may be understood as a competitive process, within a certain community, where the most successful individuals and the best suited to their surroundings tend to dominate. Thereby, the fact that natural selection favors the fittest individuals implies an innate selfishness that greatly challenge the concept of cooperation. One should not expect any sign of cooperation among individuals, as it would involve an extraordinary cost for the cooperator. In short, from a Darwinist point of view, cooperation is costly, and, as weird as it may sound to us, humans, this means that cooperation is unnatural and rather odd than rational [4, 5].

However, in Nature one may find many evidences of cooperation in all different scales, from the transition of protists to multi-cellular organisms, millions years ago, to the development of great human societies in the present, as a result of million of years of our evolutionary struggles for survival. Even if in the first case cooperation is not referred as a conscious decision, it is still an interaction between different elements, and thus following the basic principles of cooperation. This evolutionary steps were only possible due to cooperation, and so it has been identified as the third building block of evolution, next to selection and mutation.

So we now come across with this cooperation paradox: natural selection is the main engine of species evolution and it promotes the survival of the fittest, yet we verify that cooperative interactions prevail in living systems [6]. How can we then explain the emergence of cooperation? Naturally, human beings see cooperation as a very familiar and beneficial concept. However, if one thinks more carefully, the idea of offering assistance to others is rather odd from a purely rational point of view. So why do we, humans, alike many other animals, cooperate?

1.2 Topic Overview

Classical Game Theory was developed extensively in the 1950s, originally for application in economics and social science, but later in the 70s a group of biologists started to recognize how similar the games that have been studied were to the interactions within a community of individuals. The Evolutionary Game Theory (**EGT**) was then born when John Maynard Smith and George Price laid its foundations, providing a powerful theoretical framework to model Darwinian competition [7], usually know as social learning. Since then it has inspired sociologists, mathematicians, biologists, physicists and computer scientists to investigate the evolution of traits under natural selection. More specifically the evolution of cooperation has attracted wide attention in the last decades [1].

Inspired by the international research interest, some update rules of evolutionary game dynamics have been introduced, where we stand with this hot issue: how did the human cooperative behaviour evolve? Methods of statistical physics can be applied to solve this issue [4], where a comprehensive understanding of statistical physics of human cooperation is given. In fact, to analyze an evolutionary process one can, for instance, adopt the Fermi function distribution from statistical mechanics [8, 9].

The evolutionary dynamics of games are commonly studied through replicator equations [8], which provides a convenient view for the evolutionary process, however assuming infinite populations and a deterministic dynamic process [10]. The replicator equations show us the growth rate of the proportion of players using a certain strategy. In this approach, the abundance of a strategy changes according to the its relative payoff, and hence, each player will stochastically adapt their strategy prioritizing the one with the largest payoff. Therefore, this formalism allows us to study both biological evolution, where individuals with higher fitness tend to reproduce more, and social learning, where individuals with higher fitness will be imitated more often - imitation dynamics. The payoff for each strategy will now depend on the evolutionary game we are dealing with, since each game has it own rules and payoffs.

However, besides the pursuit of the highest payoffs in evolutionary social dilemmas is risky, it is also a fact that these interactions among individuals are not always driven by a selfish agenda such as fitness maximization [11], or, even if they do, they may reason slightly different. In this sense, and formally from a pairwise comparison with social learning, we bring up two new different learning rules that possibly may help us better understand the existence of cooperation among rational individuals: conformity, where individuals focus on following the most common strategy among the population [11, 12], and counterfactual thinking, where individuals reason about hypothetical past events, specifically what would have happened if those events occurred [13].

Having this new rich and complex dynamics of evolutionary game theory, with multiple available learning rules, we look to find the conditions for which the evolutionary process acts in order to promote higher cooperative standards. Optimistically, we ought to reach new conclusions and make interesting discoveries that would gradually help us to formally understand and justify why do we, indeed, cooperate.

1.3 Objectives

This thesis aims to contribute to a better understanding of the emergence of cooperation in many different scenarios. Concretely, we look to find, not only how the introduction of different learning rules, explicitly, conformity and counterfactual thinking, in a social learning environment affects the overall dynamics of different populations, but also what is the impact of population organization in the social dilemmas, in both dyadic contact processes, that is, in the 2-person framework, and collective social action, or the N-person framework.

Moreover, and by generalizing the description of Evolutionary Game Theory, one may wonder about the updating process dynamism, more specifically, how more complex updating processes may influence the evolutionary dynamics. In fact, rather than change population organization, we now look to investigate how modifying the evolutionary updating process, from an asynchronous to a synchronous updating process, affects the population's dynamics. In addition, we will also be interested in studying how do populations involving different learning rules dynamically evolve with synchronism in different levels, with particular concern to understand how a counterfactual thinker, in its more conscious way to reason, will react to synchronism.

When introducing these new learning rules in the usual social learning framework, different possibilities arise when it come to population's organization. Even when focusing specifically on well-mixed populations, one may either homogeneously mix agents resorting to different learning rule or heterogeneously separate the system into different sub-populations of individuals resorting to one same learning rule. In this composition, one may wonder how organizing the population in different ways may lead to different dynamics and what are the impacts of these changes in terms of cooperative behaviour. Notice that, in all the performed studies, we keep a focus on searching for the conditions and regimes for which cooperation is favoured, that is, we will focus on maximizing cooperation.

1.4 Thesis Outline

In order to properly study the emergence of cooperative action, and so achieving our objectives, we start by laying down in Chapter 2 the foundations of the mathematical framework in a very generic yet detailed way, on which we will base our entire study. We start by introducing Game Theory as a model to describe either dyadic or collective interactions between agents, followed by the general description of Evolutionary Game Theory for social learning. From a pairwise comparison with this latter framework, we explicitly provide all the models that describe the different learning rules to be studied, either conformity and counterfactual thinking, as well as the whole framework that is behind the different population's organization.

Having the mathematics settled down, we are now in conditions to proceed with the analyses required to reach our objectives. Regarding the impact of synchrony in the evolutionary updating process, in Chapter 3 we start by presenting the framework developed to achieve different synchronism levels, followed by the evaluation of the cooperation effects of increasing synchronism, first on a pure social learning dynamic, and followed by multi-learning rule's populations, homogeneously mixed. In this topic, the main challenge is to answer how does synchrony affects the evolutionary dynamics of population.

Regarding the analysis of multi-learning rule populations, we will divide our study in two, according to the different population's organization. While in Chapter 4 we study the evolutionary dynamics of homogeneously displayed populations, in Chapter 5 we perform the same investigation, but instead applied to heterogeneously mixed populations. For either cases, the main challenge is to analyze the evolutionary dynamics, always looking to find the conditions or regimes for which cooperation is fostered.

Finally, we emphasize the essential achievements and leave some notes on future work in Conclusions 6.

Chapter 2

Mathematical Framework

To fulfil our goals, it is first necessary to lay the foundations of the work to be developed. In this chapter, we present the mathematical framework used throughout this thesis. Most nomenclature and notation are explicitly defined here. Starting with the basics of Game Theory and with the replicator dynamics, passing through the general definition of the transition matrix, and finishing off on the gradient of selection, this chapter is an overview of all essential topics in Evolutionary Game Theory.

We look not only to follow but also to improve some of the concepts of the already existing frameworks, built on previous works, by generalizing them. With that, we aim to build a well structured and concise mathematical framework that can answer our needs and provide a good and solid basis for any further studies.

2.1 Classical Game Theory

Game Theory (**GT**) is a field of mathematics that looks to provide a convenient framework to study, understand and develop models of strategic interaction among intelligent rational decision-makers, namely models of conflict and cooperation as competition problems. More specifically, it analyzes situations in which two or more agents make decisions that will have an impact on one another's welfare, and as such, the success of an individual will depend on the decisions adopted by others [14]. These Game Theory models, commonly referred to as *games*, are described by a very well defined set of rules that govern the outcome for the moves taken by individuals, as well as by the possible outcomes, that are responsible for producing individuals earnings or losses - denoted as *payoff*. Both game's rules and resulting payoffs may be expressed either as decision trees or, more commonly, in a payoff matrix. For more complex games, we may have to resort to a payoff table instead.

The agents involved in a game, usually called *players*, are theoretical entities that model uncertainty and, from that, make a decision about its interaction *strategy* - one may understand the concept of strategy as the approach a player takes in making his moves. As stated above, generally two basic assumptions are made about players: they are rational and they are intelligent. Regarding the first one, a decision-maker is said to be *rational* whenever it makes decisions consistently in the pursuit of its objectives [15]. Following the expected-utility maximization theorem results from Decision Theory, we assume the rational player's objective is to obtain the maximal expected outcome from among all feasible actions, which may be measured on a utility-scale [14]. To summarizing, regarding strategy dynamics, rational players are always expected to adopt the strategies that maximize their earnings (or losses).

Regarding the latter assumption, an agent is said to be intelligent whenever it has the whole knowledge about the game and it can make the same inferences about the situation that we can do [14]. In other words, when describing a theory to model the behaviour of intelligent rational players, one shall expect individuals not only to be perfectly rational but also aware of other's equal rationality, and hence expect individuals to make predictions. These intelligent players may also be regarded as *Nash players* [16] (see Section 2.1.1).

In this field of interactions, one may wonder how could this individual's rationality go "deeper", as so to speak. Applications of Theory of Mind (**ToM**) on Game Theory have been studied [16, 17] in attempts to build a good framework to describe different levels of rationality and optimise mutual interactions. Following the model from [17], we may consider **ToM** at multiple levels of rationality, where the higher the level, the deeper the individual's rationality goes. This depth of rationality is associated with the ability to reason about what would the opponent choose in the current system configurations. Take, for instance, a player A that interacts with another player B, where each one of them have a certain predictable set of possible actions. We say a player A lays in the first degree of **ToM** whenever it takes into account the goals and intentions of agent B to make his strategic choice, i.e., whenever it makes a decision biased by the opponent's most likely decision. The second degree comes when the player's reasoning is aware of a first-degree agent's reasoning, and so on for all other higher theory of mind levels.

In this framework, one may consider the typical rational and intelligent player as a level-zero **ToM** agent, as individuals do not try to predict others actions. To predict an opponent move, an agent must first be aware of how the other reasons, that is, what is the other's *learning rule*. One may define the concept of learning rule as the strategy updating mechanism that players follow, to which an updating function is associated, as we will later on. Even if in most of our study we do not consider this Theory of Mind point of view, it would be interesting to formulate a new dynamics that takes it into account.

2.1.1 Nash Equilibria

As stated above, rational and intelligent individuals, having a global knowledge about the game, can also be denominated as Nash players. One of the greatest qualities of these kind of players is their capacity to predict that other's follow *Nash equilibrium* (NE) strategies [16]. This may eventually allow situations where no individual has anything to gain by only changing their strategy, even for system configurations where many individuals don't necessarily have the highest possible payoff. The system has then reached a certain kind of equilibrium: the *Nash Equilibrium*, which is the most common way to define the solution of a non-cooperative game. This equilibrium was named after the mathematician John Forbes Nash Jr., who was awarded the 1994's Nobel Prize in Economics for his PhD Thesis entitled *Non Cooperative Games* [18]. In short, the concept of Nash equilibrium states that, for any N-person game, a given set of strategies is said to be a Nash Equilibrium if no individual can increase its payoff by unilaterally changing its strategy. In other words, any strategy in a Nash equilibrium is the best response to all the N-1 others in that equilibrium [18].

Let us formalize this concept. Start by considering a game with $Z \in \mathbb{N}$ players, where we define Ψ as the strategy profile space and $\mathcal{S}$ the set of available strategies. Let S_i be the strategy adopted by a player i and $S_{\setminus i}$ be the set of strategies for all players except i, such that $\psi = \{S_i, S_{\setminus i}\}$ is strategy profile. Let $\Pi(\psi) = (\Pi_1(\psi), \ldots, \Pi_Z(\psi))$ be the payoff function evaluated at a strategy profile $\psi \in \Psi$. A given strategy profile $\psi^* = \{S_i^*, S_{\setminus i}^*\}$ is said to be a Nash equilibrium if no unilateral deviation in strategy by any single individual is profitable for that player, that is:

$$\Pi_i(\{S_i^*, S_{\setminus i}^*\}) \geq \Pi_i(\{S_i, S_{\setminus i}^*\}) \ , \forall i \in \{1, \ldots, Z\} \tag{2.1}$$

One may notice that this concept has application to both pure strategies - where players always adopt the same action - and to mixed strategies - where players probabilistically choose a strategy among the set of available pure strategies (equivalent to $\mathcal{S}$) [19]. Besides defining a mixed-strategy Nash equilibrium for any game with a finite set of actions, that is, for any game with a finite number of players and finite set of pure strategies, John Nash also proved that at least one mixed-strategy Nash equilibrium should exist in such a game [18].

2.1.2 2-Person Games

The simplest of the Game Theory models are the 2-person games. In this games, individuals interact with one another and, in terms of the simplest cooperation dynamics, they may adopt one of two pure strategies: cooperation, C, or defection, D. This means our set of available strategies is $\mathcal{S} = \{C, D\}$. While cooperative individuals contribute to the collective welfare at a personal cost, c, in order to provide a certain benefit, b, to another individual (where we imply $b > c$), defectors choose not to contribute. The outcomes for the interactions following this description may be summarized according to the matrix shown below:

$$\begin{array}{cc} & \begin{array}{cc} \boldsymbol{C} & \boldsymbol{D} \end{array} \\ \begin{array}{c} \boldsymbol{C} \\ \boldsymbol{D} \end{array} & \begin{pmatrix} (R,R) & (S,T) \\ (T,S) & (P,P) \end{pmatrix} \end{array} \tag{2.2}$$

where the first and second elements of each entry represent, respectively, the payoffs obtained by the row's and column's players. When both interacting individuals choose to cooperate, they will be awarded with a Reward, R, while mutual defection will be awarded with a Punishment, P. If individuals adopt different strategies, the defector receives Temptation, T, while the cooperator gets the Sucker's Payoff, S. Taking into account the symmetry of the game, the order of the players choosing each strategy is irrelevant, and hence, by solely taking the payoff of the row player, we may simplify the above matrix into the most commonly used payoff matrix:

$$\begin{array}{cc} & \begin{array}{cc} \boldsymbol{C} & \boldsymbol{D} \end{array} \\ \begin{array}{c} \boldsymbol{C} \\ \boldsymbol{D} \end{array} & \begin{pmatrix} R & S \\ T & P \end{pmatrix} \end{array} \tag{2.3}$$

As cooperator's resulting payoff is lower, selection pressurizes them and defectors rise as the most favoured, thus the evolution of cooperation stands as a dilemma on its own [20]. However, in all 2-person dilemmas mutual cooperation is always favored when compared to mutual defection [8], that is $R > P$. Assuming this, from the 4-dimensional space of 2-person games, one may consider a 2-dimensional subspace, the T-S parameter plane, in which $R > P$ and define four different regions as a function of the relative values of R, S, T and P, represented in the figure 2.1 below.

From all games shown in figure 2.1, in the *Harmony Game* (**HG**), also known as the *Deadlock Game*, cooperation is always favored as it is the only rational decision to make regardless of the opponent's choice. In this case, as both players adopt C, we are lead to a maximum collective return R for all individuals. As we don't have any type of antagonism between strategies, the Harmony Game is not classified as a social dilemma [21, 22].

The remaining three games are listed below:

- **Snowdrift Game (SG)** $(T > R > S > P)$

  When studying the logic of animal conflicts, John Mayard Smith and George Price have introduced the *Snowdrift Game*, under the name of *Hawk-Dove* game [7], and also known as the *Chicken Game*. In its standard version, it may be formulated as follows: two individuals are driving on a road blocked by a snowdrift and

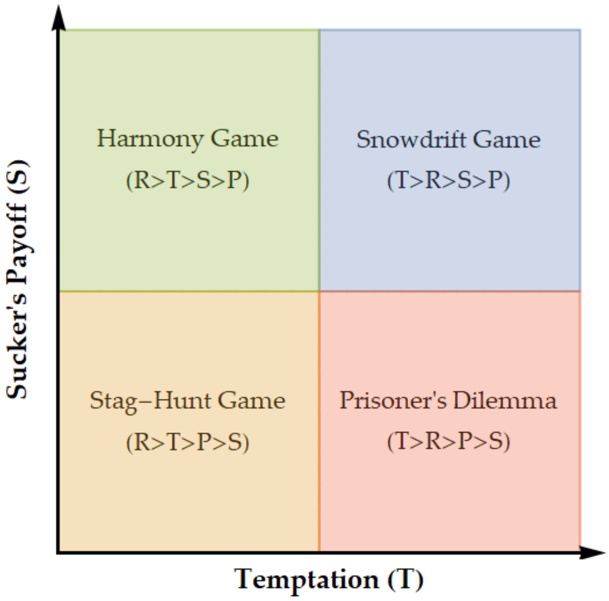

Figure 2.1: The T-S parameter plane for 2-Person games with two pure strategies, in terms of cooperation. From all the presented games, only the Harmony Game is not classified as a social dilemma.

to proceed with their journey home, to get the benefit b, the snow must be removed, incurring a cost c, with $b > c > 0$. In this scenario they have three different options: no one shovels, and hence no one gets home, the two drivers cooperate and shovel, and both get home, each one sharing half the workload of shoveling the snow, and finally, only one driver decides to shovel and so both get home, despite one driver getting the whole workload from shoveling, while the other has no costs [23]. This metaphor can be translated in the following payoff matrix:

$$\begin{array}{cc} & \begin{array}{cc} \boldsymbol{C} & \boldsymbol{D} \end{array} \\ \begin{array}{c} \boldsymbol{C} \\ \boldsymbol{D} \end{array} & \begin{pmatrix} b - \frac{c}{2} & b - c \\ b & 0 \end{pmatrix} \end{array} \tag{2.4}$$

Assuming a pure strategy game, both $(\boldsymbol{C}, \boldsymbol{D})$ and $(\boldsymbol{D}, \boldsymbol{C})$ pairs are a Nash equilibria. Intuitively, each individual is better of if the other player does the all the workload required so shovel the snow without investing anything himself, and hence it becomes a coexistence problem (as we will see further). Here we may find some traits of selfishness, characteristics of natural selection and hence the Snowdrift Game is one of the most interesting games the study of the problem of the evolution of cooperation [24]. A third Nash equilibrium appears when we consider strategies to be mixed, instead of pure. We will be discussing this topic later on, but for now let us assume strategies are pure [19]. The values for b and c can be any, as long as we always respect the Snowdrift condition $T > R > S > P$.

- **Stag-Hunt Game (SH)** $(R > T > P > S)$

  The *Stag-Hunt Game*, also know as the *Assurance Game* or *Trust Dilemma*, constitute a prototypical example of the social contract, discussed implicitly in some of the major transitions of evolution [25]. It was originally metaphorically described as a conflict between safety and social cooperation by the philosopher Jean-Jacques Rousseau in his work *Discourse on the Origin and Basis of Inequality Among Men* in 1755. In its standard version, it may be formulated as follows: two individuals go on a hunt and each of them have the option to hunt a stag, that requires the partner's collaboration, or to hunt a hare, that can be done by the self. Hunting a stag will provides a reward b while hunting a hare only provides half of it, $\frac{b}{2}$. For both cases, a cost c associated with the hunting act is applied, with $b > c > 0$. This problem may be translated by the following payoff matrix:

$$\begin{array}{cc} & \begin{array}{cc} \boldsymbol{C} & \boldsymbol{D} \end{array} \\ \begin{array}{c} \boldsymbol{C} \\ \boldsymbol{D} \end{array} & \begin{pmatrix} b-c & -c \\ \frac{b}{2}-c & 0 \end{pmatrix} \end{array} \tag{2.5}$$

Unlike the Snowdrift Game, in the Stag-Hunt Game there is an equilibrium in which both players cooperate as well as one in which both defect, that is, both $(\boldsymbol{C}, \boldsymbol{C})$ and $(\boldsymbol{D}, \boldsymbol{D})$ pure strategy pairs are a Nash equilibria - the first being payoff dominant and the latter being risk dominant. This means that the whole population tend to follow the most common strategy, whatever it is, and hence this problem is said to be a Coordination problem [19]. The values for the benefit b and the cost c can be any, as long as we always respect the main Stag-Hunt condition $R > T > P > S$.

- **Prisoner's Dilemma (PD)** $(T > R > P > S)$

Finally, we have the *Prisoner's Dilemma*, one of the most studied yet intriguing 2-Person games, as it represents the typical game-theoretical framework in which individual and group interests collide [26, 27]. Originally framed by Merril Flood and Mervil Desher, and later formalized and named by Albert W. Tucker, the Prisoner's Dilemma may be presented as follows: two criminals that are arrested and imprisoned, with no means of communicating with each other, are interrogated separately and each one is given the opportunity either to remain in silence or to testify against the other. If both cooperate and remain in silence, both will only serve one year in prison, while if they betray each other, both will serve two years. If one testifies against the other, while he remains in silence, the one who testified is set free and the other gets the full charge of three years in prison. Both prisoner's make a decision independently and simultaneously, not knowing what the other one will choose [19]. One may translate this problematic in the payoff matrix on its canonical form by taking the matrix 2.3 and the condition $T > R > P > S$. Another way to represent it is according to the special case of the *Donation Game*, that is a form of the Prisoner's Dilemma in which cooperation corresponds to offering the other player a benefit b at a personal cost c, with $b > c > 0$, which may be represented as:

$$\begin{array}{cc} & \begin{array}{cc} \boldsymbol{C} & \boldsymbol{D} \end{array} \\ \begin{array}{c} \boldsymbol{C} \\ \boldsymbol{D} \end{array} & \begin{pmatrix} b-c & -c \\ b & 0 \end{pmatrix} \end{array} \tag{2.6}$$

where we imply that $b - c = 1$.

In this game, defectors receive the benefits without spending any costs and are therefore expected to have an evolutionary advantage over cooperators [28]. This way, from a rational and evolutionary perspective, the only profitable option is defection and hence the only Nash equilibrium is the (D,D) pure strategy pair. In other words, in opposite to the Harmony Game, the Prisoner's Dilemma leads to D-dominance, which can drive the population into the *Tragedy of the Commons* [29] and thus PD represents the essence of conflict between individuals and collective interest [19].

2.1.3 N-Person Games

We saw 2-Person games are the simplest models of Game Theory and provide a solid and simple description for interactions between two individual. However, many real-life situations involve individual's collective action, and hence those interactions cannot be modelled in the same manner as in 2-person games. This is where we move to the N-Person games framework, which provides a richer spectrum of evolutionary possibilities thus best describing these collective action problems, even though more complex to analyze [27]. While in 2-Person games agents are always aware of other individual's choices, in the new N-Person framework there is the possibility of exploitation of the common good by the defectors, that go unnoticed. Moreover, while in dyadic interactions the individual's action relies completely on his partner's strategy, on multi-individual interactions all the members of the group share responsibility for the action's result [19].

As the new game dynamics become much more rich and complex, one must be equipped with new tools to better study this dynamics. Namely, we look to find the best ways to reach a public good and for that one may analyze the impact of the contributions of cooperators, or in other words, the relationship established between the level of contributions and the amount of public good produced, which is given by the *production function* [19]. Depending on the game, different functions represent the evolution of public good as a function of the number of cooperators, as one will see soon after, and hence one shall expect different dynamics. Furthermore, one may also evaluate these new dynamics through the equilibria analysis. In N-Person games new internal equilibria emerge, more specifically, it has been shown that, for n player games with d strategies, the maximum number of internal equilibria is given by:

$$(N-1)^{d-1} \tag{2.7}$$

that is, the maximum possible number of internal equilibria increases as a polynomial in the number of players, but exponentially in the number of strategies [27]. Note that for the cooperation dynamics in 2-Person games, i.e., having $n = 2$ and $d = 2$, we recover the expected at most single internal Nash equilibria [30].

Many different types of N-Person games may be defined by generalizing some of the 2-Person games, as those previously described in Section 2.1.2. In this thesis, we will study four different N-Person games, enumerated below:

- **N-Person Snowdrift Games (NSG)**

  The generalization of the Snowdrift Game to its N-Person version is very straightforward. Taking the same formulation as in the 2-Person version, we can now imagine the snowdrift occurs in a road junction, where N drivers meet. Once again, all objective is to go home, to get the benefit b, but it will require a collective action. As shoveling demands a cost c, if all shovel, then each one is awarded with $b - \frac{c}{N}$, but if only k shovel (with $k < N$) then each only gets $b - \frac{c}{k}$, while the one who refuse to shovel get home for free, hence getting b. In many **NSG** real examples, it is common that no benefit is produced unless its costs are shared by a minimum threshold of cooperators [31]. Mathematically formalizing, for a population size Z, take a group of size $N \leq Z$ where we define the threshold $1 \leq M \leq N$ such that we achieve a public good whenever the number of cooperators in the group, k, is at least M, that is, $k \geq M$. When this public good is achieved, the benefit b is produced with a workload cost c that is divided by all k cooperators. Otherwise, if $k < M$, no benefit is produced despite the current cooperators work, and hence the maximum cost each C expend is $\frac{c}{M}$ [31]. One can summarize this interpretation according to table 2.1.

  Having this, it is clear how the **NSG** is characterized by a benefit that once obtained is fixed, and thus one shall expect the production function to be a step-function [19]. Moreover, in terms of cooperation with 2 strategies, according to equation 2.7, we expect the number of internal equilibria to grow linearly with N,

Payoff Obtained	C	D
$1 \leq k < M$	$-\frac{c}{M}$	0
$M \leq k$	$b - \frac{c}{k}$	b

Table 2.1: Payoff values for a N-Person snowdrift game.

more specifically, we will have at most $N-1$ internal Nash equilibria. We shall then expect a much richer dynamics when compared to the snowdrift 2-Person version.

- **N-Person Stag-Hunt Games (NSH)**

  Taking the same analogy as in its 2-Person version, we can also describe the *N-person stag-hunt game* (**NSH**) as a hunting problem. Let us consider a group sized larger than two that go on a hunt. Two of the hunters invest in a group of prey from both sides to make them run away forward. On the other side, the remaining hunters await for the preys to run straight into them, and this way, the group of hunters make a successful hunt. It is not possible to do such a hunt with less than 3 participants, and the more, the better. Unlike the Prisoner's Dilemma, there is a cooperative equilibrium where if all others do their part, it is best for the individual to do his as well [25]. In mathematical terms, for a group of size N, each individual is given a chance to contribute with a cost c, that will be accumulated for all k cooperators, thus we have an investment of kc. These accumulated contributions will be enhanced by a factor F to produce the total benefit of kFc, to be distributed by all individuals in the group. Defectors, which did not contribute, will receive $\frac{kFc}{N}$ while cooperators must discount the cost and receive $\frac{kFc}{N} - c$. Like we mentioned in **NSG**, in most of real-world games a minimum threshold of cooperators is required to achieve a public good. Defining this threshold again as M, we can summarize this dynamics according to the table below:

Payoff Obtained	C	D
$1 \leq k < M$	$-c$	0
$M \leq k$	$\frac{kFc}{N} - c$	$\frac{kFc}{N}$

  Table 2.2: Payoff values for a N-person stag-hunt game.

  Differently to the **NSG**, we find a characteristic benefit that once obtained grows linearly with the number of cooperators, and hence one shall expect the production function to be linear. As we shall find later, the **NSH** game leads to a much richer evolutionary dynamics when compared to the **NPD** game, mainly due to the fact that in the latter game we do not have a threshold of individuals to produce a public good. Likewise on its 2-person version, but in a much wider scale, the **NSH** not only represents many wildlife hunting situations but is also present in some international relations and macroeconomics [25]

- **Public Good Games (PGG)**

  When focusing on the *Public Good Games* (**PGG**) framework, we take the most used metaphor to study **PGG**s - the N-Person version of the Prisoner's Dilemma, that is, the *N-Person Prisoner's Dilemma* (**NPD**). The description for this kind of games is fundamentally the same as for **NSH**, but with a major difference: there is no threshold below which no public good is produced, or in other words, we have $M = 0$ [25]. This way, we can define the payoffs for Cs and Ds according to the Table 2.3 below.

  This kind of collective social dilemmas comes to be the best description for problems in which the outcome obtained goes linearly with the number of cooperators in the group, as one can infer from the table 2.3. This

Payoff Obtained	C	D
	$\frac{kFc}{N} - c$	$\frac{kFc}{N}$

Table 2.3: Payoff values for a public good game.

leads to a production function that grows linearly with the value of k, similar to the **NSH**, but unlike the previous N-person games, it is not required a minimum number of cooperators to get a benefit. While in its 2-person version the only rational move is defection, independently of the values of R, S, T and P, as long as the **PD** condition is respected, the **NPD** dynamics relies mostly on the enhancement factor $\eta \equiv F/N$. For $\eta < 1$, cooperators are at a disadvantage, and hence we have D-dominance, whereas if $\eta > 1$ we have a dynamics similar to the Harmony Game's dynamic, and hence we have C-dominance. When $\eta = 1$ we will have a neutral selection, where no particular strategy is favoured [19].

- **Collective Risk Dilemma (CRD)**

  Climate change is a very real game that we cannot afford to lose [32]. Governments have taken action to reduce greenhouse gas emissions (GEE) to mitigate climate change, where new policies have been implemented as GGE should be reduced to approximately 50% of the present level by 2050. This requires international cooperation as no single country would be able to produce such a reduction by itself. And here rises a climate dilemma: on one hand the new policies to reduce GEE are likely to have a negative short-term impact on the country economy, but on the other hand failing to accomplish this goal may resulting, in the worst possible case, in a dangerous climate catastrophe, which leads to a substantial human, ecological, and economic losses [33]. This type of social dilemma is commonly called a *collective-risk dilemma* (**CRD**), and it is the standard approach framework to deal with International Environment Agreements and other problems of the same kind [32, 34–36]. It can be mathematically modelled as follows: all individuals have an initial endowment b and are given the choice to contribute with a fraction c of their endowment, i.e., to cooperate, or not, i.e., to defect. Once again, most of this collective games demand a minimum number of contributors to come into practise, which, as before, we will define as M. If the group sized N does not contain at least M cooperators, which would produce a collective effort of Mcb, all members of the group would lose their remaining endowments with a probability of risk r. Otherwise, everyone would keep whatever they have [35]. The payoffs on each scenario may be translated according to the following table:

Payoff Obtained	C	D
$1 \leq k < M$	$b(1-r) - cb$	$b(1-r)$
$M \leq k$	$b - cb$	b

Table 2.4: Payoff values for a collective risk dilemma.

There are four main reasons to distinguish **CRD** from other social dilemmas: players make decisions repeatedly before knowing the outcome, investments are not refundable, the effective value of the public good is unknown and the remaining of the private good is available with a certain probability if the target sum is not collected [33]. The imposition of the threshold M in this situation comes from trying to mimic the most common situations of the public endeavors previously described, like in international environmental agreements that demand a minimum number of ratifications to come into practice [37].

2.2 Evolutionary Game Theory

In 1928, John von Neumann, generally regarded as the foremost mathematician of his time [38], published the paper *On the Theory of Games of Strategy*, where he proved his minimax theorem, which establishes that in zero-sum games with perfect information, i.e., in which players know at each time all moves that have taken place so far, there exists a pair of strategies for both players that allows each to minimize his maximum losses. Later, in 1944, Von Neumann improved and extended this theorem to include games involving imperfect information and games with more than two players (N-person Games), publishing this result in his famous book *Theory of Games and Economic Behavior*, co-written with the economist Oskar Morgenstern [39]. These were the first times **GT** appeared as a unique field of mathematics [15], and since then it was extensively developed, originally for application in economics and social science.

In the 1970s, a group of biologists started to recognize how similar the games from classical Theory of Games were to the interactions within a community of individuals. They explicitly applied **GT** to evolving populations in biology, and by getting rid of the static description of **GT** to transform it into a dynamical process, they gave rise to the *Evolutionary Game Theory* (**EGT**). Officially it was born when John Maynard Smith and George Price laid its foundations, providing a powerful theoretical framework to model Darwinian competition that has been widely used to study dynamically evolving populations, and more particularly, for the study of cooperative behavior in animals [40].

Typically, the problem of evolution of cooperation is addressed in well-mixed populations, that is, populations in which every individual has the same probability of interaction with one another in the population. Despite real populations are far from being well-mixed and infinite, these theoretical foundations bring us a very solid framework for the analytic study of the impact of different population's internal organization. This way, from this point on we will assume populations are well-mixed, and not structured.

2.2.1 Evolutionary Stable Strategy

When John Maynard Smith and George R. Price laid **EGT** foundations, they introduced the concept of *Evolutionary Stable Strategy* (**ESS**) as the corresponding to the Nash equilibrium but now applied to evolving populations. However, there is a big difference: while Nash equilibrium comes as a consequence of individual's rationality and perfect awareness of the structure of the game in which they are playing, the **ESS** is the result of the application of the concepts og **GT** to Biology, where players are assumed to not have any saying in their strategy, as strategies are interpreted as inherited characteristics, and hence individuals play unconditionally his strategy against any opponent. We then may say a strategy is an **ESS** if, once adopted, it can't be invaded by another strategy. It is important to notice that, while the Nash equilibrium corresponds to a certain population configuration, that is, to a certain set of strategies, an **ESS** is a single strategy. Moreover, while all **ESS**s correspond to a Nash equilibria, the opposite may not be true [19].

One may formalize this concept following the same framework from Section 2.1.1. Again, for a game with Z players, we consider a player i adopts a strategy S_i while all other players strategies are organized in the set $S_{\setminus i}$. A given strategy S_i^* in the strategy profile $\psi^* = \{S_i^*, S_{\setminus i}^*\}$ is said to be an **ESS** if it obeys either one of the following conditions:

$$\Pi_i(\{S_i^*, S_{\setminus i}^*\}) > \Pi_i(\{S_i, S_{\setminus i}^*\}) \ , \forall i \in \{1, \dots, Z\} \tag{2.8}$$

$$\Pi_i(\{S_i^*, S_{\setminus i}^*\}) = \Pi_i(\{S_i, S_{\setminus i}^*\}) \ \text{ and } \ \Pi_i(\{S_i^*, S_{\setminus i}\}) > \Pi_i(\{S_i, S_{\setminus i}\}) \ , \forall i \in \{1, \dots, Z\} \tag{2.9}$$

where $\Pi(\psi) = (\Pi_1(\psi), \ldots, \Pi_Z(\psi))$ is the payoff function evaluated at a strategy profile $\psi \in \Psi$. The first condition corresponds to the definition of a strict Nash equilibrium, as presented in 2.1. The second condition may be understood as follows: if $\Pi_i(\{S_i^*, S_{\setminus i}^*\}) = \Pi_i(\{S_i, S_{\setminus i}^*\})$, we are allowing the strategy S_i to invade the population by random drift [19], however, by applying $\Pi_i(\{S_i^*, S_{\setminus i}\}) > \Pi_i(\{S_i, S_{\setminus i}\})$ we ensure that an individual adopting S_i^* still has advantage when playing against partners with different strategy, and thus we may avoid the strategy S_i invasion. Note that $S_{\setminus i}$ corresponds to any other strategy set that is different from $S_{\setminus i}^*$.

2.2.2 Strategies and Fitness

As mentioned earlier, in cooperation dynamics we typically assume two different strategies: cooperation, C, and defection, D. However, individuals may adopt other different ways to make its moves, hence emerges the need to have a general framework that is able to represent all the different strategies. This way, and as we will see throughout this thesis, we will take a framework similar to the one presented in [41].

In this sense, for a population of size Z, we consider that individuals may adopt one of the $s+1$ available strategies, that are grouped in the set $\mathcal{S} = \{S_1, \ldots, S_{s+1}\}$. As we will see more in detail, the number of individuals of the population following any strategy $S \in \mathcal{S}$ is variable over time, hence we must define the population configuration (or *state*) as time dependent: $\boldsymbol{i}(t) = \{i_1, \ldots, i_k, \ldots, i_{s+1}\}$. As the number of individuals Z is fixed, we must have $\sum_{k=1}^{s+1} i_k = Z$, meaning we can reduce the dimensionality of the system and transform the population's configuration onto $\boldsymbol{i}(t) = \{i_1, \ldots, i_k, \ldots, i_s\}$ (the frequency of players adopting strategy S_{s+1} may be obtained through normalization) [41]. In most of our cooperation dynamics study, as previously stated, we have $\mathcal{S} = \{C, D\}$ $(s = 1)$, and hence the system's configurations comes as $\boldsymbol{i}(t) = \{i_C\}$, and we may get the number of Ds by normalization $i_D = Z - i_C$. In this case, we only have to track one degree of freedom to get the the full dynamics population.

In **EGT**, the payoff individuals obtain from all interactions may be translated onto individual *fitness* as an average payoff, that is characteristic for each strategy, that is fitness is a function $f \equiv f_S$ where $S \in \mathcal{S}$. In a biological context, one may see fitness as a quantification of the reproduction success: the more successful individuals are, the more they can spread their strategy, which will then increase its frequency in the population. From a more cultural point of view, one can also think of fitness as an evaluation of an idea, where more successful ideas and learning rules tend to be more imitated and hence will spread across the whole population [19].

To generalize this fitness concept for any $s+1$ strategies scenario, let us take a population sized Z, with a given configuration $\boldsymbol{i}(t) = \{i_1, \ldots, i_k, \ldots, i_s\}$. Now, let $\boldsymbol{j}(t) = \{j_1, \ldots, j_k, \ldots, j_s\}$ be the configuration of the players in a certain group of N individuals, such that $\sum_{k=1}^{s+1} j_k = N$, and let $(\boldsymbol{j} : j_k = q)$ designate any group configuration in which there are specifically q players following strategy S_k. From this definitions we may write down the average fitness of a strategy $S_k \in \mathcal{S}$ in a population with a composition $\boldsymbol{i}$, or $f_{S_k}(\boldsymbol{i})$, as follows [41]:

$$f_{S_k}(\boldsymbol{i}) = \binom{Z-1}{N-1}^{-1} \sum_{(\boldsymbol{j}:j_k=0)}^{(\boldsymbol{j}:j_k=N-1)} \Pi_{S_k}(\boldsymbol{j}) \binom{i_k - 1}{j_k} \prod_{\substack{l=1 \\ l \neq k}}^{s+1} \binom{i_l}{j_l} \tag{2.10}$$

where $\Pi_{S_k}(\boldsymbol{j})$ stands for the payoff associated with the strategy S_k for a group with a configuration $\boldsymbol{j}$.

From the equation above one may obtain the fitnesses for all different population setup. For instance, in cooperation dynamics we have $\mathcal{S} = \{C, D\}$ and hence $s = 1$. For any group sized N, we may write down the fitnesses for strategies C and D, respectively, f_C and f_D, according to Eq. 2.10 as:

$$f_C(k) = \binom{Z-1}{N-1}^{-1} \sum_{j=0}^{N-1} \Pi_C(j+1) \binom{k-1}{j} \binom{Z-k}{N-j-1} \tag{2.11}$$

$$f_D(k) = \binom{Z-1}{N-1}^{-1} \sum_{j=0}^{N-1} \Pi_D(j) \binom{k}{j} \binom{Z-k-1}{N-j-1} \tag{2.12}$$

where we designate the number of cooperators, i_C, as k, given that it is the most common nomenclature in literature [23, 25, 31, 34, 35, 37]. This equations are valid for any N-person game, namely the ones that have been described in Section 2.1.3, and more in specific, they are valid for games with $N = 2$, i.e., for 2-person games:

$$f_C(k) = \frac{k-1}{Z-1} R + \frac{Z-k}{Z-1} S \tag{2.13}$$

$$f_D(k) = \frac{k}{Z-1} T + \frac{Z-k-1}{Z-1} P \tag{2.14}$$

where we took the payoffs from the general 2-person payoff matrix in Eq. 2.3.

These basic equations could be seen as an evaluation of the average overall score for players following that strategy. Knowing these values, as previously stated, individuals will revise their strategy, that is, individuals will consider whether or not they should change their strategy - this defines the concept of *revision*. For individuals following a social learning (**SL**) rule, this revision is only triggered by an interaction with another player. Even this process is commonly designated as an *imitation process* or the *pairwise comparison rule* [8], in this thesis, we will rather define it as a *dynamic revision*. Nevertheless, other different types of processes may occur depending on the player's learning rule [42]. For instance, individuals may proceed with their revision by autonomously evaluate the overall configuration of the population in terms of strategy payoff, and hence there is no need for interaction with another player. As such, one may define this process as a *static revision*, which is the case of counterfactual thinking (**CT**), as we will see later.

We may generally formulate the imitation process as follows: two randomly picked individuals A and B, adopting strategies S_A and S_B, respectively, will interact with one another. Intuitively, we assume that if $S_A = S_B$, then no change will occur. However, if we have $S_A \neq S_B$, the player A will replace its strategy by player's B strategy with a probability given by the Fermi function from statistical physics [31]:

$$p_{S_A \to S_B}(\boldsymbol{i}) \equiv \frac{1}{1 + e^{-\beta(f_{S_B}(\boldsymbol{i}) - f_{S_A}(\boldsymbol{i}))}} \tag{2.15}$$

where β, which in physics corresponds to an inverse temperature, controls the *intensity of selection*. More specifically, we will define $\beta \equiv \beta^{[SL]}$ to specify the individual's learning rule (in this case **SL**). The equation above is commonly designated the (strategy) updating function, or *switching probability*, and it is valid for any dynamic revision, when the individual A is following the **SL** rule. We must, however, notice that, depending on the player's A learning rule, different strategy updating functions rise. We will discuss this topic later on.

2.2.3 Replicator Dynamics

Having replicated the dynamics of a single interaction, we now wonder how can we study the evolution of this strategy dynamics in time, as players will tend to adopt different strategies. This is where we introduce to the *replicator dynamics*, as it models the evolution of strategies [19, 42]. In cooperation dynamics, for large populations, that is $Z \to \infty$, we may write the fitness equations as a function of the frequencies (or fractions) of cooperators,

x_C, and of defectors, x_D. As we saw earlier, attending that $x_D = 1 - x_C$, we can even reduce the dimensionality of the problem to one variable, $x \equiv x_C$. The growth of x in time may be given by a first order differential equation, the so-called replicator equation [19]:

$$\dot{x} = x(f_C - \langle f \rangle) = x(1-x)(f_C - f_D) \equiv g(x) \tag{2.16}$$

where $\langle f \rangle$ stands for the average fitness of the population. As one can infer from the equation above, the sign of $\dot{x}$ depends solely on the fitnesses difference $f_C - f_D$, that indicates the direction of selection: whenever $\dot{x} > 0$ cooperation is favored, otherwise defection is the preferred strategy. In this reasoning, we designate $\dot{x}$ as the *gradient of selection*, $g(x)$, as it indicates the direction of selection, i. e., the most likely outcome of evolution. The equation 2.16 will be of foremost importance in all the following discussion, as it is probably one of the strongest tools to study population dynamics. Let us, for instance, take all 2-person games referred in section 2.1.2, for which the fitnesses for cooperators and defectors are given, respectively, by equations 2.13 and 2.14, now as a function of the fraction of cooperators, x. In this case, the replicator equation from 2.16 takes the form:

$$g(x) = x(1-x)[x(R-T) + (1-x)(S-P)] \tag{2.17}$$

In this polynomial one may infer the existence of one internal root, x^*_{int}, besides the two trivial roots, $x^*_{triv} = 0$ and $x^*_{triv} = 1$, that only depends on the game's configurations [19]:

$$x^*_{int} = \frac{P-S}{R-S-T+P} \tag{2.18}$$

Depending on the stability of this internal equilibria, different dynamics emerge. Equation 2.17 is the general gradient of selection for any 2-person games, and from that four different scenarios are possible, depending on the sign of both $R-T$ and $S-P$, as one can identify in the image below.

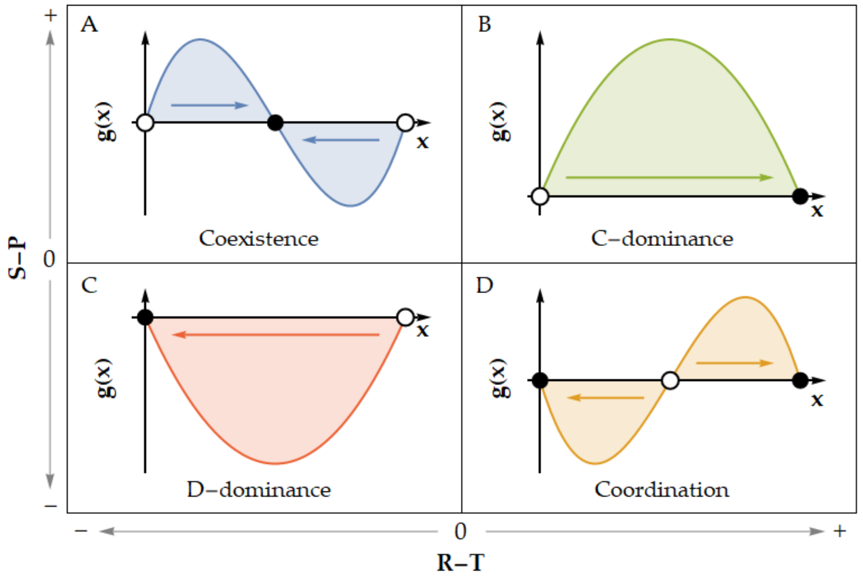

Figure 2.2: Evolutionary scenarios for 2-person games in cooperation dynamics. Panels **A** to **D** show the gradient of selection for all four different 2-person game regimes, previously described, where we consider 2 strategies. These regimes are obtained as a function of the sign of both $R-T$ and $S-P$. The full dots represent stable equilibria of the system while the open dots represent unstable equilibria.

From the image above, we can define the different regimes:

- **Coexistence (panel A):** characterized by $R - T$ negative and $S - P$ positive, this regime replicates the Snowdrift Game dynamics, as we have a balance of both populations of C's and D's, or in other words, the internal equilibrium x^*_{int} is stable while both trivial roots are unstable, and hence for $x < x^*_{int}$ ($x > x^*_{int}$) selection acts in order to increase (decrease) the number of cooperators;
- **C-dominance (panel B):** having both $R - T$ and $S - P$ positive, we enter a regime where cooperators have always a higher fitness, regardless of the current fraction of cooperators, which replicates the Harmony Game. This means that the population evolves towards achieving the full cooperative state, and hence we have an unstable fix point at $x^*_{triv} = 0$ and a stable fix point at $x^*_{triv} = 1$;
- **D-dominance (panel C):** in opposite to the C-dominance, when both $R - T$ and $S - P$ are negative we enter in a regime where defectors have the highest payoff regardless of the population's configuration, that is, the typical Prisoner's Dilemma scenario. We expect the population to evolve toward achieving the full defection state, thus we have a stable fix point at $x^*_{triv} = 0$ and an unstable equilibrium at $x^*_{triv} = 1$;
- **Coordination (panel D):** characterized by $R - T$ positive and $S - P$ negative, in this regime the internal equilibrium x^*_{int} is unstable while both trivial roots are stable, meaning that for $x < x^*_{int}$ ($x > x^*_{int}$) selection will act towards full defection (full cooperation);

2.3 Stochastic Processes

The replicator equation (2.16) is a very powerful tool that helps on describing the population's evolutionary dynamics, however it relies on the system's deterministic properties, which consequently implies continuity. To achieve this, we would require an infinite population, which in many real world scenarios is an unrealistic approximation. Moving to finite populations, we must consider fluctuations, and hence the population dynamics no longer can be described in the deterministic formulation of the replicator dynamics. The evolutionary dynamics of the propagation of strategies must now take into account the stochastic effects [19].

As we enter in a discrete domain, the description of the system may be given according to the formalism of the *Markov Processes*, which are basically stochastic processes that respect the *Markov property*. This property may be formulated as follows: let us suppose we have a system that at a time t_a has a certain configuration $\boldsymbol{i}_a$, from which we define the system state as the discrete random variable $X_{t_a} = \boldsymbol{i}_a$, where X_{t_a} is defined on a finite or countably infinite space state $\mathcal{X}$ [43]. Here, we define a as the step in the Markov process, starting from the initial state $a = 0$. A stochastic process $\{X_{t_a}\}_{a=0}^{\infty}$ is said to have a Markov property whenever:

$$P\{X_{t_a} = \boldsymbol{i}_a \,|\, X_{t_0} = \boldsymbol{i}_0, \dots, X_{t_{a-1}} = \boldsymbol{i}_{a-1}\} = P\{X_{t_a} = \boldsymbol{i}_a \,|\, X_{t_{a-1}} = \boldsymbol{i}_{a-1}\} \tag{2.19}$$

or, in other words, the state of the system at time t_{a+1} only depends on its state at a time t_a and not of all the previous history of the system starting from its initial configuration. This stochastic process is commonly called a *Markov chain* [43]. As we saw previously, in cooperation dynamics we have $\boldsymbol{i} = \{i_C\} = \{k\}$, meaning we can simplify our system representation to a Markov chain where each state is defined by the number of cooperators k.

Once we consider evolutionary dynamics, we must adopt an update mechanism that models the transitions between different states of the system, and, for that, let us establish the foundations of our reasoning. For a finite population sized Z, we have a system with $Z + 1$ states, where each state is represented by the number of cooperators k. Starting at a time t_0 with a certain initial state k, individuals start interacting with one another,

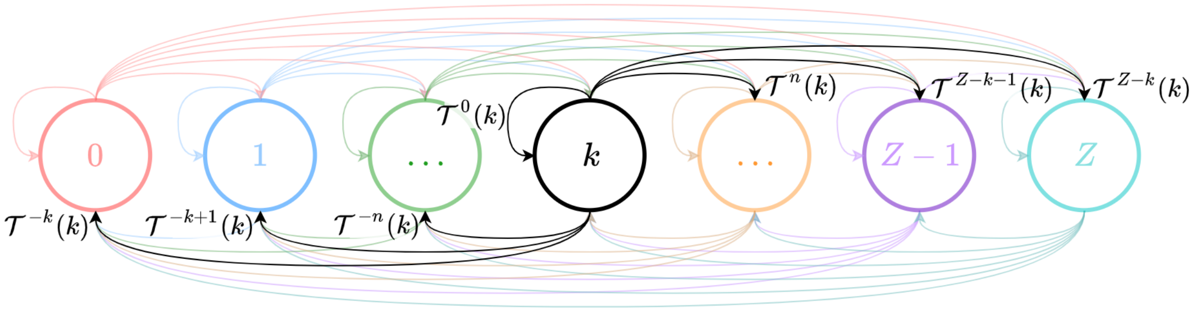

Figure 2.3: Representation of a general Markov Chain for a finite system with $Z+1$ states in cooperation dynamics, considering all transitions between states are possible.

triggering strategy revision, which consequently may lead to a change in the system's configuration. Generalizing, from a given state k at a time t_a, we represent $\mathcal{T}^n(k)$, known as the *transition probability*, as the probability that at a time t_{a+1} the system moves to the state $k+n$, i.e., as the probability that the population varies its number of cooperators by n (note that n may be either negative or positive). Obviously, we should always respect the limiting conditions that $0 \leq k+n \leq Z$. The above system's description is well represented on Figure 2.3.

2.3.1 Transition Matrix and Transition Probabilities

All transition probabilities may be summarized in the general *stochastic transition matrix* $\boldsymbol{\mathcal{T}}$, which, according to the matrix indexes i and j, may be given as $\mathcal{T}_{i,j} = \mathcal{T}^{j-i}(i-1)$, and we may obtain the following:

$$\boldsymbol{\mathcal{T}} = \left\{\mathcal{T}^{j-i}(i-1)\right\}_{i=1,j=1}^{Z+1,Z+1} = \begin{bmatrix} \mathcal{T}^{0}(0) & \mathcal{T}^{+1}(0) & \dots & \mathcal{T}^{j-1}(0) & \dots & \mathcal{T}^{+Z}(0) \\ \mathcal{T}^{-1}(1) & \mathcal{T}^{0}(1) & \dots & \mathcal{T}^{j-2}(1) & \dots & \mathcal{T}^{+(Z-1)}(1) \\ \vdots & \vdots & \ddots & \vdots & \ddots & \vdots \\ \mathcal{T}^{1-i}(i-1) & \mathcal{T}^{2-i}(i-1) & \dots & \mathcal{T}^{j-i}(i-1) & \dots & \mathcal{T}^{Z-i}(i-1) \\ \vdots & \vdots & \ddots & \vdots & \ddots & \vdots \\ \mathcal{T}^{-Z}(Z) & \mathcal{T}^{-(Z-1)}(Z) & \dots & \mathcal{T}^{j-Z}(Z) & \dots & \mathcal{T}^{0}(Z) \end{bmatrix} \tag{2.20}$$

The analytical study of the matrix $\boldsymbol{\mathcal{T}}$ is very complex. To simplify, in most studies researchers adopt a *birth-death process*, also know as *one step process*, that is, at each time-step in discrete time only one individual may revise its strategy [19, 23, 31, 41]. In our model, this means we have $\mathcal{T}^n(k)$ with at most $|n| = 1$, that is, $n = \{-1, 0, 1\}$, and hence the matrix $\boldsymbol{\mathcal{T}}$ becomes tri-diagonal, allowing us to handle major dynamics tools, such as the gradient of selection, in a very simple way, as we will see soon in Section 2.3.4.

Although we take birth-death process for the sake of simplicity, we know that in many real-world scenarios multiple strategy revisions may occur simultaneously, giving rise to many new problems. For instance, as the transition matrix becomes more complex, we are no longer able to evaluate the direction of selection as we did for the birth-death process. We must now take into account the effects of the synchronous dynamics, as we start moving away from the asynchrony. We will widely discuss the effects of synchronism later on Chapter 3. For the rest of this chapter we will adopt the typical birth-death process.

Regarding the transition probabilities, as we only assume one revision, we may write $\mathcal{T}^{\pm1}$ directly according to the outcomes of interactions between individuals with different strategies (to simplify notation, from this point on we assume $\mathcal{T}^{\pm1} = T_{\pm}$). More specifically, and according to the Fermi's switching probability in equation 2.15, one may intuitively build the transition probabilities by following this reasoning: we take a defector (cooperator) from the existing Z individuals, $x_C^{(Z)}$ ($x_D^{(Z)}$), that will interact with a cooperator (defector), now from a population with $Z-1$ individuals, $x_D^{(Z-1)}$ ($x_C^{(Z-1)}$). The transition probabilities $T_\pm$ are, then, given as a function of k:

$$T_-(k) \equiv T_{C\to D}(k) = x_C^{(Z)} \cdot x_D^{(Z-1)} \cdot p_{C\to D}(k) \tag{2.21}$$

$$T_+(k) \equiv T_{D\to C}(k) = x_D^{(Z)} \cdot x_C^{(Z-1)} \cdot p_{D\to C}(k) \tag{2.22}$$

where we define $x_S^{(Z)} = \frac{i_S}{Z}$ the fraction of individuals in the population following strategy S. In terms of cooperation, we have $x_C^{(Z)} = \frac{i_C}{Z} = \frac{k}{Z}$ and $x_D^{(Z)} = \frac{i_D}{Z} = \frac{Z-k}{Z}$. From these transition equations, we may also get the transition $\mathcal{T}^0$ by normalization, that is, $\mathcal{T}^0 \equiv T_0 = 1 - T_- - T_+$. From this, one may compute the transition matrix and get the system's dynamics for all values of k, for the one step process.

Equations 2.21 and 2.22, above described, assume that individuals are only able to adopt a strategy if it has already been adopted by one of the members of the population. In this case, the update method is said to be *non-innovative*. As such, once the system reaches any of the boundary states $k=0$ and $k=Z$, meaning we reach full cooperation or full defection, respectively, it is impossible to move out. In terms of transition probabilities, this means that both $T_+(0)$ and $T_-(Z)$ are null, and thus, whenever reached, the system would be stuck in those states. Due to this absorption capacity, both states $k=0$ and $k=Z$ are said to be *absorbing states*.

If, on the other hand, we assume that individuals have access to the whole set of strategies, $\mathcal{S}$, allowed by the rules of the game, even if no individual in the population is currently adopting one of them, the update method is said to be *innovative* and we no longer have absorbing states [19]. This update method may be formalized by adjusting the equations 2.21 and 2.22 with the introduction of a small mutation rate μ, where the randomly chosen individual may either mutate to the either strategy, with probability μ, or follow the standard update method, with probability $1-\mu$. The transition probabilities ${}^{\mu}T_\pm$ of the transition matrix $\boldsymbol{\mathcal{T}}^{\mu}$, are now given as:

$${}^{\mu}T_-(k) = (1-\mu)\, T_-(k) + \mu \cdot x_C^{(Z)} \tag{2.23}$$

$${}^{\mu}T_+(k) = (1-\mu)\, T_+(k) + \mu \cdot x_D^{(Z)} \tag{2.24}$$

where, once again, $x_C^{(Z)} = \frac{k}{Z}$ and $x_D^{(Z)} = \frac{Z-k}{Z}$. With this formulation, when the population reaches a monomorphic state (either all Cs or all Ds), an individual revising his strategy can change to a different one. Some examples of of innovative update methods are the *Best-Response* and the *Reinforcement Learning* [19].

2.3.2 Fixation Probability and Fixation Times

For non-innovative update mechanism, it may be relevant to compute the *fixation probability*, ϕ_i, that is, the probability that i cooperators invade the population while the remaining $Z-i$ individuals are defectors. For a birth-death process, and always considering well-mixed populations, it may be given as [44, 45]:

$$\phi_i = \frac{1 + \sum\limits_{k=1}^{i-1} \prod\limits_{j=1}^{k} \gamma_j}{1 + \sum\limits_{k=1}^{Z-1} \prod\limits_{j=1}^{k} \gamma_j} \tag{2.25}$$

where we define $\gamma_j = \frac{T_-(j)}{T_+(j)}$. For neutral selection, we have $T_-(j) = T_+(j)$, which results in $\gamma_j = 1$. In the case we only have 2 absorbing states ($k=0$ and $k=Z$), the probability $1-\phi_i$ defines the opposite to fixation probability, the *extinction probability*, that is, the probability that cooperation goes extinct when we have i cooperators in a population sized Z.

Other quantity of interest in evolutionary dynamics of finite population is the average time until fixation occurs. For a two strategy setup, $\mathcal{S} = \{S_1, S_2\}$, two of the most relevant fixation times are:

- the *unconditional fixation time*, τ_j, is defined as the average time until either one of the two absorbing states is reached when starting from state j. The average unconditional fixation time for a any j may be given as:

  $$\tau_j = -\sum_{k=j}^{Z-1}\left(\tau_1 \prod_{m=1}^{k}\gamma_m - \sum_{l=1}^{k}\frac{1}{T_+(l)}\prod_{m=l+1}^{k}\gamma_m\right) \tag{2.26}$$

  where we have:

  $$\tau_1 = \underbrace{\frac{1}{1+\sum_{k=1}^{Z-1}\prod_{j=1}^{k}\gamma_j}}_{\phi_1}\sum_{k=1}^{Z-1}\sum_{l=1}^{k}\frac{1}{T_+(l)}\prod_{m=l+1}^{k}\gamma_m \tag{2.27}$$

  One shall notice that these fixation times is usually quantitatively high, depending on the population parameters Z, β and the game. Particularly, in coexistence games, such as Snowdrift games, fixation times do not only diverge with the population size and the intensity of selection, but they represent averages of a very broad distribution [45]. The unconditional fixation time is independent of the strategy.

- the *conditional fixation time*, $\tau_j^{S_1}$, specifies the average time the system takes to reach the absorbing state S_1, starting from state j, knowing that S_1 is eventually reached. If fixation of strategy S_1 is almost certain ($\phi_{S_1} \approx 1$), then it is clear that $\tau_j^{S_1} \approx \tau_j$, that is, the unconditional and conditional fixation times are very similar. For a general j, the conditional fixation time may be given by:

  $$\tau_j^{S_1} = -\sum_{k=j}^{Z-1}\left(\tau_1^{S_1}\frac{\phi_1}{\phi_j}\prod_{m=1}^{k}\gamma_m - \sum_{l=1}^{k}\frac{\phi_l}{\phi_j}\frac{1}{T_+(l)}\prod_{m=l+1}^{k}\gamma_m\right) \tag{2.28}$$

  where we have:

  $$\tau_1^{S_1} = \sum_{k=1}^{Z-1}\sum_{l=1}^{k}\frac{\phi_l}{T_+(l)}\prod_{m=l+1}^{k}\gamma_m \tag{2.29}$$

  As mentioned, one may verify that for certain fixation, that is, $\phi_1 = \phi_j = 1$, the time τ_1^A is reduced to the unconditional fixation time τ_1. The same way, we can obtain the conditional fixation time for the other absorbing state S_2 starting from an arbitrary number of S_1 individuals:

  $$\tau_j^{S_2} = -\sum_{k=1}^{j}\left(\tau_{Z-1}^{S_2}\frac{\tilde{\phi}_{Z-1}}{\tilde{\phi}_j}\prod_{m=1}^{k}\frac{1}{\gamma_{Z-m}} - \sum_{l=1}^{k}\frac{\tilde{\phi}_{Z-l}}{\tilde{\phi}_j}\frac{1}{T_-(Z-l)}\prod_{m=l+1}^{k}\frac{1}{\gamma_{Z-m}}\right) \tag{2.30}$$

  where we have:

  $$\tau_{Z-1}^{S_2} = \sum_{k=1}^{Z-1}\sum_{l=1}^{k}\frac{\tilde{\phi}_{Z-l}}{T_-(Z-l)}\prod_{m=l+1}^{k}\frac{1}{\gamma_{Z-m}} \tag{2.31}$$

  Along with the fixation probabilities, both fixation times are relevant to characterize the evolutionary process, as they give us insights that include information about all transition probabilities [45].

Note, however, this is only valid for non-innovative update mechanisms in birth–death processes. For more complex processes, these quantities may be obtained following a different derivation, as done in Chapter 3.

2.3.3 Stationary Distribution

From the general transition matrix 2.20 one can compute the *stationary distribution*, which basically defines the fraction of time the system spends on each state, or in other words, it defines the probability of finding the system at a certain state k at any time. Formalizing the concept, let us define the state distribution at a time t as the row vector $s_t \in \mathbb{R}_+^{\mathcal{X}}$, which is the vector whose j-th coordinate indicates the probability of finding the system in a state j at a certain time t, i.e., we have $(s_t)_j = P(X_t = j)$. This way, having $s_{t_0} = P(X_{t_0})$ as the initial state distribution, one may compute the state distribution at any point in time as:

$$s_{t_a} = s_{t_0}\boldsymbol{\mathcal{T}}^a \ , \ \forall a \geq 0 \tag{2.32}$$

where, once again, we define a as the step in the Markov process.

After a long period of time, there are many cases where the system reaches an equilibrium in which no better system's configuration leads to an increase on the individual's payoff. In these situations, the Markov chain is said to converge to a *stationary distribution*, $\bar{s}$, which is given by:

$$\begin{aligned} \bar{s} &= \lim_{a\to\infty} s_{t_0}\boldsymbol{\mathcal{T}}^a \\ &= \lim_{a\to\infty} s_{t_0}\boldsymbol{\mathcal{T}}^{a+1} \\ &= \left(\lim_{a\to\infty} s_{t_0}\boldsymbol{\mathcal{T}}^a\right)\boldsymbol{\mathcal{T}} \\ \implies \bar{s} &= \bar{s}\boldsymbol{\mathcal{T}} \end{aligned} \tag{2.33}$$

which means that $\bar{s}$ is the left eigenvector of $\boldsymbol{\mathcal{T}}$ for the eigenvalue 1 (the highest eigenvalue) [19]. Note that $\bar{s}$ may be written as a function of the systems configuration, that is, generally we have $\bar{s} \equiv \bar{s}(\boldsymbol{i})$, for any configuration $\boldsymbol{i}$. It should also be noted that not all Markov chains admit a stationary distribution but, however, if it is irreducible then it will admit a unique stationary distribution, which is the case of the birth-death process [43].

Notice that, for non-innovative update mechanisms, one should expect a peak on each the two absorbing states, as the system would stay there for a infinitely long time. This way, when studying the evolutionary dynamics of a certain game, it would be advisable to adopt an innovative update mechanism, such as the one previously presented in equations 2.23 and 2.24. In order not to lose the essence of the game's dynamics, it would be better to use a low value for μ, for instance, $\mu \sim \mathcal{O}\left(\frac{1}{Z}\right)$ or $\mu \sim \mathcal{O}\left(\frac{1}{Z^2}\right)$. The stationary distribution is, thus, a great tool that stochastically predicts the outcome for infinitely long evolutionary games.

Having the fraction of time the system spends on each state, one may now obtain the *expected fraction of cooperators*, EFC, that is, the fraction of cooperators one should expect to find in the system whenever evaluated at a random moment in time. Noticing the stationary distribution may be explicitly defined as a function of the fraction of cooperators, expressly $\bar{s} \equiv \bar{s}(x)$, we may define the EFC as:

$$EFC = \sum_{x=0}^{1} x \cdot \bar{s}(x) \tag{2.34}$$

This quantity may be very important on a system's evaluation, as it may be indicative of the system's most likely outcome at any point in time. However, it should only be used as an auxiliary tool for system's evaluation, as it may bring missleading conclusions. For example, suppose we have a system's stationary distribution with two peaks, respectively centered at the fractions of cooperators x_1 and x_2. Assuming the values for the rest of the distribution are low enough to be negligible, one may expect an $EFC \approx \frac{x_1+x_2}{2}$, which is obviously missleading, as the probability to find the system on this point is very low. It would be much more likely to find the system in one of the two more probable peaks. Therefore, it is imperative to take into consideration the shape of the distribution. More specifically, it would be more advisable to use this measurement solely for a single peak shaped distribution.

Another quantity of interest, will be the *average group achievement*, commonly designated by η_G, which is a measure of cooperation in a population. For each possible configuration $\boldsymbol{i}$, we make use of the multivariate hypergeometric sampling to compute the (average) fraction of groups that overcome the threshold of M contributors (commonly defined as η_{PG}), which is designated as $a_G(\boldsymbol{i})$. Formally, this quantity may be obtained when replacing the $\Pi_{S_k}(\boldsymbol{j})$ term by $\Theta(\sum_{k=1}^{s} j_k - \eta_{PG})$ in equation 2.10, for any general case [41]. Recall that, overcoming the threshold M is equivalent to achieving a contribution of $M\,c\,b$, and hence successfully achieving the public good. The average group achievement may then be computed by averaging over all possible configurations $\boldsymbol{i}$, each weighted with the corresponding stationary distribution [36]:

$$\eta_G = \sum_{\boldsymbol{i}} \bar{s}(\boldsymbol{i}) \cdot a_G(\boldsymbol{i}) \tag{2.35}$$

To summarize, the average group achievement provides the overall probability of achieving success, and hence it becomes another very important tool to evaluate the game dynamics in the N-person framework.

2.3.4 Deterministic Gradient of Selection

Let us retake the previously defined Markov process $\{X_{t_a}\}_{a=0}^{\infty}$, and more specifically, let us have $X_{t_a} = i_a$, and thus having the system defined as a Markov chain $\{i_a\}_{a=0}^{\infty}$. The study of a Markov process often subsist in finding its probability density function (PDF) evolution [42]. The probability density function, $p_{\boldsymbol{i}}(t)$, defined as the predominance of configuration $\boldsymbol{i}$ at a (continuous) time t, evolves according to the *Master equation* [42]:

$$\frac{dp_{\boldsymbol{i}}(t)}{dt} = \sum_{\boldsymbol{i}'} \{T_{\boldsymbol{i}\boldsymbol{i}'} P_{\boldsymbol{i}'}(t) - T_{\boldsymbol{i}'\boldsymbol{i}} P_{\boldsymbol{i}}(t)\} \tag{2.36}$$

where $T_{\boldsymbol{i}\boldsymbol{i}'}$ denotes the transition probability from configuration $\boldsymbol{i}$ to $\boldsymbol{i}'$. This is known as the *gain-loss* equation - the first term on the right-hand side is associated to the gain due to transitions from other states $\boldsymbol{i}'$ to the state $\boldsymbol{i}$ while the second term corresponds to the loss due to transitions from $\boldsymbol{i}$ to other states $\boldsymbol{i}'$.

Solving the Master equation is, however, complicated. Following the derivation shown in [19, 42, 45], and assuming $Z \to \infty$ and for two strategies, we will finally obtain the *deterministic gradient of selection* as a deterministic differential equation:

$$G(x) \equiv \dot{x} = T_{+}(x) - T_{-}(x) \tag{2.37}$$

which is equivalent to the replicator equation 2.16. It may also be addressed as *drift*. This procedure is extensible for systems with more than two strategies although in this case, the mathematics is considerably more complex [45]. Note, however, that we have only considered the limit $Z \to \infty$, keeping all other variables fixed. To perform the thermodynamic limit, or macroscopic limit, the intensity of selection, β, in the Fermi process from equation 2.15 should scale with Z, which means that, for finite populations, the approximation of the process is only valid for large Z and can be used to address the evolutionary dynamics only under weak selection, that is, $\beta \ll 1$ [45].

Notice that, until now, we have been representing the typical 2-dimensional cooperation dynamics, with 2 strategies, C and D, for well-mixed populations, in a **SL** environment. However, and as we will see soon after, all these concepts may be generalized for any other learning rules and strategies, independently of their formulation, most of them through a direct pairwise comparison with social learning.

2.4 Other Learning Rules

Until now, most of population dynamics in Evolutionary Game Theory had its mathematical framework based on social learning. We assumed that decision-makers are rational and therefore they look to obtain the maximal expected outcome from among all feasible actions. However, besides the pursuit of highest payoffs in evolutionary social dilemmas is risky, it is also a fact that individual's interactions are not always driven by a selfish agenda such as fitness maximization [11]. In many real world scenarios, one may verify that some individuals will prefer to adopt different ways of reasoning. For instance, individuals may opt to follow the most common strategy in the population (conformity, **C**) or they may autonomously reason about a past event that did not occur yet (counterfactual thinking, **CT**), as we will see later more in detail. These are just two examples from a great number of different updating mechanisms that are yet to be profoundly studied.

As earlier mentioned, the concept of *learning rule* may be defined as the strategy updating mechanism that some individuals follows at a certain point in time. In other words, we say an individual has a certain learning rule, L_j, from the set of the l available learning rules in the system, $\mathcal{L} = \{L_1, \ldots, L_j, \ldots, L_l\}$, for a certain amount of time, in which the individual will update its strategy according the update mechanism associated to that rule. If, for instance, a player has a social learning (**SL**) rule for a certain time, as we assumed until now, then it will update its strategy according to the Fermi function 2.15 during that period of time.

However, temporally speaking, the learning rule may be either inherent to the individual or not, that is, it characterizes the individual and does not change over time - we say it is *fixed* - or it is a state of mind that varies over time - it is *flexible*. In this latter case, one could assume the learning rule changes follow a certain distribution, where the individuals would change their rule probabilistically according to that distribution, that could go as a function of the cumulative period time the player has been following that learning rule. From this point, regarding learning rules, many different population setups could be studied. In fact, for further studies, it would be interesting to investigate different distributions for learning rule changing in flexible-rule populations, as we should expect a richer and more complex dynamics. However, for the scope of this thesis, we will focus our study on populations where individuals have one learning rule $L \in \mathcal{L}$, with $\mathcal{L} = \{SL, C, CT\}$, that is fixed and hence constant over time.

2.4.1 Conformity

As some individuals might not opt to imitate those with higher fitness, they may ignore the relative payoffs of the game and focus on choosing the most common strategy among their partners. This learning rule may be defined as *conformity* (**C**), and individuals following this learning rule are said to be conformity-driven or conformists. In fact, there exists compelling evidence that favours the fact that conformity plays an important role in cooperation dynamics, especially among humans and social animals [11]. Intuitively, conformists players tend to minimize their risk while ensuring they still receive some kind of payoff, not much lower than the average. In this topic, previous work have been done, mostly on structured populations [11, 12]. In most these studies it is adopted a framework very similar to the one previously built for social learning, although specifically applied to structured populations.

To take into account well-mixed populations, one can very elegantly define a framework for conformity by simply making a pairwise comparison with the previously defined **SL** dynamics. In the latter, we saw the switching probability goes as a function of the difference between the strategy fitnesses, $f_{S_B}(\boldsymbol{i}) - f_{S_A}(\boldsymbol{i})$, of the two interacting individuals, A and B, for a certain configuration $\boldsymbol{i}$. In this population, we will have n_{S_A} and n_{S_B} individuals following strategies S_A and S_B, respectively. The difference between these number of individuals, $n_{S_B} - n_{S_A}$, will tell us which of the strategies is the most common in that population, and this constitutes the base function of conformity.

Formally, we can define the switching probability for individuals following the conformity rule, C, as:

$$p^{[C]}_{S_A \to S_B}(\boldsymbol{i}) \equiv \frac{1}{1 + e^{-\beta^{[C]}(n_{S_B}(\boldsymbol{i}) - n_{S_A}(\boldsymbol{i}))}} \tag{2.38}$$

where we specifically define $\beta^{[C]} \neq \beta^{[SL]}$ as the *intensity of conformity*. Please notice this does not require individual B to be conformist, only individual A must be identified as a conformist. Likewise as in **SL** interactions, we assume individual A requires an interaction with B to trigger the strategy revision, that is, we assume the conformity behavior is associated to dynamic revision processes. The function $n_{S_B} - n_{S_A}$ may be normalized, which in this case leads to the simple transformation on the intensity $\beta^{[C]} \to Z * \beta^{[C]}$. As an example, for the typical 2 strategy cooperation dynamics, we will have the normalized functions $n_C(x) = x_C^{(Z-1)}(k)$ and $n_D(x) = x_D^{(Z-1)}(k)$.

From this new switching probability, we may define the other tools to study evolutionary dynamics of the population. The conformity transition probabilities, again by analogy to equations 2.21 and 2.22, may be written as:

$$T_-^{[C]}(k) \equiv T^{[C]}_{C \to D}(k) = x_C^{(Z)} \cdot x_D^{(Z-1)} \cdot p^{[C]}_{C \to D}(k) \tag{2.39}$$

$$T_+^{[C]}(k) \equiv T^{[C]}_{D \to C}(k) = x_D^{(Z)} \cdot x_C^{(Z-1)} \cdot p^{[C]}_{D \to C}(k) \tag{2.40}$$

which will define the deterministic gradient of selection for conformity:

$$G^{[C]}(k) \equiv T_+^{[C]}(k) - T_-^{[C]}(k) \tag{2.41}$$

This is the basis to define a framework for conformity, simply by a pairwise comparison with **SL**. In the previous works, it was shown that the presence of conformity-driven players enhances network reciprocity, and thus aids the favourable resolution of social dilemmas. The effectiveness of conformity to do so, however, depends on the fraction of conformists within the population [12]. Later in this thesis, we will more profoundly investigate the impact of conformity in non-structured populations.

2.4.2 Counterfactual Thinking

Another learning rule of interest is counterfactual thinking (**CT**), which is widely studied for an N-person game scenario in [13]. Counterfactual thinking is a human cognitive ability where individuals capture the process of reasoning about hypothetical past events, specifically what would have happened if those events occurred. This reasoning would be take into account in the next player moves. Therefore, and recalling the **ToM** definition in section 2.1, the counterfactual thinker may be already considered a **ToM** level-one agent, contrary to a social learner or a conformist, that stand at the lower level of **ToM**. For the simpler cases, as for the birth-death process currently in study, this doesn't bring much complexity to the transition probabilities, formally speaking. However, in chapter 3 we will see how synchronous processes may become more and more complex as we take into consideration the implications of assuming **CT** individual as a first-degree **ToM** agent.

Differently to **SL**, individuals that are **CT**-driven evaluate all possible alternatives to their current returns, had they chosen an alternative strategy to what actually took place. Players will reason about how the outcome could have worked if their decision (strategy, in the case) would have been different. In its simplest form, this may be modelled as an initial form of myopic best response rule at the population level, by considering the fitness of the agent in a system configuration that did not, but could have occurred [13]. From a pairwise comparison to the **SL** framework, the switching probability may be given as:

$$p_{S_A \to S_B}^{[CT]}(\boldsymbol{i}) \equiv \frac{1}{1 + e^{-\beta^{[CT]}(f'_{S_B}(\boldsymbol{i}) - f'_{S_A}(\boldsymbol{i}))}} \tag{2.42}$$

where we specifically define $\beta^{[CT]}$ as the *intensity of counterfactual thinking*. As one can see, the probability increases non-linearly with the different between the fitness the individual would have had if it had chosen strategy S_B, designated as $f'_{S_B}(\boldsymbol{i})$, and the fitness it actually got by playing S_A, designated as $f'_{S_A}(\boldsymbol{i})$. Specifically applying this in the typical 2-strategy cooperation dynamics, one can easily rewrite equation 2.42 by considering the fitness C players, or D players, would have had in a population having an extra cooperator, or extra defector, depending on the alternative strategy the individual had chosen [13]. This way, we will have:

$$p_{C \to D}^{[CT]}(k) \equiv \frac{1}{1 + e^{-\beta^{[CT]}(f_D(k-1) - f_C(k))}} \tag{2.43}$$

$$p_{D \to C}^{[CT]}(k) \equiv \frac{1}{1 + e^{-\beta^{[CT]}(f_C(k+1) - f_D(k))}} \tag{2.44}$$

From this we may define the other tools to study evolutionary dynamics of the population, just like we did before for conformity. The **CT** transition probabilities may be obtain by analogy to equations 2.21 and 2.22, but now taking into account that the revision process is static (see section 2.2.2), that is, individual **A** does not require an individual **B** to revise its strategy. These equations may be written as:

$$T_{-}^{[CT]}(k) \equiv T_{C \to D}^{[CT]}(k) = x_C^{(Z)} \cdot p_{C \to D}^{[CT]}(k) \tag{2.45}$$

$$T_{+}^{[CT]}(k) \equiv T_{D \to C}^{[CT]}(k) = x_D^{(Z)} \cdot p_{D \to C}^{[CT]}(k) \tag{2.46}$$

which will define the deterministic gradient of selection for counterfactual thinking:

$$G^{[CT]}(k) \equiv T_{+}^{[CT]}(k) - T_{-}^{[CT]}(k) \tag{2.47}$$

Firstly, one shall note that, differently from **SL** or **C** learning rules, the the transition probabilities do not have a second fraction of individuals term $x_S^{(Z-1)}$, with $S \in \{C, D\}$, hence a relative higher order of magnitude is expected for **CT**. This effect will be clearly manifested in the later results, as we will be discussing in Chapters 4.

In previous works it is suggested that counterfactual reasoning fosters coordination in collective action problems in large populations, with a limited impact on cooperation dilemmas in which coordination is not essential. Furthermore, it is shown that a small prevalence of individuals following counterfactual thinking is enough to direct an entire population towards an highly cooperative community [13]. It is now our intention to investigate the impact of counterfactual thinking in other different and possibly more complex populations, not only for all the previously defined games but also in the joint presence of conformity.

2.4.3 Multiple Learning Rules Populations

Setting all this learning rules together, one may define a new population dynamics based on how the different individuals associated to each one of the heuristics. In real-world populations, all individuals, regardless of their way to reason, may belong to one same community. In one first case, we may consider individuals are equivalent as they may resort to any of the available heuristics to their strategies. They may resort to different learning rules, yet all share the same probabilities of using each, and hence the equivalent characteristic between them. In this case, we say individuals are arranged in an *homogeneous population*. In other case, individuals may adopt a different, yet fixed, learning rule, displayed in separated sub-populations. In this case we say individuals are organized in an *heterogeneous population*. It seems obvious that the overall dynamics for both cases won't be the same and, as that, a different framework shall be adopted. Even though these dynamics are general, along this thesis we will focus on a frameworks with only two leaning rules.

Homogeneous Populations

When addressing a certain population as homogeneous, we are assuming the individual's leaning rule does not have an impact on the well-mixed characteristic of the population. In other words, we recover the well-mixed concept definition: any individual in the population may interact with one another with equal probability, regardless of the individual's leaning rule. In this framework, we will assume the equivalent individuals resort to a certain learning rule $L \in \mathcal{L}$ with a given fixed probability $\delta^{[L]}$, in a way that $\sum_{L\in\mathcal{L}} \delta^{[L]} = 1$. Formally speaking, this is the same as redefine the system's transition probabilities to take into account all the different rules:

$$T_{\pm}(k) = \sum_{L\in\mathcal{L}} \delta^{[L]} T_{\pm}^{[L]}(k) \tag{2.48}$$

which can be applied for the case of study, with $\mathcal{L} = \{SL, C, CT\}$, as:

$$T_{\pm}(k) = \delta^{[SL]} T_{\pm}^{[SL]}(k) + \delta^{[C]} T_{\pm}^{[C]}(k) + \delta^{[CT]} T_{\pm}^{[CT]}(k) \tag{2.49}$$

where, by normalization, we may rewrite $\delta^{[SL]} = 1 - \delta^{[C]} - \delta^{[CT]}$.

Directly from this equation, one can write the novel gradient of selection as:

$$G(k) = \delta^{[SL]} G^{[SL]} + \delta^{[C]} G^{[C]} + \delta^{[CT]} G^{[CT]} \tag{2.50}$$

As we will see later on, this equation will be of foremost importance in the study of population's dynamics, when assuming the population is mixed homogeneously. Please notice that the redefinition of the transition probabilities in 2.48 does not have a negative impact regarding the validity of the framework previously shown in section 2.3. It becomes obvious that, taking both $\delta^{[C]} = 0$ and $\delta^{[CT]} = 0$, one may recover the regular social learning dynamics.

Notice that we have been assuming populations with fixed leaning rules probabilities. If we, however, consider flexible dynamics, some of the quantities above described should be defined also as flexible. For instance, we may have to redefine all the heuristic probabilities as a function of time, that is, $\delta^{[L]} \equiv \delta^{[L]}(t)$. This could potentially lead to a much richer population dynamics, that would be interesting to investigate. However, and for the scope of this thesis, we will leave this for future work.

Heterogeneous Populations

When a population is organized in multiple smaller communities of same-rule individuals, a different approach shall be taken. In this thesis, we will follow a framework similar to the one presented in [41], where a certain population is divided into two sub-populations according to individual's wealth classes (rich or poor). In our case, we will divide our population according to each individual's learning rule, that is fixed and unchangeable, treating each sub-population independently, however always considering all interactions between different sub-populations are possible. As previously mentioned, we will focus our studies in populations divided only in two sub-populations.

We start by defining $Z^{[L]}$ as the number of individuals that drive its reasoning according to leaning rule $L \in \mathcal{L}$. It is easy to understand that these quantities must be normalized to the total number of individuals on the population, that is, we will have $\sum_{L\in\mathcal{L}} Z^{[L]} = Z$.

This framework creates an interdependent behavioral ecosystem, where every individual in a group knows about all other member's actions and where one's own decisions and achievements are influenced by others. Particularly, for instance, decisions taken by a conformist may potentially have an impact on a social learner actions and achievements (and vice versa), even though they belong to distinct sub-populations. However, individuals may be more receptive to decisions of those that follow the same learning rule as its own, thus selecting preferentially those of their learning rule as peers. To take this effect into account, one may define an *homophily* parameter, $0 \leq h \leq 1$, such that when $h = 1$, individuals are restricted to influence (and be influenced) by those of the same sub-population, whereas when $h = 0$, anyone in this population may influence and be influenced by anyone else [41]. This latter definition, for $h = 0$, is equivalent to assume the population is well-mixed, in such a way that we may recover the homogeneous case, whereas having maximum homophily highlights the true definition of heterogeneity. In this sense, homophily may be seen as a (normalized) measure of the level of heterogeneity, from an homogeneous organization to a pure heterogeneous one.

Let us take a population sized Z that is subdivided into two sub-populations with $Z^{[L_1]}$ and $Z^{[L_2]}$ individuals, respectively for each of the two available learning rules, $\mathcal{L} = \{L_1, L_2\}$. Having two strategies $\mathcal{S} = \{S_1, S_2\}$, but treating each sub-population distinctively, we will have the system configuration as $\boldsymbol{i} = \{i_{S_1}^{[L_1]}, i_{S_1}^{[L_2]}\}$, always bearing in mind that the configuration for the opposite strategy is given by $i_{S_2}^{[L]} = Z^{[L]} - i_{S_1}^{[L]}$, with $L \in \mathcal{L}$. The transition probabilities, which gives the probability that an agent A with strategy $S_A \in \mathcal{S}$ in the sub-population $L_A \in \mathcal{L}$ changes to a strategy $S_B \in \mathcal{S}$, both from the same sub-population L_A and $L_B \in \mathcal{L}$, with $L_B \neq L_A$, can all be written in terms of the following expression [41]:

$$T_{S_A \to S_B}^{[L_A]} = \frac{i_{S_A}^{[L_A]}}{Z} \left\{ \frac{i_{S_B}^{[L_A]}}{Z^{[L_A]} - 1 + (1-h) Z^{[L_B]}} \left(1 + e^{\beta^{[L_A]} (f_{S_A}^{[L_A]} - f_{S_B}^{[L_A]})} \right)^{-1} \right. \\ \left. + \frac{(1-h) i_{S_B}^{[L_B]}}{Z^{[L_A]} - 1 + (1-h) Z^{[L_B]}} \left(1 + e^{\beta^{[L_A]} (f_{S_A}^{[L_A]} - f_{S_B}^{[L_B]})} \right)^{-1} \right\} \tag{2.51}$$

in which it is visible how it replicates the definition of homophily.

Notice this equation could be generalized for more than two sub-populations, that is, for more than two different learning rules. For this, different homophilies should be defined for each different combination of interactions, as different sub-populations may have different influence over the others. In this case, the homophilies should be defined with explicit identification of the sub-populations involved. Supposing we have an individual from the sub-population L_A interacting with another individual from sub-population L_B, the homophily between the two different sub-populations may be defined similarly to the transition population, that is, as $h_{L_A \to L_B}$. Notice that the opposite homophily, $h_{L_B \to L_A}$, may not be the same, meaning the sub-population L_B does not have the same influence on L_A than L_A has on L_B. However this could bring a whole new dynamics to the populations evolution, we will focus on bi-directional homophilies, that is, we will assume $h_{L_A \to L_B} = h_{L_B \to L_A} \equiv h$ as the only general homophily.

From the transition probabilities, one may now build the gradient of selection, but now defined in a 2-dimensional space, as each direction is associated to a different learning rule. This means that, differently from homogeneous populations, we take each rule's gradient of selection, $G^{[L]}$ with $L \in \mathcal{L}$, as a single coordinate. We define this gradient of selection as $\nabla(\boldsymbol{i})$, which, for each configuration $\boldsymbol{i} = \{i_{S_1}^{[L_1]}, i_{S_1}^{[L_2]}\}$, may be given by:

$$\nabla(\boldsymbol{i}) \equiv \{G^{[L_1]}(\boldsymbol{i}), G^{[L_2]}(\boldsymbol{i})\} = \{T_+^{[L_1]}(\boldsymbol{i}) - T_-^{[L_1]}(\boldsymbol{i}), T_+^{[L_2]}(\boldsymbol{i}) - T_-^{[L_2]}(\boldsymbol{i})\} \tag{2.52}$$

Using this framework, one may now look for new internal equilibria and, with that, study these new and more complex dynamics in heterogeneous populations, and eventually retrieve some knowledge for further application in real-world networks. We will focus on studying the effects of different homophilies on the evolutionary dynamics of populations, from the homogeneous case to the pure heterogeneity case.

Just like previously described for the usual **SL** dynamics, both the homogeneous or heterogeneous layout of populations may be evaluated, in terms of cooperation maximization, through both the expected fraction of cooperation, EFC, or the group achievement, η_G, defined in the same reason as previous equations 2.34 and 2.35, respectively. Notice that in the heterogeneous case, having each sub-population distinctively separated, we may also compute the EFC for each sub-population, as we will see later on Chapter 5.

2.5 Final Notes

We have used Game Theory to describe interactions among individuals, which evolution in time will make rise the so-called Evolutionary Game Theory. When applying to Biology, scientists have formulated the Social Learning dynamics, intending to describe individuals' cooperative dynamics, although it is not enough to explain cooperative learning rule in societies. In this sense, we bring up two new different learning rules that possibly may help us better understand the existence of cooperation among rational individuals.

Along this chapter, we presented the mathematical tools that allow us to study the evolution of populations. We started by describing the whole social learning framework, that has been widely studied in the past years, followed by the formulations for both conformity and counterfactual reasoning, from a pairwise comparison with social learning. Regardless of the dynamic in the study, either for a single or a multiple learning rule population, through the birth-death process Markov chain previously described, one may characterize the system in its finite form. With the transition probabilities between two different states, we are able to compute both the stationary distribution and the (deterministic) gradient of selection. The first one, not only allow us to compute both the expected fraction of cooperation, EFC, and the group achievement, η_G, that evaluate the system in terms of cooperation maximization, but also gives us the average population configuration, that is, population composition averaged over time. The latter, on the other hand, allows us to evaluate the real population dynamics, giving us the most probable path and its fastness at each point of the configuration space.

Having all these foundations established, we have now conditions to perform different studies on the evolutionary dynamics of populations. We will begin with studies on analyzing the impacts of synchronism in the updating process, on Chapter 3, followed by a deep study of multiple learning rule populations dynamics, in both homogeneously and heterogeneously displayed communities, respective on Chapters 4 and 5.

Chapter 3

Synchronism and Asynchronism

In this chapter, we analyze and discuss the impact of different updating processes on the general cooperating dynamics for a finite population. More specifically, we will analyze the impacts on the stationary distribution and convergence of the dynamics along the spectrum of synchronism, from a completely asynchronous to a completely synchronous process. We start by developing the general formulation for the transition matrix, that will allow us to produce the results to be assessed later in the chapter.

3.1 Synchronism versus Asynchronism

In evolutionary games, individuals interact with one another several time steps through a given game, which, as we saw, is used as a metaphoric description of the interaction that is being studied. After each interaction session, or generation, some or all of the agents, depending on the update dynamics used, may update their strategies. A dynamics is said to by *synchronous* if all the agents in the population update their strategies simultaneously at each generation, that models a strong correlation of moments at which agents are updated. This is not the case of asynchronous dynamics where only some agents, possibly even just one, update their strategy at each step [46].

Perfect synchronism is an abstraction that assumes the existence of a global clock by which all individuals in the population time their actions. However, actions being strongly correlated does not imply they are perfectly timed. For instance, populations of *Pteroptyx malaccae* fireflies are able to synchronize their flashes so they occur approximately at the same time, although not perfectly simultaneous. Despite perfect synchronism being a concept that is far from being real, in a variety of scientific fields synchronization processes have been the most common way of modelling the update dynamics of real systems, even though this practice is very questionable [46]. Following this reasoning, even assuming perfect synchronization as an abstraction of reality, one may consider synchronization processes as a valid approximation of real simultaneous updating processes.

The most common alternative of synchronous updating is the sequential updating, that is a special case of asynchronism: at each generation, exactly one element is updated, which is the case of the birth-death process. Despite both synchronous and sequential updating being opposite ways to model the update dynamics of a system, most real dynamical systems, and biological ones in particular, actually lie between these two different extreme processes. Moreover different systems may have different synchrony rates [46]. This panoply of possibilities for updating processes allow us to define a *spectrum of synchrony*, which may characterize updating systems according to their level of synchronism, from a completely asynchronous to a perfectly synchronous process.

To understand the differences between different updating processes along the spectrum, let us start by building the general framework that will allow us to define some of the major tools to study population dynamics. More specifically, we will study the impact of intermediate synchronous processes on the stationary distribution. Notice, however, this whole framework is specifically built for a cooperation dynamics with only two strategies, C and D, and hence the system's configuration is reduced to the number of cooperators. For other more complex system's architectures, a generalization of this framework would be required.

3.2 The General Transition Matrix

The general transition matrix, that was previously described according to equation 2.20 (in the previous chapter), summarizes all the possible transition probabilities. However, and as mentioned, in most studies researchers adopt an asynchronous process, namely the birth-death process, that is, we assume that, at each time-step in discrete time, one individual only will proceed with its strategy revision. This would produce a tri-diagonal matrix, and, consequently, some of the major tools to study the population dynamics, such as the gradient of selection, could be defined in a very simple way. We know, however, this assumptions are, in many cases, far from reality and thus the need of building a general framework that describes any updating process along the spectrum of synchrony.

We start by defining the *number of revisions*, n_r, as the number of individuals that will revise their strategy on each time step. For sake of simplicity we will assume that n_r is a constant variable, although it could indeed follow a different distribution in time. For example, one could consider a system where n_r would follow a discrete Gaussian distribution around a given mean value μ_{n_r}, thus having the synchrony level as a new variable. Nevertheless, we will take n_r as constant. In this case, we define the updating process according to its number of revisions, that is, for a given n_r we say the system's evolutionary dynamics evolves according to a n_r-step process, that is, a process that is on the n_r-th level of the synchrony scale. Some particular cases of this are the one-step process, or birth-death process, characterized by $n_r = 1$, and the Z-step process, also known as the *Wright-Fisher process*, characterized by $n_r = Z$, which is the same as a perfectly synchronous process.

As previously seen, when adopting a birth-death process, the only possible transitions are $\mathcal{T}^{-1}$, $\mathcal{T}^{0}$ and $\mathcal{T}^{+1}$, that is, $\mathcal{T}^{n}$ with $n \in \{-1, 0, 1\}$, and consequently, our matrix $\boldsymbol{\mathcal{T}}$ becomes tri-diagonal. Following this reasoning, one may generalize the transition probabilities for every value of n_r as $\mathcal{T}^{n}$ with $n \in \{-n_r, \ldots, 0, \ldots, n_r\}$, which may be summarized in a transition matrix with the $2n_r + 1$ central diagonals, as shown in the matrix bellow:

$$\boldsymbol{\mathcal{T}} = \left\{\mathcal{T}^{j-i}(i-1)\right\}_{i=1,j=1}^{Z+1,Z+1} = \begin{bmatrix} \mathcal{T}^{0} & \mathcal{T}^{+1} & \ldots & \mathcal{T}^{+n_r} & 0 & \ldots & 0 & 0 \\ \mathcal{T}^{-1} & \ddots & & & \ddots & & \ddots & 0 \\ \vdots & \ddots & \ddots & & & \ddots & & \vdots \\ \mathcal{T}^{-n_r} & & \ddots & \ddots & & & \ddots & 0 \\ 0 & \ddots & & \ddots & \ddots & & & \mathcal{T}^{+n_r} \\ \vdots & & \ddots & & \ddots & \ddots & & \vdots \\ 0 & & & \ddots & & \ddots & \ddots & \mathcal{T}^{+1} \\ 0 & 0 & \ldots & 0 & \mathcal{T}^{-n_r} & \ldots & \mathcal{T}^{-1} & \mathcal{T}^{0} \end{bmatrix} \tag{3.1}$$

where the green, red and gray regions represent the probabilities to increase, decrease and maintain, respectively, the number of cooperators. The remaining regions are null, that is, are impossible to reach.

The major challenge is now trying to understand how to obtain the values for each of the transition probabilities. For that, we will have to take into account all the interactions that are possible at each generation. For instance, if we have $n_r = 2$, there are $n_r^2 = 4$ possible scenarios: chose two cooperators, chose two defectors, chose a cooperator and then a defector, and the opposite. Notice that the order individuals are chosen is important as it will have an impact on the effective population from which the probabilities are computed. As things get more complex now, it is necessary to build a general framework, that works for any system's configuration.

3.2.1 The Transition Probabilities' Algorithm

While studying cooperation dynamics, consider a finite population with size Z, where only two strategies are available, $\mathcal{S} = \{C, D\}$. For the sake of simplicity, we assume the only available learning rule is social learning. To generally define each the n-th transition probability, $\mathcal{T}^n$, one may follow four different steps:

1. Firstly, we choose n_r different individuals that will interact. Notice that the individuals are allowed to interact with any of the remaining, including to any others from the n_r chosen individuals, expect the self.
2. For each revision $i \in \{1, \ldots, n_r\}$, the system varies its number of cooperators by $\boldsymbol{v}_i$. For each possible variation and for each strategy, we will compute the individual transition probabilities, specified for cooperation dynamics. All the n_r revisions will occur sequentially and each sequence is unique.
3. For each value of n, we get the subset of all the possible sequences of revisions such that the sum of all variations produces a transition of n in the system.
4. Finally, we multiply all transition probabilities for each sequence and sum over all possible combinations in the subset that corresponds to n. This way, we will be able to obtain the transition probability $\mathcal{T}^n$.

Each of the points will be explained in detail soon after. After having all values of $\mathcal{T}^n$, we are able to compute the transition matrix, and hence the stationary distribution.

3.2.2 Developing the Framework

We start by generally defining the *individual transition probability*, $T_{\boldsymbol{v}}^S$, as the probability that the systems varies its configuration by $\boldsymbol{v}$ when picking an individual following strategy $S \in \mathcal{S}$. In other words, it is the probability that a general system with a certain configuration $\boldsymbol{i}$, at a certain time t_a, varies to a configuration $\boldsymbol{i'} = \boldsymbol{i} + \boldsymbol{v}$, at a time t_{a+1}, when a randomly chosen individual follows strategy S. Notice that the variation is a vector $\boldsymbol{v} = \{v_1, \ldots, v_k, \ldots, v_{s+1}\}$, with the same size of the non-normalized configuration $\boldsymbol{i}$, as the variation may not be regular. However, by considering the system as the equivalent to a closed system in physics, the variation's norm must be null, that is $|\boldsymbol{v}| = 0$, and, consequently, this allows us to normalize the variation vector as $\boldsymbol{v} = \{v_1, \ldots, v_k, \ldots, v_s\}$ with $v_{s+1} = -\sum_{k=1}^{s} v_k$.

Specifying for cooperation in its simplest case, with $\mathcal{S} = \{C, D\}$, we will have $\boldsymbol{i} = \{i_C, i_D\}$, which respectively corresponds to the number of cooperators and the number of defectors. As we previously saw in Chapter 2, we will only focus on the normalized version of $\boldsymbol{i}$ and $\boldsymbol{v}$, for matters of simplification, and so we we have $\boldsymbol{i} = \{i_C\} = \{k\}$. From any two-individual interaction only three different outcomes are possible: a cooperator switches its strategy, and so $\boldsymbol{v} = \{-1\}$; a defector switches its strategy, and thus $\boldsymbol{v} = \{+1\}$; or no strategy switching occurs, where $\boldsymbol{v} = \{0\}$. In this latter case, one must also include the same-strategy individuals' interactions, as we assume individuals only change their strategy whenever facing an individual following a different strategy. Naturally, if a cooperator (defector) is chosen to interact with another individual, it will not be possible for it to increase (decrease) the number of cooperators k, as this is a binary variable.

Having this, the most basic individual transition probabilities, for any $S \in \{C, D\}$ and any $v \in \{-1, 0, 1\}$, may be given similarly to equations 2.21 and 2.22 as:

$$T_{-1}^{C}(k) = x_{C}^{(Z)} \cdot x_{D}^{(Z-1)} \cdot p_{C\to D}(k) \qquad T_{-1}^{D}(k) = 0 \tag{3.2}$$

$$T_{+1}^{C}(k) = 0 \qquad T_{+1}^{D}(k) = x_{D}^{(Z)} \cdot x_{C}^{(Z-1)} \cdot p_{D\to C}(k) \tag{3.3}$$

$$T_{0}^{C}(k) = x_{C}^{(Z)} \left(x_{C}^{(Z-1)} + x_{D}^{(Z-1)} \cdot (1 - p_{C\to D}(k)) \right) \quad T_{0}^{D}(k) = x_{D}^{(Z)} \left(x_{D}^{(Z-1)} + x_{C}^{(Z-1)} \cdot (1 - p_{D\to C}(k)) \right) \tag{3.4}$$

where we assume, for now, that all individuals follow the **SL** rule. Notice that, in this form, we have the previously defined simpler equations as $T_{-} = T_{-1}^{C}$ and $T_{+} = T_{+1}^{D}$, and thus one may rewrite equations 3.4 as a result of the normalization $T_0 \equiv T_0^C = T_0^D = 1 - T_{-1}^{C} - T_{+1}^{D}$. However, having a number of revisions higher than one, this normalization is no longer possible.

Having more than one individual revising their strategy, the functions above get more complex. We now must take into account the number of available individuals for each strategy, and for the population itself. For instance, let us suppose we will proceed with two revision processes. We pick a first individual that will interact with another one, and for that interactions the possible transitions' probabilities may be computed according to equations 3.2 and 3.3. Next, the chose a second individual to proceed similarly, although now one must be aware that the first individual was already chosen. This means that, as revisions are being processed, one must update the number of individuals that are available to get picked from, not only for each strategy but for the whole population. And this reasoning must be applied successively until we reach the n_r-th revision.

To solve this issue, we define u_Z as the update for the available population size and u_{i_C} (or u_k to simplify) as the update for the available cooperators. Previously in subsection 2.3.1, we defined the fraction of individuals following strategy S as a function of Z as $x_{C/D}^{(Z)} \equiv x_{C/D}^{(Z)}(k) = \frac{i_{C/D}}{Z}$. Now, we shall redefine it as $x_{C/D}^{(Z,u_Z)}(k, u_k) = \frac{i_{C/D} - u_{i_{C/D}}}{Z - u_Z}$. Simplifying things, and by normalization, we will have:

$$x_{C}^{(Z,u_Z)}(k, u_k) = \frac{k - u_k}{Z - u_Z} \qquad x_{D}^{(Z,u_Z)}(k, u_k) = \frac{(Z - u_Z) - (k - u_k)}{Z - u_Z} \tag{3.5}$$

As we mentioned previously, individuals are allowed to interact with any others, including the ones picked for revision. This means the second term on the transition probabilities 3.2, 3.3 and 3.4 remain unchanged, that is, with no updates. Having this in mind, and now using the definition 3.5, we may redefine the transition probabilities as:

$$T_{-1}^{C}(k, Z, u_k, u_Z) = x_{C}^{(Z,u_Z)}(k, u_k) \cdot x_{D}^{(Z-1,0)}(k, 0) \cdot p_{C\to D}(k) \tag{3.6}$$

$$T_{+1}^{D}(k, Z, u_k, u_Z) = x_{D}^{(Z,u_Z)}(k, u_k) \cdot x_{C}^{(Z-1,0)}(k, 0) \cdot p_{D\to C}(k) \tag{3.7}$$

$$T_{0}^{C}(k, Z, u_k, u_Z) = x_{C}^{(Z,u_Z)}(k, u_k) \left(x_{C}^{(Z-1,0)}(k, 0) + x_{D}^{(Z-1,0)}(k, 0) \cdot (1 - p_{C\to D}(k)) \right) \tag{3.8}$$

$$T_{0}^{D}(k, Z, u_k, u_Z) = x_{D}^{(Z,u_Z)}(k, u_k) \left(x_{D}^{(Z-1,0)}(k, 0) + x_{C}^{(Z-1,0)}(k, 0) \cdot (1 - p_{D\to C}(k)) \right) \tag{3.9}$$

where both T_{+1}^{C} and T_{-1}^{D} probabilities were not considered already since they are are null, as this scenarios are unrealistic in this specific setup, as previously discussed in this subsection.

One may now group these transition probabilities all together into the *set of transition probabilities*, that we will be temporarily designated as Q, that is defined as the set of functions:

$$Q = \{T_{-1}^{C}, T_{+1}^{D}, T_{0}^{C}, T_{0}^{D}\} \tag{3.10}$$

which will be the basis for computing all the possible combinations of transition probabilities.

At each generation, a certain combination of revisions will occur in a specific order and each combination defines an unique possibility. It is important to notice that the order of the revisions is important, as the updates on Z and k will depend on that. Having defined the set of the possible transition probabilities, Q, one may now compute the set of all the possible combinations of transition probabilities, where each combination directly defines a sequence of revisions, as obvious. This way, we define the *set of sequences of revisions*, $\mathcal{R}^{n_r}$, as a function of n_r, as follows:

$$\mathcal{R}^{n_r} = \underbrace{Q \times Q \times \cdots \times Q}_{n_r \text{ times}} \tag{3.11}$$

As the size of P is 4, the total number of terms of the set $\mathcal{R}^{n_r}$ is 4^{n_r}, and hence we may rewrite $\mathcal{R}^{n_r}$ as:

$$\mathcal{R}^{n_r} = \{R_1, \ldots, R_i, \ldots, R_{4^{n_r}}\} \tag{3.12}$$

where each R_i defines a sequence of revisions $R_i = \{T^{S_1}_{v_1(i)}, \ldots, T^{S_j}_{v_j(i)}, \ldots, T^{S_{n_r}}_{v_{n_r}(i)}\}$, with $i \in \{1, \ldots, 4^{n_r}\}$. Notice that each combination is independent and its i index does not have any implication on the sequence of transition probabilities, being merely indicative and will be helpful as we will see later on.

As mentioned, each sequence of revisions defines an unique situation, that produces a specific variation on the system's configuration. For instance, a generic sequence of revisions such as $R = \{T^{S_1}_{v_1}, \ldots, T^{S_j}_{v_j}, \ldots, T^{S_{n_r}}_{v_{n_r}}\}$ will modify the number of cooperators by $n = \sum_j v_j$, that is, if this sequence of revisions occur, the system will move from a state k to a state $k + n$. Having this in attention, it is now trivial how to get the subset of sequences that will produce a transition n in the system, so one can compute the system's transition probability $\mathcal{T}^n$ afterwards. In fact, to accomplish this, we just have to get all the sequence of transition probabilities such that the sum of their variations is equal to n. Mathematically speaking, we have the set of sequences of revisions that produces a transition n as the subset $\mathcal{R}^n \in \mathcal{R}^{n_r}$, defined as:

$$\mathcal{R}^n = \left\{ R_i \in \mathcal{R}^{n_r} : \sum_{j=1}^{n_r} v_j = n \mid T^{S_j}_{v_j(i)} \in R_i \right\} \tag{3.13}$$

Each revision is an independent event. This means that the probability of a certain sequence of revisions may be obtained simply by the multiplication of the probabilities for each revision. In other words, the probability of $R \in \mathcal{R}^n$, $P(R)$, may be given by the successive multiplication of all $T^{S_j}_{v_j(i)} \in R_i$, where at each multiplication, the number of available individuals is sequentially decreased by one. This way, we may write down:

$$P(R_i) = \prod_{j=1}^{n_r} T^{S_j}_{v_j(i)}(k, Z, u_k, j-1) \tag{3.14}$$

Regarding the update on the number of cooperators, we will only decrease then number of available cooperators whenever a cooperator was picked in the previous revision. In other words, we will only increase u_k if the strategy of the player in the sequence's previous revision was C. Formally speaking, we may redefine $P(R)$ as:

$$P(R_i) = \prod_{j=1}^{n_r} T^{S_j}_{v_j(i)}(k, Z, u_k, j-1) \ , \ \text{ with } u_k = \begin{cases} 0 & j = 1 \\ u_k & S_{j-1} = D \\ u_k + 1 & S_{j-1} = C \end{cases} \tag{3.15}$$

Having the probability for each sequence of revisions, and noticing that each sequence is independent, one may now obtain the system's n-th transition probability as $\mathcal{T}^n = P(\mathcal{R}^n)$, which is equivalent to summing up the probabilities for all the elements of $\mathcal{R}^n$. Formally speaking, this is:

$$\mathcal{T}^n = \sum_i P(R_i) \tag{3.16}$$

For a given value of n_r, the possible values of n stand in the interval $[-n_r; n_r]$. Following combinatorics, the total number of terms for each $\mathcal{R}^n$ will follow the same order as the $2n_r$-th line of the Pascal's Triangle. This means each $\mathcal{R}^n$ have a size of $\binom{2n_r}{n_r+n}$. As an example, for the lowest possible values we have:

$n_r = 1$ $\quad n = \{-1, 0, +1\}$ $\quad$ nº of terms: $\{1, 2, 1\}$

$n_r = 2$ $\quad n = \{-2, -1, 0, +1, +2\}$ $\quad$ nº of terms: $\{1, 4, 6, 4, 1\}$

$n_r = 3$ $\quad n = \{-3, -2, -1, 0, +1, +2, +3\}$ $\quad$ nº of terms: $\{1, 6, 15, 20, 15, 6, 1\}$

$n_r = 4$ $\quad n = \{-4, -3, -2, -1, 0, +1, +2, +3, +4\}$ $\quad$ nº of terms: $\{1, 8, 28, 56, 70, 56, 28, 8, 1\}$

$n_r = n_r$ $\quad n = \{-n_r, \ldots, 0, \ldots, +n_r\}$ $\quad$ nº of terms: $\left\{\binom{2n_r}{0}, \ldots, \binom{2n_r}{n_r+n}, \ldots, \binom{2n_r}{2n_r}\right\}$

Finally, we are able to define the general equation for the system's transition probability as:

$$\boxed{\mathcal{T}^n = \sum_{i=1}^{\binom{2n_r}{n_r+n}} \prod_{j=1}^{n_r} T_{v_j(i)}^{S_j}(k, Z, u_k, j-1)\ , \ \text{ with } u_k = \begin{cases} 0 & j = 1 \\ u_k & S_{j-1} = D \\ u_k + 1 & S_{j-1} = C \end{cases}} \tag{3.17}$$

where $T_{v_j(i)}^{S_j} \in R_i \in \mathcal{R}^n$. From this, the transition matrix becomes trivial to compute, as show in the matrix 3.1.

The above formula is quite complex to compute. As the number of revisions increases, computing $\mathcal{T}^n$ quickly becomes computationally extremely extensive, as we will have a very large number of sequences to compute. Hence, we find ourselves in this limiting situation, where on one hand we must have a large population size, but on the other hand, we are not able to study scenarios where the number of revisions is high. For further work, it would be helpful to find a formulation that accomplishes the results from equation 3.17 in a much more simple way. Nevertheless, we will proceed to the study of the impact of increasing synchronism level in the updating process.

3.3 Synchronism in Social Learning

As previously mentioned in section 2.3.3, the stationary distribution is propitious to the formation of two peaks on both extremes of the fraction of cooperators, due to the absorption characteristics of the Markov chain that defines the system. To contrary this issue, we consider the updating process to be innovative, instead of non-innovative, and hence we introduce a small mutation rate μ, just like in equations 2.23 and 2.24. Applying the same reasoning to the previously defined individual transition probabilities, equations 3.6-3.9, we will be able to obtain:

$${}^{\mu}T_{-1}^{C}(k, Z, u_k, u_Z) = (1-\mu)\, T_{-1}^{C}(k, Z, u_k, u_Z) + \mu\, x_C^{(Z, u_Z)}(k, u_k) \tag{3.18}$$

$${}^{\mu}T_{+1}^{D}(k, Z, u_k, u_Z) = (1-\mu)\, T_{+1}^{D}(k, Z, u_k, u_Z) + \mu\, x_D^{(Z, u_Z)}(k, u_k) \tag{3.19}$$

$${}^{\mu}T_{0}^{C/D}(k, Z, u_k, u_Z) = (1-\mu)\, T_{0}^{C/D}(k, Z, u_k, u_Z) \tag{3.20}$$

where the probabilities with $v = 0$ only have one term due to the normalization process. More specifically, we have that the sum of all transition probabilities above written is one, as one should expect.

We are now in conditions to proceed to the analysis of the impact of increasing synchronism on the updating processes along the spectrum of synchrony. We will be building up the transition matrix for some different values of n_r, and from that we will be obtaining the stationary distribution for the four different social games, previously described in section 2.1.2.

Let us suppose we have a population of social learners with a size of $Z = 50$, with a certain mutation rate. It was experimentally verified that, for this population size, having $\mu \sim \mathcal{O}\left(\frac{1}{Z^2}\right)$ would still lead to the formation of two peaks in the stationary distribution, meaning the mutation rate was low enough to be negligible and hence it becomes unpractical to make a proper evaluation of this distribution. We also verified that having $\mu \sim \mathcal{O}\left(\frac{1}{Z}\right)$ would be more suitable regarding the system's stationary distribution analysis, as it is low enough to remove the system's absorption states and high enough to not corrupt the game dynamics, and for this reason, we will take $\mu = \frac{1}{50} = 2\%$.

In the figure below we present 4 panels, one for each of the social games. For all these, we impose the condition $1 > 0.75 > 0.25 > 0$ for the order of the R, S, T, P variables. For instance, for the **SG**, as we have $T > R > S > P$, we get $T = 1$, $R = 0.75$, $S = 0.25$ and $P = 0$. The same reasoning will be applied for the other games. To simplify, having an intensity of selection of $\beta = 1.0$, and for all the numbers of revisions $n_r = \{1, 3, 5, 7\}$, we were able to obtain the stationary distributions, presented below in the Figure 3.1.

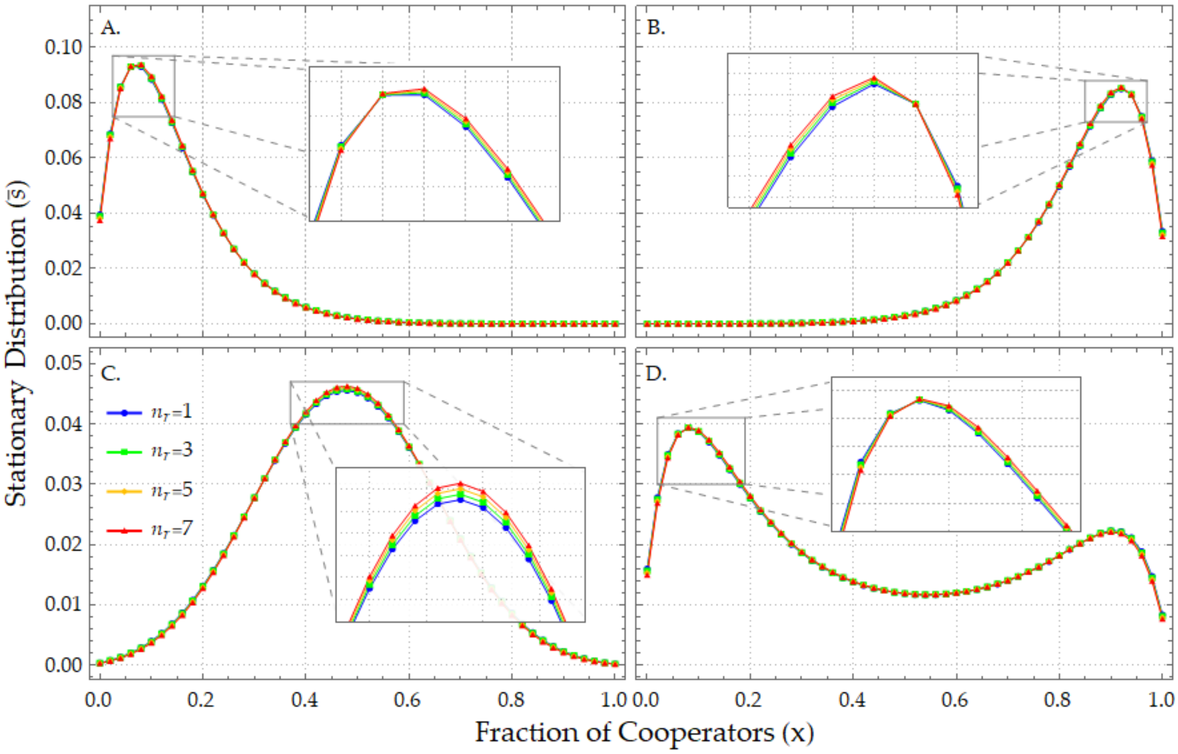

Figure 3.1: The effects of progressive increasing levels of synchronization on a well-mixed population of social learners. We present the stationary distribution for $n_r = \{1, 3, 5, 7\}$, in four different 2-person social games, specifically, the **PD**, **HG**, **SG** and **SH**, respectively on panels from **A** to **D**. It is noticeable that, as we increase the level in the spectrum of synchrony, the stationary distribution is getting further away from its original asynchronous form, even though this variation is very small. This insight is independent on the game, as the results is visible in all panels.

As previously mentioned, as we increase the level of synchronism in the synchrony spectrum, the computational process becomes more and more extensive, and due to computational power limits, we were not able to obtain the transition matrix for values above $n_r = 7$ in a feasible time. Nevertheless, from the results above shown we will try to get as much information as possible, although always being aware it may be insufficient to some conclusions.

At first sight, it is noticeable how small is the impact of a small increase on the synchronization level. From the graphs above one may infer how similar the stationary distribution curves are, only presenting a progressive deviation relative to the previous curve, starting from the one-step process curve and moving further and further away as we increase the number of revisions.

For all cases with exception of panel **D.**, the $n_r = 1$ curve is peak-shaped, and hence, as previously discussed in section 2.3.3, we might be on conditions to perform a study on the evolution of the expected fraction of cooperators, as a function of the number of revisions. One may take, for instance, the snowdrift game and, for each the available stationary distributions, that is, for each $n_r = \{1, 3, 5, 7\}$, we compute the EFC according to equation 2.34, as we intend to obtain the relation $EFC(n_r)$ and find any possible trend. Results are shown below in the Figure 3.2.

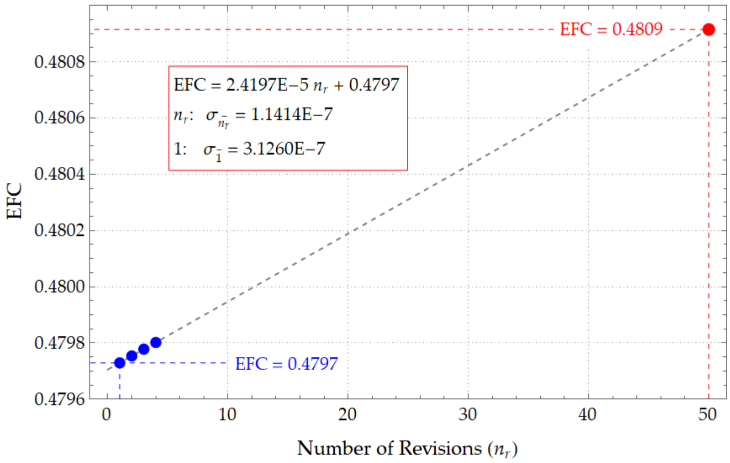

Figure 3.2: The evolution of the expected fraction of cooperators as a function of the number of revisions, for the 2-Person Snowdrift game. If the trend follows the same patter as for the initial points, we could expect a linear variation with a positive slope, that, even though is very small, would be indicative of an progressive increase of the EFC. The red dot represents the predicted value if the update process was perfectly synchronous, that is, for $n_r = Z$, while the blue dots correspond to the values of EFC for the previous displayed stationary distributions.

As the stationary distribution only slightly changes with increasing n_r, it is predictable that the expected fraction of cooperators evolves with very subtle changes. In fact, in Figure 3.2 it is evident how close are the EFC values for the available previously computed stationary distributions, the differences between them being almost negligible.

Even though the number of computed points is very small, it is already noticeable a certain pattern in the evolution of EFC, where it is apparent a linear relation with a positive slope. As that, in order to find a forecast for EFC for higher values of n_r, a linear regression was performed in the four available points (in blue in the figure) so we obtain the relation $EFC(n_r)$. As expected, the regression slope is extremely low, in the order of $\mathcal{O}(10^{-5})$, indicating that a large variation of n_r has a very little impact on the EFC. Moreover, using the regression model, one may compute the predicted value for the maximum possible number of revisions, $n_r = Z = 50$, and obtain a value that corresponds to an increase of at most $\approx 0.25\%$ of the EFC, when compared to the one-step process. This clearly indicates that, as we progressively increase the level of synchronism in the spectrum of synchrony, EFC increases almost negligibly.

Notice these results were obtained specifically for the 2-person **SG**, which may question any try of generalization, even though similar results can be obtained for the remaining games (to which corresponds a peak-shaped stationary distribution). Nevertheless, we will take into consideration the fact these insights were specific for a single example. To better support any conclusions, we will investigate other cases, namely, we will see the impact of synchronism in N-person games and analyze their stationary distribution with the help of some other different tools.

Results above shown for 2-person games are very similar to the ones obtained for all the N-person games, previously described in section 2.1.3. In the same way as previously done, in the figure below we present 4 panels, one representing each of the N-person social games. More expressly, from panels **A** to **D**, we have the **NSG** with $(N, M, b, c) = (10, 5, 1.0, 0.5)$, **NSH** with $(N, M, F, c) = (10, 5, 10, 0.25)$, **PGG** with $(N, F, c) = (10, 10, 0.25)$, **CRD** with $(N, M, b, c, r) = (10, 5, 1.0, 0.15, 0.6)$. The choice of these values was based on the search for a wide variety of the population dynamics, as we intend to generalize the conclusions.

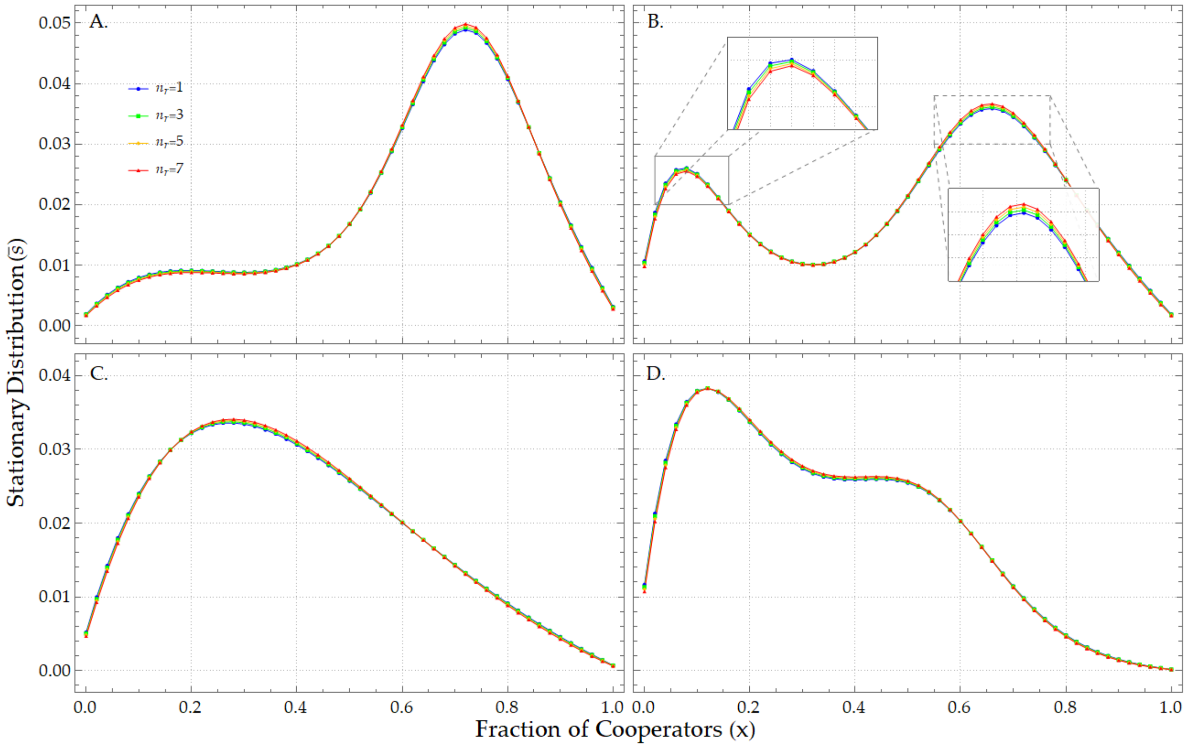

Figure 3.3: The effects of progressive increasing levels of synchronization on well-mixed population of social learners. We present the stationary distribution for $n_r = \{1, 3, 5, 7\}$, in four different N-person social games, specifically, the **NSG**, **NSH**, **PGG** and **CRD**, respectively on panels from **A** to **D**. Once again, one may notice that, as we increase the level in the spectrum of synchrony, the stationary distribution is getting further away from its original asynchronous form, even though this variation is very small. This insight is independent on the game, as the results is visible in all panels.

For all the results from both Figures 3.1 and 3.3 one may notice something very interesting: in some intervals in x, the curves relative to more synchronous processes stand above the asynchronous process' curve, while for other intervals they stand below. These insights are very visible, for instance, in the mini zoomed plots in panel **B**. As that, one should expect some points on which all the curves touch, which define values for $\bar{s}$ that are completely independent of the synchronism level. This may be indicative that the transformations resulting from increasing synchrony level are more like fluctuations around the asynchronous process' curve than a translation. Attending that any stationary distribution should be normalized to 1, that is $\sum_x \bar{s}(x) = 1$, this result shouldn't be surprising: with increasing n_r, if in some points the stationary positively deviates from the asynchronism curve, it must negatively deviate in some other points, such that the integral difference between both curves is null.

Another important quantity to measure the probability to achieve success, in terms of cooperation, is the group achievement. Following the definition in equation 2.35, and being aware that it is applicable for all N-person games in which $M > 0$ (we will see the effects for $M = 0$), one may compute η_G evolution as a function of the number of revisions. If any change occurs, and following the same trend hitherto seen, one should expect it to be very slight.

Keeping the previous game's configuration, the obtained results are shown in the Figure 3.4 below.

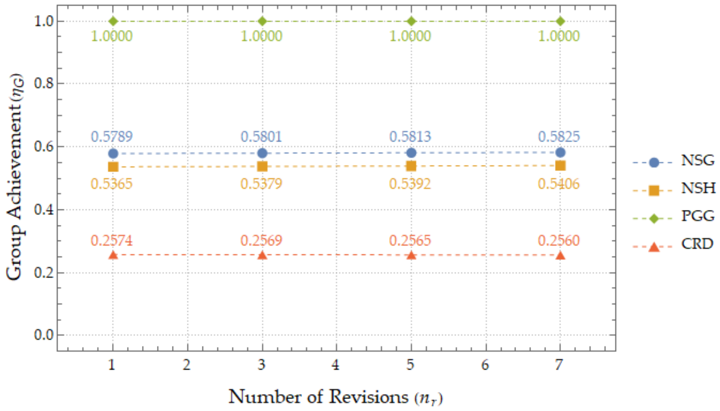

Figure 3.4: Group achievement as a function of the number of revisions, for all the studied N-person games. It is noticeable an almost constant line, which indicates the progressive increasing of the synchronism level does not have a very significant effect on the group achievement. Notice that, for the **PGG**, the η_G is always maximum (one), due to the fact the threshold M is null.

Firstly, for the **PGG**, in its **NPD** description, we verify a group achievement with constant value of 1 regardless of the number of revisions. This is due to the fact that we define the null threshold of $M = 0$, and hence the multivariate hypergeometric sampling takes into account all the possible cases, and thus the sum becomes one.

For the other N-person games, as expected, one may infer how small are the effects of increasing level of synchronism on the evolution of the group achievement. Although almost negligible, we notice an increase of η_G for both **NSG** and **NSH**, while for the **CRD** we notice a slight decrease. Before take any conclusions, it is important to be aware about the formulation taken on each game's description. Being highly configurable, many different outcomes are possible for a certain game, and, as such, for one same game it is possible to verify either synchronism 'positive and negative effects. This way, we are tempted to assume the existence of a correlation between the synchronism effect and the game's configuration.

To confirm these insights, for different game setups we compute η_G for both $n_r = 1$ and $n_r = 3$, from which we calculate the difference $\eta_G(3) - \eta_G(1)$. An increase of the synchrony level, from $n_r = 1$ to $n_r = 3$, affects positively the group achievement whenever this difference is positive, and affects negatively otherwise. As we previously saw in Figure 3.4, the evolution of $\eta_G(n_r)$ seems to be uniform with n_r, and hence we will assume that, from the difference $\eta_G(3) - \eta_G(1)$, one may conclude about the whole $\eta_G(n_r)$ evolution. Therefore, for both **NSG** and **CRD**, we vary some of the quantities that characterize each game, more specifically, we vary the ratios c/b and M/N, for the **NSG**, and r and M/N for the **CRD**. Finally, for each combination of values we compute the difference $\eta_G(3) - \eta_G(1)$ as an indicative of the effects of synchronism. The results are shown bellow, in Figure 3.5.

The previous made insights look valid: there is in fact a correlation between the game's setup and the synchronism effects. In some regions in the game's setup space (for instance, in the **NSG** we have the (N, M, b, c)-space), increasing the level on synchronism along the spectrum of synchrony produces a positive effect on the probability to achieve success, while in other regions the opposite occurs. Between these two, one may find a region on the effects of synchronism are null, meaning in some cases the group achievement is completely independent of the synchrony level on the spectrum. Generally, we may conclude that an increase of the synchrony level may or may not be beneficial to achieving success, depending on the game's setup. Not wanting to compromise the validation of the results, attending to the very small magnitude of those values, and due to the increasing complexity with increasing n_r, one must be aware of the possible computational errors associated to all the required calculations.

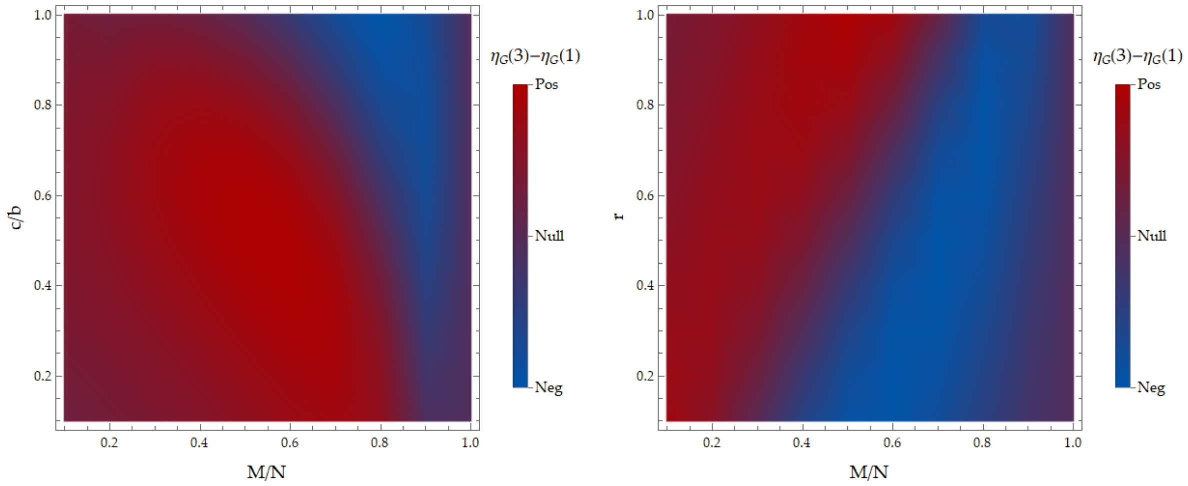

(a) N-Person Snowdrift Game

(b) Collective Risk Dilemma

Figure 3.5: Synchronism effects on η_G as a function of the game's configurations. For the **NSG**, it is clear how the effects of synchronism depend on the game's configuration, more specifically, being mostly negative for higher values of M/N, while positive in the remaining regions. For the **CRD**, the higher the risk, the less likely it is for synchronism to produce an negative effect.

3.3.1 Fixation Probability and Fixation Times

Another important determinant of the dynamics is given by the probabilities of fixation, that looks forward to answer the following question: if a mutation leads to a new strategy, how likely is it that this individual takes over the entire population? [44] In the previous chapter, in section 2.3.2, we explicitly present the formula for the fixation probability, ϕ_i, for i of cooperators that invade the population. However, as with fixation times, these expressions are only valid for the birth-death process, and thus one need to find a generalized form to compute these quantities.

Following the reasoning in [44], let us consider the transition matrix of the discrete-time Markov chain as $\boldsymbol{\mathcal{T}}_{s\times s}$, with at least one absorbing state, where s is the total number of states. In our cooperation dynamics case, as previously discussed, we will have two absorbing states, for both $k = 0$ and $k = Z$. After that, we renumber the states such that the t transient states are first and the a absorbing states are last, where $t + a = s$, and, this way, the transition matrix is said to be in its canonical form:

$$\boldsymbol{\mathcal{T}}_{s\times s} = \begin{bmatrix} \boldsymbol{Q}_{t\times t} & \boldsymbol{R}_{t\times a} \\ \boldsymbol{0}_{a\times t} & \boldsymbol{I}_{a\times a} \end{bmatrix} \tag{3.21}$$

As transitions are not possible from absorbing states to transient states, the lower left block of the matrix is null. Once absorbed, the system will stay there forever, hence the lower right block is the identity matrix. From this, we may now compute the fundamental matrix of the Markov chain as:

$$\boldsymbol{F} = \sum_{n=0}^{\infty} \boldsymbol{Q}^n = (\boldsymbol{I} - \boldsymbol{Q})^{-1} \tag{3.22}$$

which multiplied by the block $\boldsymbol{R}$ provides both the fixation and extinction probabilities, together as:

$$\boldsymbol{\Phi} = \boldsymbol{F} \cdot \boldsymbol{R} \tag{3.23}$$

Both extinction and fixation probabilities may be specified as the columns of $\boldsymbol{\Phi}$, respectively, as $\boldsymbol{\Phi}_i^1$ and $\boldsymbol{\Phi}_i^2$, for any number of cooperators $i \in \{1, \ldots, Z-1\}$. For the extreme values of i, that is, for the absorbing states, we follow the definition of fixation and extinction and we have:

$$\mathbf{\Phi}_0^1 = 1 \qquad \mathbf{\Phi}_Z^1 = 0 \qquad \mathbf{\Phi}_0^2 = 0 \qquad \mathbf{\Phi}_Z^2 = 1 \tag{3.24}$$

To assess the total time the process spends before absorption, we look at the so-called unconditional fixation time, which we define as τ_j. It is said to be unconditional since it is not sensitive to which of the absorption states it reaches. It is independent of the strategy and it may be given by:

$$\tau_i = \sum_{j=1}^{Z-1} \boldsymbol{F}_{i,j} \tag{3.25}$$

For each the absorbing states $k = 0$ and $k = Z$ we associate an index $A = 1$ and $A = 2$, respectively. Contrary to τ_i, the conditional fixation time depends on the strategy and, as that, we define:

$$\tau_i^A = \sum_{j=1}^{Z-1} \left(\frac{\Phi_j^A}{\Phi_i^A} \boldsymbol{F}_{i,j} \right) \tag{3.26}$$

For some clarification, in this case, $A = 1$ ($k = 0$) is the defectors absorbing state, while $A = 2$ ($k = Z$) is the cooperators absorbing state. In short, each absorbing state is associated to the strategies' monomorphic state.

To verify the impact of synchronism in these measures, we start by computing the fixation probabilities for the snowdrift game, in both 2-person and N-person versions. In specific, we will take $(R, S, T, P) = (0.75, 0.25, 1.0, 0.0)$ for **SG** and, as before, we take $(N, M, b, c) = (10, 5, 1.0, 0.5)$ for the **NSG**. Following the trend of results obtained so far, with increasing n_r one should expect only a very slight change on fixation probability curve shape, compared to the asynchronous curve. Attending to the normalization of $\mathbf{\Phi}_i^A$, these changes will occur in the form of fluctuations and not translations, just like we saw for the stationary distribution. These predictions go along with the results obtain, as shown in the Figure 3.6 below.

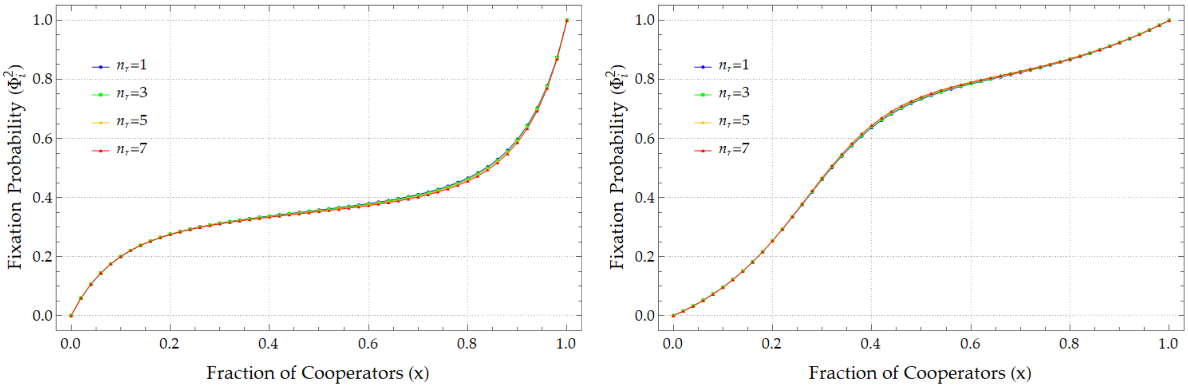

(a) 2-Person Snowdrift Game

(b) N-Person Snowdrift Game

Figure 3.6: Fixation probabilities as a function of n_r, for both **SG** and **NSG**. Once again, it is clear how small is the impact of increasing synchrony level on the fixation probability, in either the cases. Attending to the normalization of the fixation probability, the curves for higher n_r correspond to fluctuations around the asynchronism curve.

Regarding the fixation times, as we increase the number of revisions, it would be expectable a faster convergence to each of the absorbing states, regardless of the dynamics' complexity. Let us suppose an one-step process where one defector changes its strategy to cooperation in a first generation. In the next generation, the same happens, and hence in the two generations the system moved from k to $k+2$. If, on the other hand, we have $n_r = 2$, we have the possibility to produce such a result in only one generation. Generalizing this reasoning, one may expect the convergence time to decrease linearly with increasing number of revisions. This way, instead of directly computing both τ_i and τ_i^A with $a \in \{1, 2\}$, we will compute these quantities multiplied by the number of revisions, that is, $\tau_i \cdot n_r$ and $\tau_i^A \cdot n_r$, and so obtaining an average fixation time for each revision. This way, we may properly investigate if synchronism really affects the systems' convergence time.

In this reasoning, and for the same games as for the fixation probabilities before, we compute both the average unconditional and conditional fixation times, $\tau_i \cdot n_r$ and $\tau_i^A \cdot n_r$. The results are shown below in Figure 3.7.

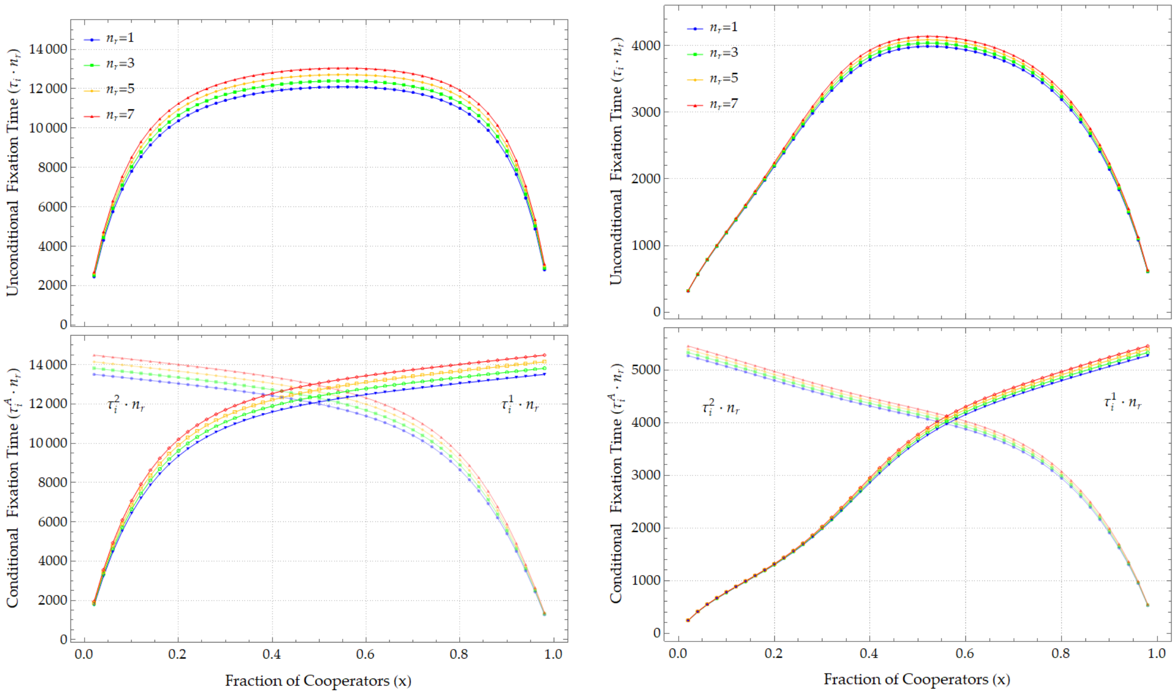

(a) 2-Person Snowdrift Game

(b) N-Person Snowdrift Game

Figure 3.7: Average unconditional and conditional fixation times as a function of n_r, for both **SG** and **NSG**. In the first case (the graphics on the left), the curves for all different n_r are further away from each other when compared to the **NSG**, which may be due to the fact the magnitude of the time values are much higher, possibly from computational errors.

In both cases, we verify the average time curves are very similar in shape, although they progressively translate positively in the y-axis with the increasing of n_r. This effect is more visible in the 2-person **SG**, the curves for all different n_r are further away from each other when compared to the **NSG** case. This effect may be due to the higher magnitude magnitude of the time values for this latter case, having, at most, an magnitude order of $\mathcal{O}(\tau_i \cdot n_r) \sim 10^3$, while for **SG** we have $\mathcal{O}(\tau_i \cdot n_r) \sim 10^4$ (the same occurs for $\tau_i^A \cdot n_r$). This may be indicative that, even though synchronism accelerates the system's convergence for either one of the absorption states, the average fixation time, conditional or unconditional, will progressively increase with n_r.

To summarize, and specifically for social learning, from all the performed experiments it is possible to conclude the effects of an increase of the synchronism level, in the updating process, are globally very small, being nearly negligible in some cases, when compared to the asynchronous process. However, although small, there are indeed some effects that one should take into consideration. We not only saw how synchrony could increase the expected fraction of cooperators, and how it may slightly enhance the group achievement, depending on the game's setup, but also how the average fixation times increase, even knowing the total fixation time linearly decreases with n_r.

Nonetheless, and as a reminder, one must be aware of the computational limitations that we are subjected, only having been possible to viably reach a level of synchronism corresponding, at most, to approximately 14% (7/50) of the synchrony spectrum. The effects of higher levels of synchronism may be contradictory of some of the conclusions above taken, or maybe even totally disprove them. It is, then, imperative to find a formulation for $\mathcal{T}^n$ that would allow us to compute more and more complex transition matrices, hence allowing us to investigate more profoundly the effects of synchronism along all the synchrony spectrum.

3.4 Synchronism in Other Learning Rules

In the same way as for social learning, we may also study the effects off synchronism on environments where individuals may also follow other learning ruless beside social learning, such as **C** and **CT**. In specific, we investigate how synchronism affects well-mixed populations with multi-rule dynamics. As we don't intend to go much deeper, we will focus our study in homogeneous populations. Before evaluating the population dynamics, considering multi revision process, some slight changes on the transition probabilities may be required.

Let us start with conformity. In the description we have been taking so far, the conformist individual, as a zero-degree **ToM** agent, does not reason about other's most probable response, and thus its strategic choice is independent of the level of synchronism in the update process. In other words, we say the conformist is not sensitive to other simultaneous revisions, only caring about the opponent's strategy in its own revision process. Therefore, no changes will be necessary for the conformity transition probabilities, previously defined in equations 2.39 and 2.40.

Regarding **CT**, things aren't so simple. Previously in section 2.4.2, we discussed how we could categorize a **CT** individual as a first-degree **ToM** agent [13]. This means the individual is aware of others intentions and takes them into account for its strategic choice. When facing a scenario with multiple revisions occurring simultaneously, the individual must reason about every single possible scenario and find what would probably be the most beneficial for itself. As one can predict, this has severe implications for the description of the switching probability: not only the individual reasons hypothetical past events, but he must also take into consideration all the hypothetical responses of all the other $n_r - 1$ individuals that are revising their strategy simultaneously.

3.4.1 Reassembling the Model

To take into account the new **CT** dynamics in the updating process, one must reformulate the switching probabilities for both possible interactions, $C \to D$ and $D \to C$. Previously in section 2.4.2, we explicitly defined the switching probabilities for the birth-death process, that we will retake in order to build our new model. For a more clear visualization, we start by taking both equations 2.43 and 2.44 in the following representation:

$$p^{[CT]}_{C\to D}(k) \equiv p^{[CT]}_{-} = \left\{1 + \text{Exp}\left[-\beta^{[CT]}\left(f_D(k-1) - f_C(k)\right)\right]\right\}^{-1} \tag{3.27}$$

$$p^{[CT]}_{D\to C}(k) \equiv p^{[CT]}_{+} = \left\{1 + \text{Exp}\left[-\beta^{[CT]}\left(f_C(k+1) - f_D(k)\right)\right]\right\}^{-1} \tag{3.28}$$

Besides being rational and intelligent, the counterfactual thinker is aware of the game's updating process. More precisely, it is aware that, at each generation, there are n_r individuals that will proceed with their revision process. This means that, besides itself, each one of the other $n_r - 1$ entities is given the possibility to move the system's state from k to $k \pm 1$. Having all the $n_r - 1$ individuals producing an impact of ± 1, the system's configuration will move in total, at most, from k to $k \pm (n_r - 1)$. Knowing this, the **CT** individual will take into consideration what would happen if any of those states would be reached in the end of the generation, if it haven't played. In other words, the **CT** will evaluate its strategic choice for each of the possible state resulting from the other $n_r - 1$ revisions. Assuming every single scenario would occur with the same probability, one may reformulate equations 3.27 and 3.28 as follows:

$$p^{[CT]}_{C\to D}(k) \equiv p^{[CT]}_{-} = \left\{1 + \text{Exp}\left[-\frac{\beta^{[CT]}}{2n_r - 1}\sum_{\delta=-n_r+1}^{n_r-1}\left(f_D(k+\delta-1) - f_C(k+\delta)\right)\right]\right\}^{-1} \tag{3.29}$$

$$p^{[CT]}_{D\to C}(k) \equiv p^{[CT]}_{+} = \left\{1 + \text{Exp}\left[-\frac{\beta^{[CT]}}{2n_r - 1}\sum_{\delta=-n_r+1}^{n_r-1}\left(f_C(k+\delta+1) - f_D(k+\delta)\right)\right]\right\}^{-1} \tag{3.30}$$

where we have divided the intensity of **CT** by $2n_r - 1$ for the sake of normalization.

Although this new formulation seems to describe the new dynamics, the latest assumption is compromising. Each possible outcome from the $n_r - 1$ first revisions, which we will designate by k', does not have the same possibility to occur, and hence there is a need to find a weighting function that differentiates every single scenario.

In our research, we have wonder if we could base our weighting function in the probability to have a certain amount of cooperators in the group of n_r individuals. For instance, in order to provisionally reach the state $k' = k - n_r + 1$, all the $n_r - 1$ individuals must be cooperators, as only they may produce a state variation of $v = -1$. The probability to pick all these cooperators, given by $\sum_{i=0}^{n_r-2} x_C^{(Z,i)}(k,i)$, is dependent of the current number of cooperators, and it may be different from any other scenario. The reasoning above described may be translated according to the scheme on Figure 3.8, shown below.

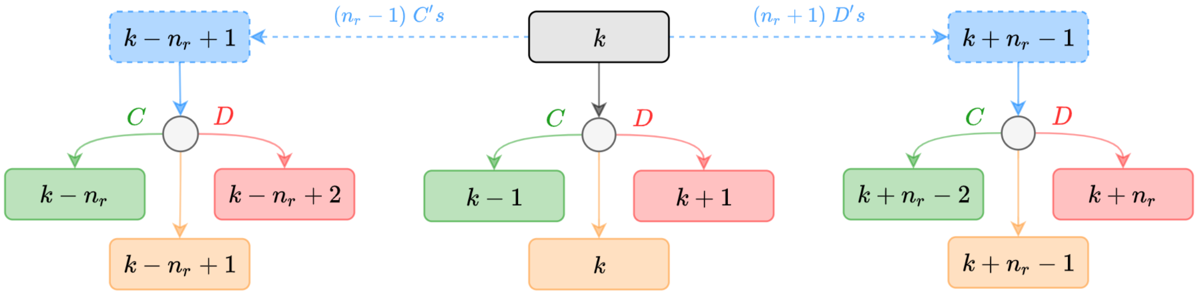

Figure 3.8: Scheme of CT's reasoning in the updating process.

If, for instance, we have $k' = k - n_r + 2$, it is mandatory that at least $n_r - 2$ individuals are cooperators. Notice, however, that this also includes the scenario where we have $n_r - 1$ cooperators, meaning the weighting function is cumulative on all scenarios that, at least, accomplish the required number of cooperators. Defining α as the weighting function, we may rewrite equations 3.29 and 3.30 as follows:

$$p^{[CT]}_{C\to D}(k) \equiv p^{[CT]}_{-} = \left\{1 + \text{Exp}\left[-\frac{\beta^{[CT]}}{n_r}\sum_{\delta=-n_r+1}^{n_r-1}\alpha(k, n_r - 1, \delta)\left(f_D(k+\delta-1) - f_C(k+\delta)\right)\right]\right\}^{-1} \tag{3.31}$$

$$p^{[CT]}_{D\to C}(k) \equiv p^{[CT]}_{+} = \left\{1 + \text{Exp}\left[-\frac{\beta^{[CT]}}{n_r}\sum_{\delta=-n_r+1}^{n_r-1}\alpha(k, n_r - 1, \delta)\left(f_C(k+\delta+1) - f_D(k+\delta)\right)\right]\right\}^{-1} \tag{3.32}$$

where:

$$\begin{aligned}\alpha(k, n'_r, \delta) &= \sum_{\beta=\text{Max}(\delta,0)}^{\text{Min}(\delta+n'_r,n'_r)}\binom{nr'}{\delta}\frac{\left(\prod_{i=0}^{\delta-1}(k-i)\right)\left(\prod_{j=0}^{n'_r-\delta-1}(Z-k-j)\right)}{\prod_{i=0}^{n'_r-1}(Z-i)}\\ &= \sum_{\beta=\text{Max}(\delta,0)}^{\text{Min}(\delta+n'_r,n'_r)}\binom{nr'}{\delta}\frac{k!(Z-k)!(Z-n'_r)!}{Z!(k+\delta)!(Z-n'_r-k+\delta)!}\end{aligned} \tag{3.33}$$

Although the weighting function is apparently complex, its formulation is very simple. The limits on the summation are given according to the possible number of cooperators that allow each scenario, following the reasoning of the examples previously mentioned. In a much simpler way, we may rewrite equation 3.33 as:

$$\alpha(k, n_r', \delta) = \sum_{\beta=\text{Max}(\delta,0)}^{\text{Min}(\delta+nr',nr')} \left(\prod_{i=0}^{\delta-1} x_C^{(Z,i)}(k,i) \right) \left(\prod_{i=0}^{\delta-1} x_D^{(Z,\delta+i)}(k,\delta) \right) \tag{3.34}$$

following the definitions in equation 3.5, for both x_C and x_D.

Having reformulated the switching probabilities for **CT**, to take into account the **ToM** first-degree characteristic, all the remaining functions in the dynamic's study may be given naturally just by following the description on sections 2.4.2 and 3.2.2, and hence, we are ready to proceed to the evaluation of the impact of synchronism in well-mixed populations in the presence of multiple different learning rules.

3.4.2 Synchronism in Conformity

Regarding conformity, in all its dynamics, there is not an explicit dependency on the number of revisions, and, as that, the results on the impact of synchronism should not be any different from the ones in the **SL** dynamics, that we previously saw in section 3.3.

In order to better evaluate a new dynamic that includes conformity, we believe that, firstly, it would be convenient to show the typical conformity dynamics, that is, the dynamics for the usual asynchronous updating process. The dynamics may be described, for example, in terms of the stationary distribution. Following the previously described formulation, from section 2.4.1, we will take population sized $Z = 50$, with a mutation rate of $\mu = \frac{1}{Z}$, in which all individuals behave according to the conformity principles, that is, a purely conformist population. This is the same as taking a multi-rule homogeneous population with $\delta^{[C]} = 1.0$. For this case, we will vary the intensity of conformity, $\beta^{[C]}$, and for each we compute the stationary distribution. The results are given below in Figure 3.9.

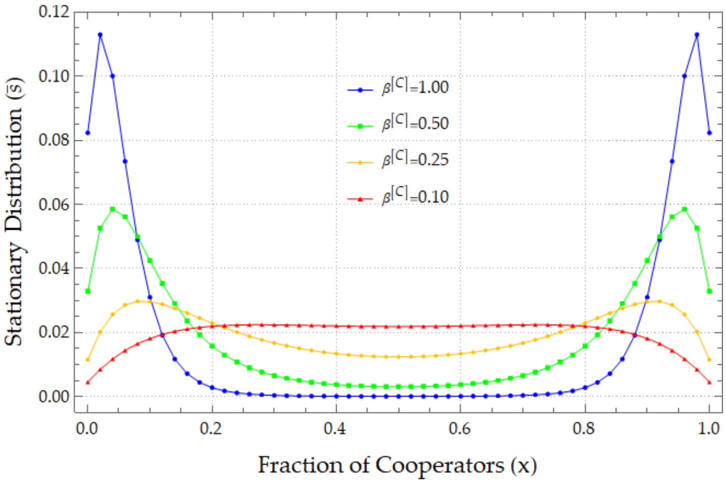

Figure 3.9: Stationary distribution for a pure conformist population, that is, we have $\delta^{[C]} = 1.0$. This also means the dynamics is completely independent of the game. For a population sized $Z = 50$, and with $\mu = \frac{1}{Z}$, we take different intensities of conformity as $\beta^{[C]} = \{0.1, 0.25, 0.5, 1.0\}$.

Firstly, note that, regardless on the learning rules, the lower the intensity associated to a certain rule, the lower the impact of the learning rule's corresponding function. In this sense, as expected, one may observe that decreasing the value of the intensity of conformity progressively leads to a lower influence of the difference between the fractions of cooperators and defectors on the revision process. It is to be noted that, as a consequence, the decreasing $\beta^{[C]}$ progressively twists the typical coordination dynamics to a co-existence one, which contradicts the formal definition or conformity (we will retake this topic later on section 4.1.1).

The conformity switching probability is given as a function of the difference between the fraction of individuals for each strategy, C and D. This may be suggestive of a dynamics characterized by two fixed points, one for each strategy, that is, one for defectors, at $k = 0$, and other for cooperators, at $k = Z$. Notice that this dynamic is equivalent to the 2-person **SH**, as both may be considered dynamics of coordination (see section 2.2.3). In this reasoning, we expect that, by well-mixing conformity-driven individuals in a **SL** environment, the two peaks relative to each of the fixed points will be increasingly highlighted, as we increase the probability of conformity.

Once again, we take the same population as in the case above, on Figure 3.3, but now fixing both intensities of conformity and selection at $\beta^{[C]} = 1.0$ and $\beta^{[SL]} = 1.0$, respectively. Having 20% of conformity-driven individuals, that is, for a conformity probability of $\delta^{[C]} = 0.2$, and varying the number of revisions in the updating process, with $n_r = \{1, 3, 5, 7\}$, we investigate the N-person previously studied games, specifically obtaining the stationary distributions presented in the Figure 3.10 below.

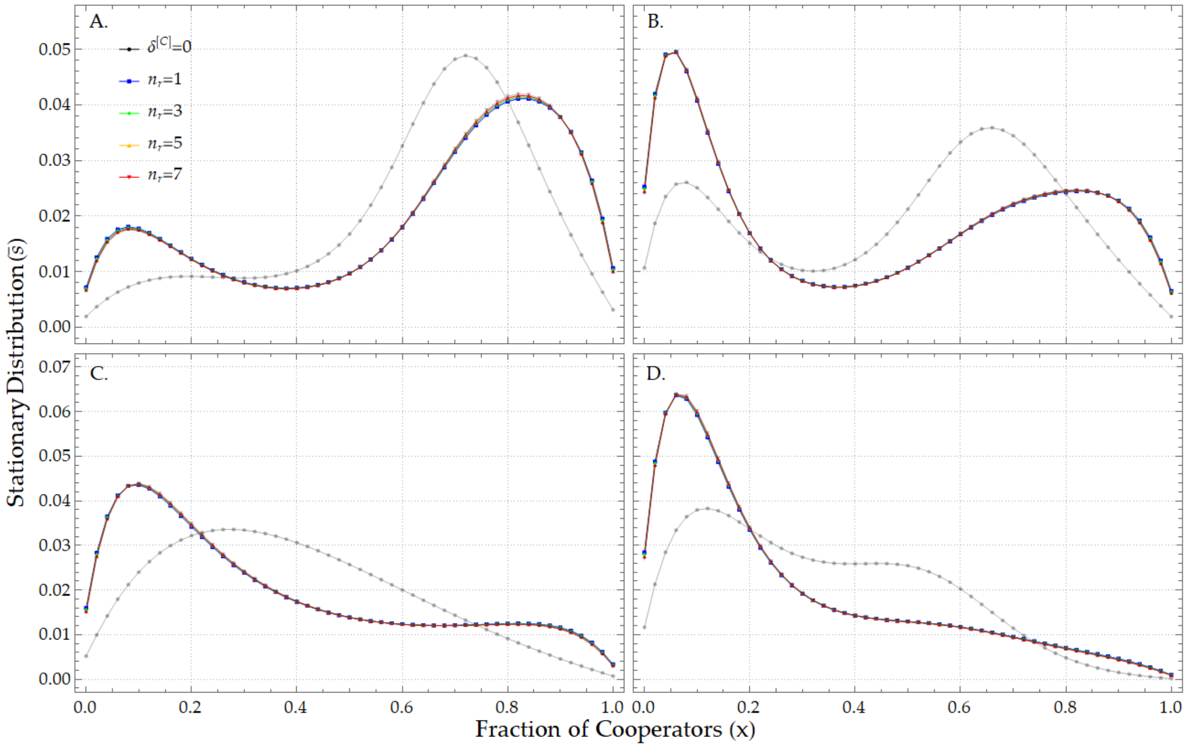

Figure 3.10: The effects of progressive increasing levels of synchronization on a well-mixed homogeneous population, in a **SL** environment with $\delta^{[C]} = 0.2$. We present the stationary distribution for $n_r = \{1, 3, 5, 7\}$, in four different N-person social games, specifically, the **NSG**, **NSH**, **PGG** and **CRD**, respectively on panels from **A** to **D**. The curve in black represents the asynchronous process, with $\delta^{[C]} = 0$, for matters of comparison. The results on synchronism do not generally differ much from what we obtained for a full **SL** population, due to the fact that conformity does not have a dependency on synchronism variables.

Regarding the curves' overall shape, the results go as expected, as they accomplish the homogeneous mixing of conformity individuals on a social learning environment, having now two protrusions, one corresponding to each the monomorphic states, that are associated to the conformity dynamics.

The results on synchronism effects go along, very similarly, with the ones previously obtained in both cases of Figures 3.1 and 3.3: not only the curves for different n_r are very close to each other, acting like fluctuations around the asynchronous process', but also there is no direct impact on fostering cooperation, as the effects on both EFC and η_G are highly dependent on the system's set of parameters. Generally, this indicates that conformity has only an impact on the general population dynamics, not being dependent on the system's level of synchronism.

3.4.3 Synchronism in Counterfactual Thinking

Contrary to conformity, the **CT** dynamics, with its new switching probability description, does have a dependency on the number of revisions, and hence, one should expect a non null impact on the system when increasing the level of synchronism. Moreover, the results from [13] show that a small prevalence of **CT** individuals is enough to nudge an entire population towards highly cooperative standards. This way, as a measure of validation, we hope our new model' results match these insights.

To evaluate the impact of synchronism in homogeneous populations, like before, we will take a population sized $Z = 50$, with a mutation rate of $\mu = \frac{1}{Z}$, with $\beta^{[SL]} = 1.0$ and $\beta^{[CT]} = 5.0$, where 5% of all individuals follow the **CT** learning rule, that is, $\delta^{[CT]} = 0.05$. We will vary the number of revisions as $n_r = \{1, 3, 5\}$, for all the N-person previously studied games, and for each we compute the stationary distribution, as shown in the Figure 3.11 below.

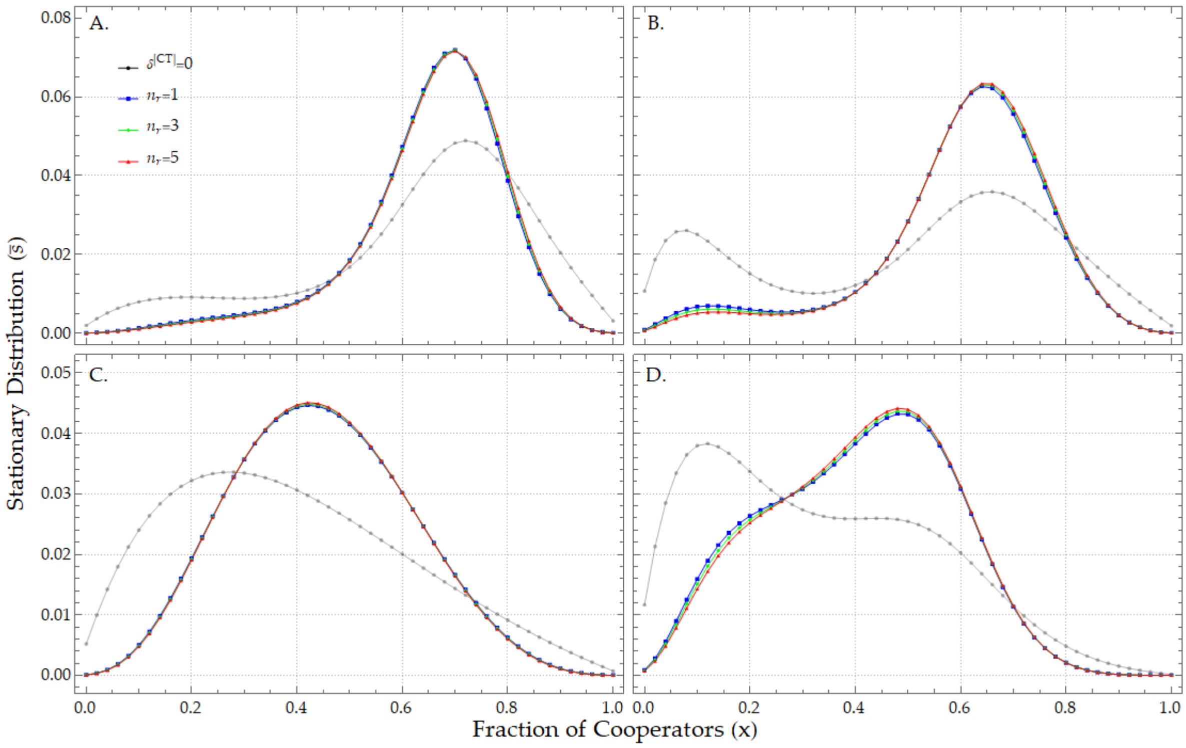

Figure 3.11: The effects of progressive increasing levels of synchronization on a well-mixed homogeneous population, in a **SL** environment with $\delta^{[CT]} = 0.05$. We present the stationary distribution for $n_r = \{1, 3, 5\}$, in four different 2-person social games, specifically, the **NSG**, **NSH**, **PGG** and **CRD**, respectively on panels from **A** to **D**. Even though the **CT** dynamics is explicitly dependent on the level of synchronism, it is visible how small that impact is, on the overall system's dynamics.

The results on the synchronism effects follow the same trend of the results for both conformity and social learning, where, regardless on the level of synchronism, the stationary distribution curves present a very similar shape, being displayed very close to each other, seemingly behaving as fluctuations around the asynchronous' curve. However, in this case, one may notice these variations occur more strongly for counterfactual reasoning than for other learning rules, as we may more easily infer from both **NSH** and **CRD**. Moreover, although we were only able to produce these results, in feasible time, for low values of n_r, due to the **CT** more complex formulation, it is already possible to notice a non-negligible deviation of the curve, even for $n_r = 5$. This way, even lacking more support information, these insights could suggest that, unlike other learning rules, counterfactual reasoning is significantly affected by increasing synchronism, as the higher the synchronism level is in the spectrum of synchrony, the more deviated from the asynchronous curve the stationary distribution is. Nevertheless, we must take into consideration that this lack of data could be critical, as for higher levels of synchronism the system dynamics could fall into a different tendency.

Furthermore, we notice that a small probability of **CT** has already an huge impact on the general system's dynamics, which go along with the expected, as shown in [13]. For both **C** and **D** panels, corresponding to the **PGG** and **CRD**, respectively, it is clear how **CT** does, indeed, move the entire population to much higher standards of cooperation. Regarding the other two cases, it may not be that clear. To clarify the results, and as previously done in Figure 3.3, it might be relevant to compute the overall achievement group as a measurement of the probability of success, and to compare them with the expected results for a full of social learner population. This way, for each game and for each number of revisions we compute η_G, not only to show the overall evolution as a function of the synchronism, but also to compare it with what would we expect in a full **SL** population. The results are shown in Figure 3.12.

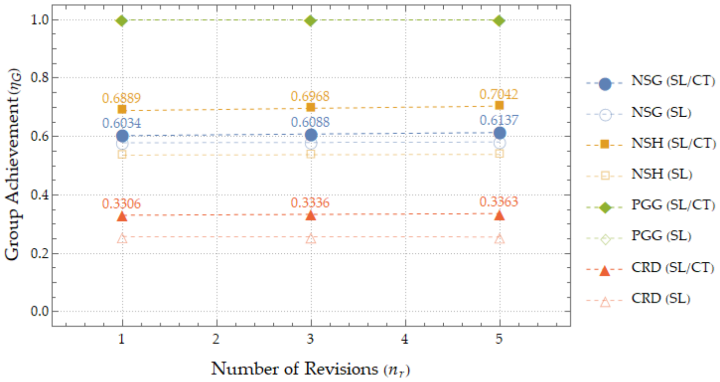

Figure 3.12: Group achievement as a function of the number of revisions, for all the studied N-person games. It is noticeable an almost constant line, which indicates the progressive increasing of the synchronism level does not have a very significant effect on the group achievement. Notice that, for the **PGG**, the η_G is always maximum (one), due to the fact the threshold M is null.

Generally, regardless on the social game, one may observe that a small probability of counterfactual thinkers is enough to push the entire population towards higher cooperative standards, which goes as expected, according to [13]. When it comes to the effect of synchronism, we notice that, comparatively to the pure social learning population, the **CT** learning rule is much strongly affected by increasing the number of revisions on the updating process. In fact, attending to Figure 3.4, we notice that from $n_r = 1$ to $n_r = 5$, the group achievement has increased 0.415%, 0.503% and -0.349%, respectively for **NSG**, **NSH** and **CRD** in the pure-**SL** framework, while homogeneously mixing a small amount of **CT** individuals in a **SL** environment modifies these values to 2.221%, 1.707% and 1.724%, respectively. This result suggests that counterfactual reasoning is, in absolute terms, strongly more influenced by synchronism than social learning.

Interestingly, we notice that, in all the performed examples, the group achievement grows with the increasing synchronism level, which could suggest a very new exciting conclusion: a small prevalence of counterfactual thinkers, homogeneously well-mixed in a **SL** environment, not only leads to a significant increase of the group achievement, when compared to a pure **SL** population, but also promotes higher probabilities of success for higher levels of synchronism, in the synchrony spectrum. Although this results sound interesting, we cannot take them as certain, due to many factors. Firstly, to achieve such results, very complex calculations had to be computed, to which a propagation of computational error may be underlying. Moreover, we have only been able to test the outcomes for relatively low levels of synchrony, and, therefore, our insights may lack the information necessary for their generalization. Furthermore, these studies have only been performed specifically for the game's configuration above explicit, but however, as we saw on Figure 3.5, different game configurations may lead to negative impacts on the group achievement with increasing synchronism level.

Attending to all the previous insights, we suggest that more profound studies on synchrony effects on **CT**-based populations should be performed. To do so, due to their high complexity, it would firstly be advisable to obtain a new simpler formulation to compute both the stationary distribution and the **CT** transition probabilities, so one could perform studies for higher levels of synchronism, along the whole synchrony spectrum. In addition, it should also be interesting to evaluate the dependency of these conclusions on the game's configuration variables, in order to find any direct dependency of the effects of synchronism in **CT** on the game's variable.

3.5 Final Notes

The effects of increasing the synchronism level, along the spectrum of synchrony, on the overall population dynamics is very small, to the point of being negligible, either in the 2-person or the N-person framework. In fact, along this chapter, we have verified how insignificant are the consequences of progressively increasing the number of revisions, on the evolutionary updating process, not only for a pure social learning population, but also for homogeneously well-mixed populations of social learners and conformists. For all cases we verified that, regardless of the social game, synchrony leads to a dynamic characterized by a the stationary distribution which curve fluctuates around the asynchronous process curve, oscillations that progressively become more intense as we increase the level of synchronism, yet still very small.

Following this reasoning, we have also obtained an almost negligible impact of the evolution of the cooperation evaluation tools, both the EFC (in the 2-person framework) and the η_G (in the N-person framework). Even though very small, we saw that the evolution of $\eta_G(n_r)$ shows to be either positive or negative, depending on the game's configuration variables, directly meaning that, regarding cooperation optimization, synchronism may either have positive or negative impact, depending on the game. Formally, we can say $\eta_G \equiv \eta_G(v, n_r)$, where v is the set of game's configuration variables. When it comes to convergence, we saw, through the fixation times, that, even though synchronism generally accelerates the system's convergence for either one of the absorption states, approximately linearly with n_r, the average fixation time, that is, the fixation time for each revision, conditional or unconditional, will progressively increase with increasing n_r. This suggests the total number of revisions, which should not be confused with total time steps, increase with n_r.

It is noteworthy that, specifically in the case of **CT**, the dynamics shows to be more sensitive to synchrony than to the other learning rules, fundamentally due to the fact they new transition probabilities directly depends on n_r. In fact, for one same game, increasing the synchronism level on the **CT** framework shows to promote an increase on η_G, in some cases, up to five times larger than on a pure-**SL** population. Moreover, might be interesting to notice that, specifically for the studied cases, increasing the synchronism level progressively leads to higher group achievements which, contrary to conformity or social learning, no longer are so small to be negligible. However, attending to the lack of relevant information to sustain these latter insight, it would be very premature to generalize these conclusions.

Chapter 4

Population Dynamics in Homogeneous Populations

In this chapter, we explore the dynamics of different social games, in the case of well-mixed, homogeneous and finite populations, on a scenario with multiple available learning rules. More specifically, we investigate the evolutionary dynamics through analyzing the stochastic gradient of selection, along with other relevant evaluation tools such as the EFC, in the case of 2-person games, and the η_G, for N-person games, aiming to discover how the introduction of different learning rules in a social learning environment affects the overall population's evolutionary most likely outcome. For this new population dynamics, we ought to find any correlations between the population's configurations and the overall cooperation expectations, hopefully finding any relations that foster cooperation maximization.

4.1 Dynamics in 2-Person Games

It is in 2-person games where we find the simplest dynamics. We begin our study by evaluating the effects of the introduction of different learning rules, namely conformity and counterfactual thinking, in an homogeneous and well-mixed population of social learners, following each of the 2-person games previously described in section 2.1.2. Regarding cooperation optimization, we resort to the expected fraction of cooperation, EFC (see equation 2.34), as an evaluation tool, but only whenever it is valid.

4.1.1 Conformity in 2-Person Games

We start by investigating population's dynamics in communities with a fixed number of conformity-driven individuals, in a social learning environment. Attending to the multi-rule formulation, as previously shown in section 2.4.3, and specifically for homogeneous populations, in the case where $\mathcal{L} = \{SL, C\}$, we may define the deterministic gradient of selection equivalently to equation 2.50:

$$G(x) = \delta^{[SL]} G^{[SL]} + \delta^{[C]} G^{[C]} \tag{4.1}$$

Attending to the conformity formulation in section 2.4.1, both these learning rules are associated with dynamic revision processes, whose effect is taken into account when formulating the transition probabilities for both **SL** and

C. In fact, and assuming a similar magnitude for both switching probabilities, $p^{[SL]}_{S_A \to S_B}$ and $p^{[C]}_{S_A \to S_B}$, it wouldn't be unreasonable to expect similar orders of magnitude for both $T^{[SL]}_{\pm}$ and $T^{[C]}_{\pm}$. Very roughly, this means the conformity impact on the overall population dynamics is dimensionally equivalent to the social learning's impact, and hence, one shall expect to visually verify a very smooth increase of the conformity effects as we increase the probability of conformity, $\delta^{[C]}$, in a social learning environment. Even though the learning rule's functions, that is, the functions associated to each learning rule ($f_S(x)$ and $n_S(x)$, respectively for **SL** and **C**), involve variables or different kind, and assuming they are similarly weighted with the respective learning rule's intensities, $\beta^{[SL]}$ and $\beta^{[C]}$, the difference on their magnitudes is not enough to justify a significant difference between the switching probabilities, hence not being sufficiently relevant to change the magnitude of the gradient of selection.

Proceeding with the investigation, we start with a full **SL** population ($\delta^{[C]} = 0$) and we progressively increase the value of the probability of conformity until reaching a full conformist population ($\delta^{[C]} = 1.0$). For each step, we compute the gradient of selection, as an explicit function of the fraction of cooperator x, and analyze the system's dynamics. Recall that, in this setup, we assume $\delta^{[C]}$ as a constant fixed value, that is characteristic of the population, and hence the G variations with $\delta^{[C]}$ should not be considered as part of the population's evolution. Along with the gradient of selection it might be relevant to compute the expected fraction of cooperators, EFC, as a qualitative measure, assuming our objective is to maximize cooperation. Notice, however, that the EFC analysis may be escorted by misleading conclusions, namely for coordination dynamics, as previously explained in Chapter 3, and thus it must be taken solely as an auxiliary tool.

For all the four 2-person games previously described, we impose the condition $1 > 0.75 > 0.25 > 0$ for the order of the R, S, T, P variables respective to each game, following the same reasoning as in section 3.3. In order to force the same relative impact, we have both intensities of selection and conformity set to $\beta^{[SL]} = 1.0$ and $\beta^{[C]} = 1.0$, respectively, and, for a population sized $Z = 50$ with a mutation rate of $\mu = \frac{1}{Z}$, we may obtain the relative gradient of selection for all $x \in [0;1]$, and for all possible $\delta^{[C]} \in [0;1]$. We say the gradient of selection is relative as the computed values of G are then normalized between the minimum (negative) value to the maximum (positive) value of G. The results for all the described setup are shown below in Figure 4.1.

The obtained results generally go as expected: the effects of conformity increase approximately linearly with increasing probability of conformity, as one may visually verify. In other words, the variations on the system's dynamics progressively increase with increasing $\delta^{[C]}$, and hence the effects of conformity apparently become more visible for larger probabilities of conformity. For instance, for both **HG** and **PD** (panels **A** and **D**, respectively), for values of $\delta^{[C]} > 0.50$, approximately, conformity is responsible for the formation of a new regions with opposite sign to the dominant sign of the gradient, which occurs in a very smooth way, not abruptly. In the case of **SG** (panel **B**), we perceive that conformity completely switches the population dynamics, quite rapidly, within a certain region of $\delta^{[C]}$, but still in a very smooth way. In opposite, for the **SH** (panel **C**) nothing much occurs, as the general dynamics of this game matches the full conformity population's dynamics. In fact, all these results could be predicted attending to the fact that a population full of conformity-driven individuals is characterized by a coordination dynamic, regardless of the current social game. These means that the progressive effects of conformity in the population will depend on the original social learning game dynamics. Generally, the further away a game dynamics is from coordination, in the 2-person game space, the more conformity affects the population dynamic is, an effect that progressively grows with increasing probability of conformity.

In terms of cooperation optimization, one may observe that, for certain social games, conformity may be responsible for improving the expected fraction of cooperation, but for other cases this is not true, as conformity may even work against the EFC maximization. Although these conformity effects, positive or negative, on EFC mostly

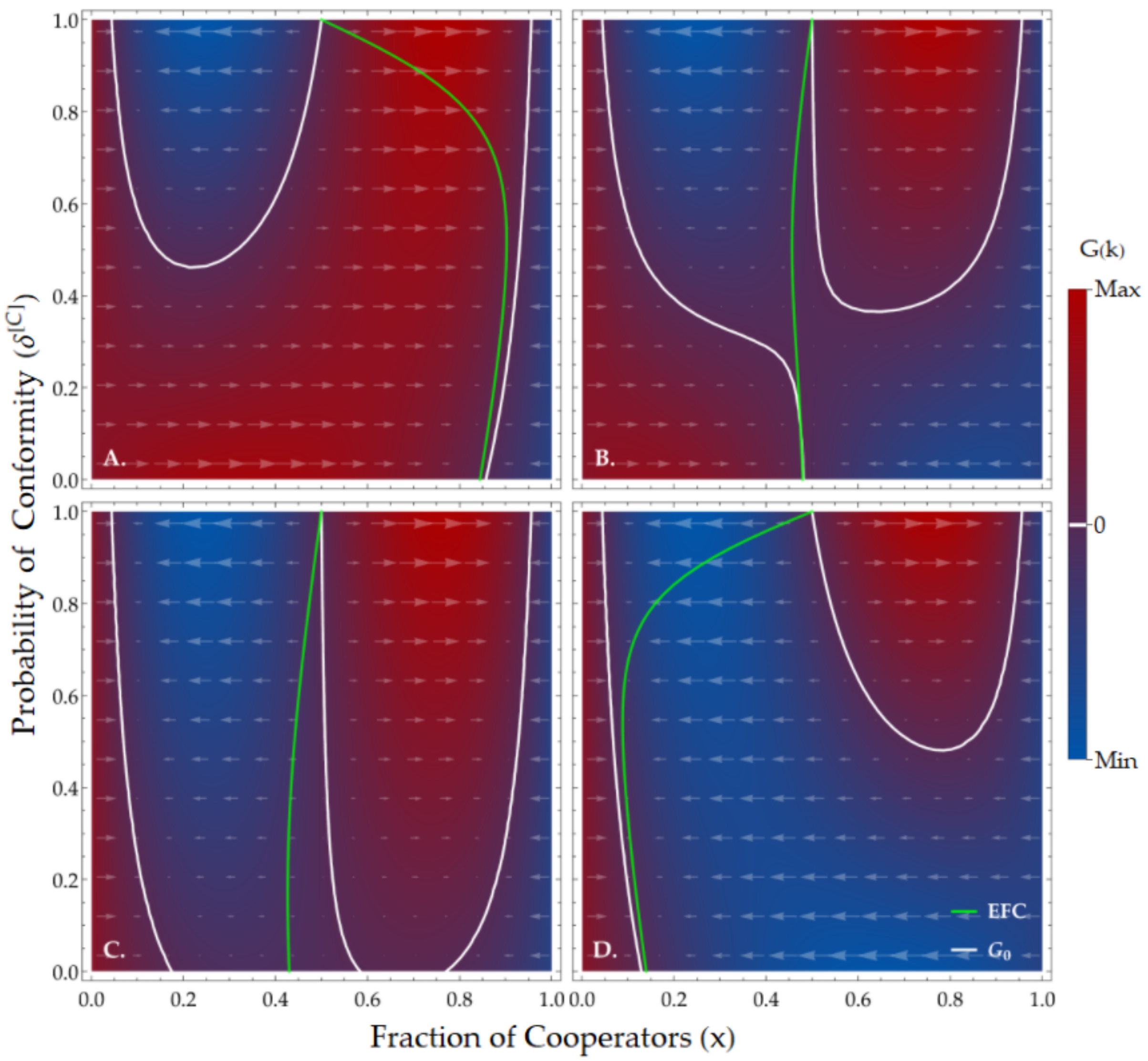

Figure 4.1: Relative gradient of selection in 2-person games, for well-mixed, homogeneous and finite populations of conformists and social learners. We take a population sized $Z = 50$, with a mutation rate of $\mu = \frac{1}{Z}$, with both intensities of social learning and conformity as $\beta^{[SL]} = \beta^{[C]} = 1.0$. Panels from **A** to **D** respectively show the results on the **HG**, **SG**, **SH** and **PD** games. The gradient of selection is given relatively through normalization, from its minimum to its maximum values. The line in white represent the points of null gradient, while the green line represents the evolution of the EFC with increasing $\delta^{[C]}$. Recall that the gradient of selection, being explicitly defined as a function of x for a fixed value of $\delta^{[C]}$, evolves horizontally in the graphic, and not vertically. Generally, the impacts of conformity increase smoothly with increasing $\delta^{[C]}$, meaning one must have a considerable amount of conformists in the population in order to get a significant impact of **C**. Regarding the effects on EFC, the most significant variations are given for very large $\delta^{[C]}$ (panels **A** and **D**), while for others the effects can be considered close to negligible. However, recall the EFC may be missleading for non peaked-shaped stationary distributions, such as the 2-person **SH**.

depend on the current social game dynamics, there are also a dependency on the value of $\delta^{[C]}$. Let us take, for instance, the **HG** (panel **A**). Here we notice that conformity progressively leads to an increase of the EFC, which goes along with the **HG** stable fix point motion to the left, but only until a certain maximum value, on $\delta^{[C]} \approx 0.5$, from where EFC starts decreasing until it reaches the final value of $EFC = 0.5$. Despite that, and regardless on the social game, as one would expect, we notice that, the same way conformity leads to a pure coordination dynamic, conformity also pushes the EFC towards the unstable fix point in the middle, exactly at $x = 0.5$, that is characteristic of the coordination dynamics.

The convergence to the coordination dynamics visually occurs very smoothly as we increase $\delta^{[C]}$. However, one may expect this convergence to be faster or slower depending on the relation between both intensities of selection and conformity: having $\beta^{[C]} > \beta^{[SL]}$, one would expect a faster convergence to coordination, while for $\beta^{[C]} < \beta^{[SL]}$ we would expect a slower one. These statements are merely empirical speculations and lack a more formal foundation. In this manner, for better evaluating the impact of the intensity of conformity, we may compute the homogeneous gradient of selection for one same population, but varying the value of $\beta^{[C]}$. Specifically in this study, for the **SG** with $(R, S, T, P) = (0.75, 0.25, 1, 0)$, we take a well-mixed, homogeneous and finite population with $\delta^{[C]} = 0.5$, where $Z = 50$, $\mu = \frac{1}{Z}$ and $\beta^{[SL]} = 1.0$. For each value in the range $\beta^{[C]} = \{0.1, 0.5, 1, 10\}$, we compute the gradient of selection. The results are shown below in Figure 4.2.

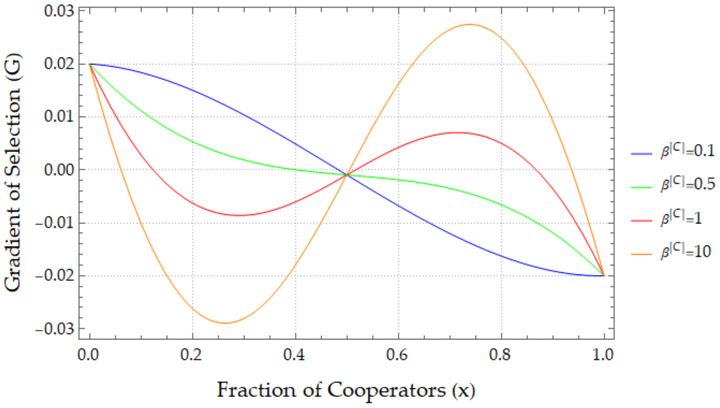

Figure 4.2: Gradient of selection in well-mixed, homogeneous and finite populations with $Z = 50$, $\mu = \frac{1}{Z}$ and $\delta^{[C]} = 0.5$, for $\beta^{[SL]} = 1.0$ and $\beta^{[C]} = \{0.1, 0.5, 1, 10\}$. We notice how the dynamics progressively change from co-existence to coordination as we increase the intensity of conformity.

Firstly, we can't help noticing that these results go along with the conformity stationary distributions, shown previously in Figure 3.9, where lower values of $\beta^{[C]}$ would promote a co-existence dynamics, while higher values would favour coordination. In the graphic above, we notice mostly the same: for the lower values of $\beta^{[C]}$, the dynamics appears to be one of co-existence kind, whereas for higher values we recover the typical coordination dynamic. As we keep increasing $\beta^{[C]}$, the gradient takes on much larger magnitude values, progressively enhancing an abrupt transition from the negative gradient peak, on the lower half ($x < 0.5$), to the positive gradient peak, on the upper half ($x > 0.5$). In its limit ($\beta^{[C]} \to \infty$), we achieve the true nature of conformity: individuals facing a population with more cooperators strongly tend to choose cooperation, while in the opposite case they opt for defection.

As we can see, this result does not depend on the social game, meaning that the (pure) conformity dynamics will only depend on the intensity of conformity, which, only for lower values promotes co-existence, while for the wide majority of the cases it favours coordination. Although all these scenarios are mathematically possible, in its formal definition, conformity promotes a coordination dynamic, and hence, configurations with the lower values of $\beta^{[C]}$ lose their physical meaning. As that, we are more prone to assume that conformity always promotes coordination, notwithstanding the social game's dynamics.

To summarize, regardless on the social learning game, conformity will always lead to a perfect coordination dynamics, characteristic of a pure conformity population ($\delta^{[C]} = 1$). For intermediate levels of conformity ($\delta^{[C]} < 1$), however, the resulting dynamics are dependent on the **SL** environment. The same result is replicated when it comes to cooperation optimization: although increasing $\delta^{[C]}$ will lead to the expected $EFC = 0.5$, characteristic of conformity, for intermediate levels the effects are unknown apriori and dependent on the social game dynamics (recall, however, that the EFC indicator may be escorted by misleading conclusions). Moreover, having both gradients $G^{[SL]}$ and $G^{[C]}$ dimensionally equivalent, it is required a fair prevalence of conformity-driven agents to significantly modify the social game dynamics.

4.1.2 Counterfactual Thinking

Now, we investigate population's dynamics in communities with a fixed number of counterfactual thinking-driven individuals, in a social learning environment. Again, specifically for homogeneous populations, but now in the case where $\mathcal{L} = \{SL, CT\}$, we may define the deterministic gradient of selection equivalently to equation 2.50:

$$G(x) = \delta^{[SL]}G^{[SL]} + \delta^{[CT]}G^{[CT]} \tag{4.2}$$

Contrary to conformity, counterfactual thinking is characterized by a static revision process rather than a dynamic one, which automatically implies transition probabilities some orders of magnitude above the typical for the **SL** transition probabilities. Consequently, **CT** comes with a much larger impact on the overall gradient of selection for homogeneous populations, when compared to **SL**. Formally speaking, this means that a small prevalence of **CT** individuals, that is, a small value of the probability of counterfactual thinking is enough to drastically change the population's dynamics. Regarding the switching probabilities, as the learning rules' functions for both **SL** and **CT** are very similar ($f_S(x)$ and $f_S^i(x)$, respectively), and assuming a same order intensities for the learning rules, we should not expect any significant difference between $p^{[SL]}_{S_A \to B}$ and $p^{[CT]}_{S_A \to B}$.

To study the impact of **CT** in a **SL** environment, we may start by investigating the dynamics, through the (relative) gradient of selection, of population's with variable probability of **CT**. Specifically, and likewise that in conformity, we start by building a full **SL** population ($\delta^{[CT]} = 0$) and progressively increase the probability of counterfactual thinking until reaching a full **CT** population ($\delta^{[CT]} = 1$). For each step, we compute the gradient of selection, once again, explicitly as a function of the fraction of cooperators, x, and analyze the system's dynamics. Attending to the previous insights, for the same intensities order, one may verify that **CT** impact is much larger than **SL**, that is, $G^{[CT]} \gg G^{[SL]}$. To contrary these effects, we will set $\beta^{[SL]} = 5$ while having $\beta^{[CT]} = 1$, significantly increasing the overall strength of **SL** in order to balance the gradient of selection for both learning rules. Again, along with $G(x)$ we also present the expected fraction of cooperators as a qualitative measure, however always keeping in mind the possible misleading conclusions its analysis may bring.

For all the four 2-person games previously described, we impose the condition $1 > 0.75 > 0.25 > 0$ for the order of the R, S, T, P variables respective to each game, just as before. As mentioned, we have both intensities of selection and conformity set to $\beta^{[SL]} = 5.0$ while $\beta^{[CT]} = 1.0$, respectively, and, for a population sized $Z = 50$ with a mutation rate of $\mu = \frac{1}{Z}$, we may obtain the relative gradient of selection for all $x \in [0; 1]$, and for all possible $\delta^{[C]} \in [0; 1]$. The results for all the described setup are shown below in Figure 4.3.

Firstly, in all the above graphics it is easy to notice how much larger is $G^{[CT]}$ when compared to $G^{[SL]}$, especially if we take attention to the colour gradient, which represents the overall range of values for G in this setup. For all the above games, we notice that, when the population is full **CT**-driven, both minimum and maximum values of G correspond, respectively, to the minimum and maximum values of the color bar. On the other hand, when the population is full **SL**-driven, the values of G stand very close to the origin, independently of their sign, meaning the values for $G^{[SL]}$ are relatively much smaller than $G^{[CT]}$.

Another interesting thing to notice is that counterfactual thinking favours a co-existence dynamic. However, and

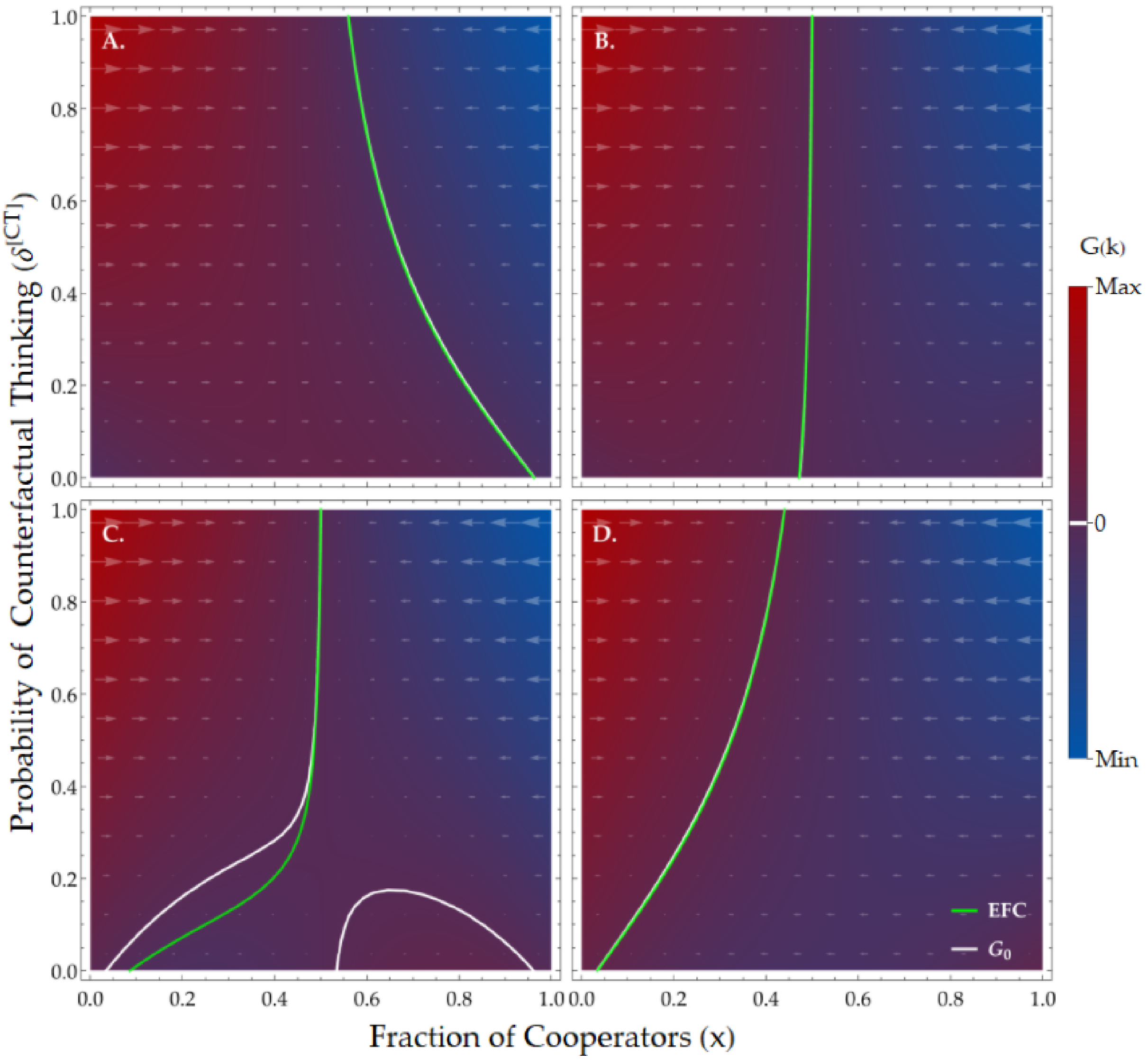

Figure 4.3: Relative gradient of selection in 2-person games, for well-mixed, homogeneous and finite populations of counterfactual thinkers and social learners. We take a population sized $Z = 50$, with a mutation rate of $\mu = \frac{1}{Z}$, with both intensities of social learning and conformity as $\beta^{[SL]} = 5.0$ and $\beta^{[CT]} = 1.0$. Panels from **A** to **D** respectively show the results on the **HG**, **SG**, **SH** and **PD** games. The gradient of selection is given relatively through normalization, from its minimum to its maximum values. The line in white represent the points of null gradient, while the green line represents the evolution of the EFC with increasing $\delta^{[CT]}$. Recall that the gradient of selection, being explicitly defined as a function of x for a fixed value of $\delta^{[CT]}$, evolves horizontally in the graphic, and not vertically. With exception to **SH** (panel **C**), the progressive addition of **CT** individuals does not have a greater impact on the overall game dynamics, being a stable equilibrium progressively favored as we increase the value of $\delta^{[CT]}$. It is noticeable how much more intense is the gradient of selection for higher probabilities of **CT** when compared to a full **SL** population. This goes as expected, attending on the difference of magnitudes on the transition probabilities for both **SL** and **CT**. Regarding **SH**, we verify a very small probability of **CT** is enough to drastically change the game dynamics, from a point where we have 3 fix points, to 1.

contrarily to conformity, the final learning rule dynamics does depend on the social game individuals are playing. This result should be expected as the rule function associated with **CT** does have a dependency on the game's configuration, in this case, on (R, S, T, P), while in the conformity case the function goes solely as a function of x. In fact, we notice that for all games but the **SH** the EFC line seems to overlay the null gradient line, emphasizing a very strong co-existence dynamics, which go according to the previous insights.

Regarding the **SH** case, one may verify something very interesting: increasing the probability of counterfactual thinking rapidly leads to a drastic change in the game's dynamics. Specifically, increasing the number of **CT** individuals in the **SL** environment leads to a progressive disruption of the **SL** dynamics, from a point where we have 3 fix points, that characterizes the typical **SH** coordination dynamics, passing through 2 fix points for a specific value of $\delta^{[CT]}$, and ending up with solely 1 fix point, that characterizes the coordination fix point. This modification in the dynamics is responsible for a sharp increase in the EFC, from a very small value ($EFC \approx 0.1$) when $\delta^{[CT]} = 0$, until we reach a more stable regime ($EFC \approx 0.5$) when $\delta^{[CT]} \approx 0.4$. This increase of $\approx 400\%$ in the expected fraction of cooperation go along with the insights from [13], that, despite being specific for the N-person version of the **SH**, shows how a small probability of **CT** is enough to foster cooperation significantly.

Generally, for this specific population setups, counterfactual thinking seems to foster a co-existence dynamics, characterized by a positive gradient for lower values of x and a negative gradient for higher values of x, pushing the population's dynamics towards the stable fixed point for some x in the middle. However, according to [13], in collective action problems, and specifically for **NSH**, one should expect counterfactual reasoning to promote coordination dynamics. Taking **NSH** simply as a generalization of the **SH**, it wouldn't be unreasonable to think that, for this latter case, **CT** would approximately follow the same coordination dynamics, rather than co-existence dynamics. Although it appears to be a contradiction, one must be aware of the dependency on the intensity of **CT**: the higher it is, the more the f_S^i functions influence the switching probabilities. As the population's dynamics depend mostly on this probability, it is logical to think that $\beta^{[CT]}$ may have a great impact in the overall population dynamics.

To verify this suggestion, and proceeding as before for conformity, we compute the gradient of selection for one same population, but varying the intensity of counterfactual thinking. For the **SH** with $(R, S, T, P) = (1, 0, 0.75, 0.25)$, we take a well-mixed, homogeneous and finite population with $\delta^{[CT]} = 0.5$, where $Z = 50$, $\mu = \frac{1}{Z}$ and $\beta^{[SL]} = 5.0$. For each value of the intensity of **CT**, in the range $\beta^{[CT]} = \{1, 5, 10, 25\}$, we compute the gradient of selection. The results are shown below in Figure 4.4.

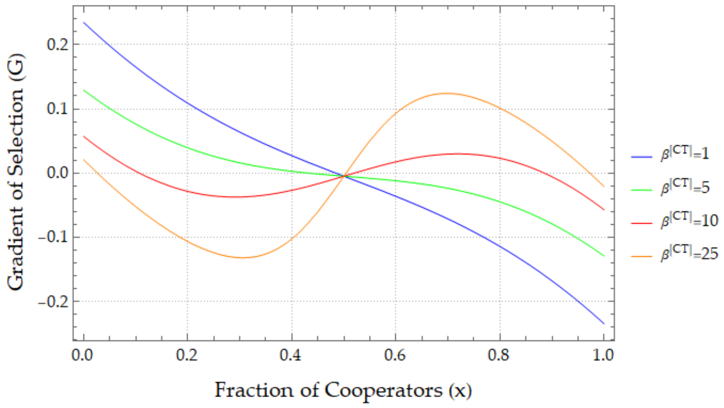

Figure 4.4: Gradient of selection in well-mixed, homogeneous and finite populations with $Z = 50$, $\mu = \frac{1}{Z}$ and $\delta^{[CT]} = 0.5$, for $\beta^{[SL]} = 5.0$ and $\beta^{[CT]} = \{1, 5, 10, 25\}$. We notice how the dynamics progressively change from co-existence to coordination as we increase the intensity of **CT**.

The previous insights are proved to be correct: varying the intensity of **CT** may lead to greater modifications on the system's dynamics. More specifically, we observe that, as we increase the value of $\beta^{[CT]}$, we progressively transform the dynamics from co-existence to coordination. Having this, one can justify both results from Figure 4.3 and from [13] in terms of the relation between $\beta^{[SL]}$ and $\beta^{[CT]}$, and hence we may verify our framework is valid.

To summarize, counterfactual reasoning dynamics are sensitive to the population's configurations, namely to the game's configuration (R, S, T, P), population's size and mutation rate (that we do not investigate here), and to the intensities of social learning and counterfactual thinking ($\beta^{[SL]}$ and $\beta^{[CT]}$). As we previously saw in Figure 4.4, specifically for the $\beta^{[CT]}$, changing any of these variables may result in a drastic change in the population dynamics. In our specific case, with $\beta^{[SL]} = 5$ and $\beta^{[CT]} = 1$, we saw that **CT** fosters co-existence dynamics, whereas having $\beta^{[SL]} = 5$ and $\beta^{[CT]} > 5$ progressively leads to a dynamics characterized by coordination. A more complete study on **CT** dynamics, to compare the results with the ones from [13], will be performed later on.

4.2 Dynamics in N-Person Games

When moving to the N-person framework, the population dynamics gets much more rich and complex. Proceeding similarly as for the 2-person framework, in this study we evaluate the effects of different learning rules, namely conformity and counterfactual thinking, in an homogeneous and well-mixed population of social learners, now following each the N-person games previously described in section 2.1.3. In this case, regarding cooperation optimization, we resort to the so called group achievement, η_G (see equation 2.35), to evaluate the overall dynamics, as a measure of the probability to achieve success.

4.2.1 Conformity

While in 2-person games agents are always aware of other individual's choices, in the N-person framework opes the possibility to exploit the common good by defectors, that go unnoticed [19]. This implies game dynamics to become much more rich and complex, specifically for social learning. However, notice that, even in this N-person framework, conformity-driven individuals are still aware of the other's choices, as they have the knowledge about the fraction of cooperators and defectors, meaning they may potentially block the possibility of defector's exploitation. In fact, following the reasoning from the previous results in Chapter 4, one would expect that, regardless on the **SL** original dynamics, conformity would always favour coordination dynamics.

Following the same reasoning as in the previous chapter, we start by investigating population's dynamics in communities with a fixed number of conformity-driven individuals, in a social learning environment. Attending to the multi-rule formulation where $\mathcal{L} = \{SL, C\}$, specifically for homogeneous populations we may define the deterministic gradient of selection equivalently to equation 4.1. Along with G, in the N-person framework, it would also be relevant to compute the group achievement as a measure of the probability to achieve success, like we previously did in Chapter 3. Note, however, that for games with a null threshold ($M = 0$), as in the case of the **NPD**, this measurement loses its effect, has we would have $\eta_G = 1$ independently on the population dynamics.

We will proceed the say way as before: we vary the probability of conformity in the interval $\delta^{[C]} \in [0; 1]$ and for each value we compute the relative gradient of selection, that is, G normalized between its minimum (negative) value to its maximum (positive) value. We will do this for each one of the four N-person games, previously described in section 2.1.3, more specifically, for **NSG** with $(N, M, b, c) = (10, 5, 1, 0.2)$, **NSH** with $(N, M, F, c) = (10, 5, 12, 0.5)$, **PGG** with $(N, F, c) = (10, 10, 0.7)$ and **CRD** with $(N, M, b, c, r) = (10, 6, 1, 0.15, 0.75)$. As in section 4.1.1, to force the same relative impact, we take both intensities of selection and conformity as $\beta^{[SL]} = 1.0$ and $\beta^{[C]} = 1.0$, respectively, and we take a population sized $Z = 50$ with a mutation rate of $\mu = \frac{1}{Z}$, so one can finally compute the relative gradient of selection for all $x \in [0; 1]$. All the results are shown below in Figure 4.5.

Generally, the results go along with the ones previously obtained for the 2-person framework: regardless of the social learning game, increasing the number of conformity-driven individuals will progressively favour a pure

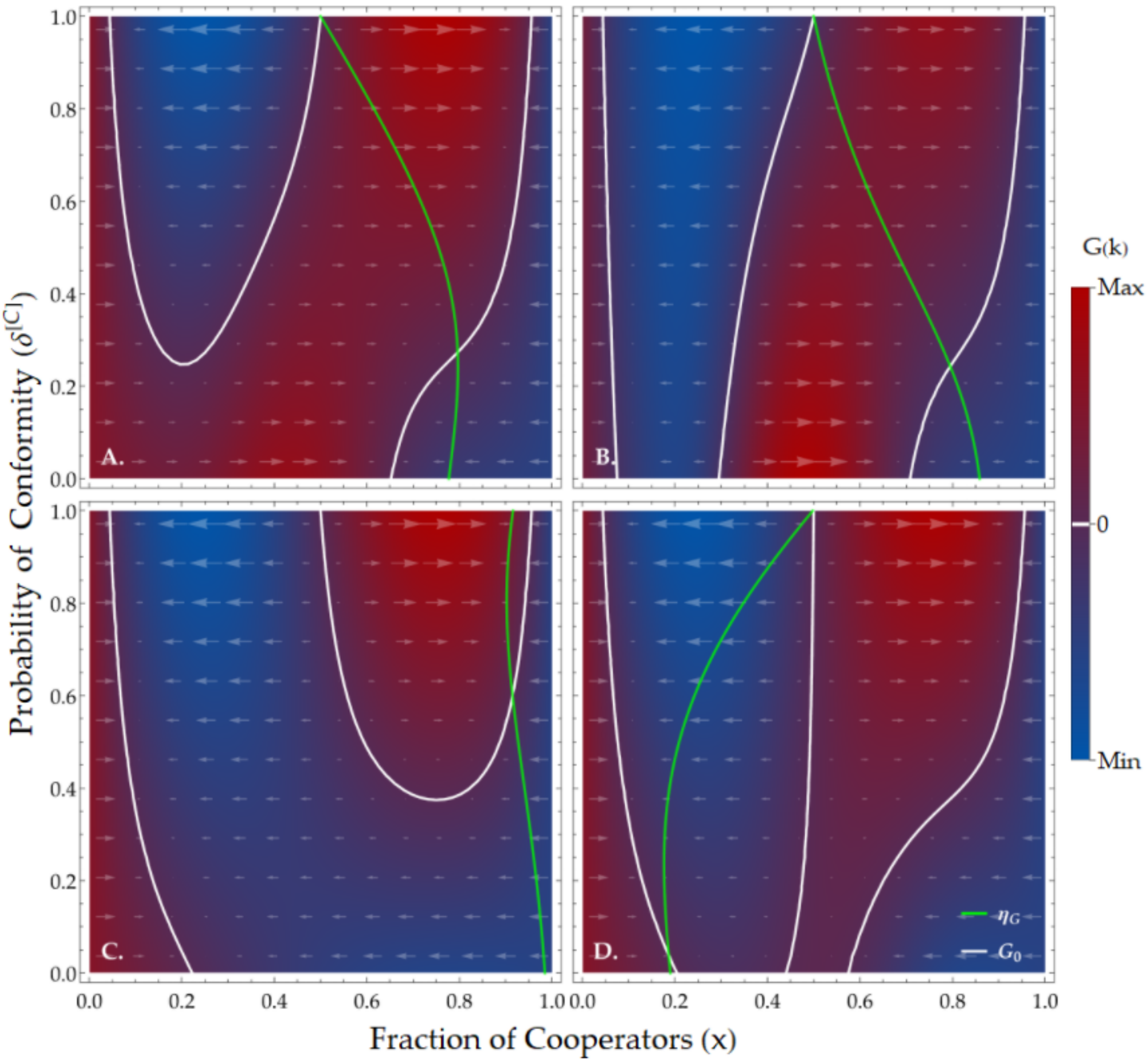

Figure 4.5: Relative gradient of selection in N-person games for populations of conformists and social learners, homogeneously well-mixed. We take a population sized $Z = 50$, with a mutation rate of $\mu = \frac{1}{Z}$, and with both intensities of social learning and conformity respectively as $\beta_{SL} = 1.0$ and $\beta^{[C]} = 1.0$. Panels from **A** to **D** respectively show the results on the **NSG**, **NSH**, **PGG** and **CRD** games. The gradient of selection is given relatively through normalization, from its minimum to its maximum values. The line in white represent the points of null gradient, while the green line represents the evolution of the group achievement (η_G) as we increase the value of $\delta^{[C]}$. Recall that the gradient of selection, being explicitly defined as a function of x for a fixed value of $\delta^{[C]}$, evolves horizontally in the graphic, and not vertically. Again, the conformity effects smoothly increase with increasing $\delta^{[C]}$, but when comparing to the 2-person framework, the general changes on the dynamics seem more accentuate. Regarding the group achievement, as we increase $\delta^{[C]}$, the n_G moves toward the conformity coordination fix point, regardless of the original game dynamics, with exception of **PGG**.

coordination dynamic, with a single unstable fix point at exactly $x = 0.5$, which is characteristic of the pure conformity dynamic. Notice that, contrarily to **CT**, this final dynamic is independent on the system's configuration.

Regarding the group achievement, irrespective on the social game dynamics, increasing the probability of conformity progressive moves the η_G towards the coordination fix point, at $x = 0.5$. If in the pure **SL** dynamic we have $\eta_G < 0.5$, we could expect conformity to be beneficial in the overall cooperation dynamics, as we can see in panel **D**, whereas, if we have $\eta_G > 0.5$, conformity would generally become prejudicial to the cooperation dynamics, as we can see in both panels **A** and **B**. Notice, however, that this does not mean that we cannot have an higher value for η_G in between the two extremes, $\delta^{[C]} = 0$ and $\delta^{[C]} = 1$. In fact, we notice that in panel **A** the maximum value for η_G stands for a value of $\delta^{[C]} \approx 0.25$, while in panel **B** the maximum value for η_G stands for $\delta^{[C]} = 0$. Generally, this means that, even when $\eta_G > 0.5$ for $\delta^{[C]} = 0$, conformity may either lead to an increase or decrease of the group achievement, depending on the probability of conformity, while when $\eta_G < 0.5$ for $\delta^{[C]} = 0$, conformity will always lead to an increase of the η_G, specially for higher values of $\delta^{[C]}$.

The conclusions above suggested are only valid for those certain game's configurations, that were carefully chosen, and, like that, one may wonder about the generalization of these results. For other different game's configurations, very different dynamics may rise, as we previously shown in both Figures 4.2 and 4.4, where modifying the intensity of a learning rule may lead to a drastic dynamic change. Besides these intensities, the game's configuration variables may also strongly transform the population dynamics. To show this, for one same N-person game, we may vary one of the game's configuration variable and analyze how it impacts the group achievement. In Figure 4.6, we take the three most interesting N-person games, in terms of η_G analysis, and for each we will take two of the game variables (one at a time) and vary them in a specific range, while the remaining variables remain untouched. Finally, for each value of $\delta^{[C]} \in [0; 1]$, we compute η_G, in the same way as previously, so one can analyze the dependency of η_G in the system's configurations. Essentially, we want to show that $\eta_G \equiv \eta_G(v)$, where v stand for the set of variables that define each game.

In the Figure 4.6, there are a lot of many different insights that may be taken, depending on the social game. For instance, for the **NSG**, in sub-figure **(a)**, the group achievement linearly decreases with the threshold, a trend that seems to occur independently on the probability of conformity, although, for higher values of $\delta^{[C]}$, this decrement on η_G no longer occurs as regularly as for a pure **SL** population. As a consequence, while for lower thresholds conformity may lead to a decrease in η_G, for higher thresholds conformity is actually promoting cooperation, leading to higher group achievements. Regarding the cost, in sub-figure **(b)**, the results matches the intuition that lower costs promote higher group achievements. Notice, however, that, when we have a full conformity population, we recover the expected $\eta_G = 0.5$, corresponding to conformity fix point. As that, and attending conformity dynamics are independent on the game's configuration, regardless of the initial value of η_G, increasing the probability of conformity will always lead to the conformity characteristic $\eta_G = 0.5$. This result may be observed in all graphics, with exception to the **(a)**, as the group achievement has a dependency on the multivariate hypergeometric sampling in its formal definition (equation 2.35), thus directly depending on N and M.

Regarding the **NSH**, from sub-figure **(c)**, and as one would expect, the higher the enhancement factor, the more likely we are to achieve success. However, and likely to sub-figure **(b)**, increasing conformity will be beneficial whenever the pure **SL** group achievement stands below 0.5, while for populations with $\eta_G > 0.5$ conformity will become a disadvantage. Relatively to the cost, in sub-figure **(d)**, we observe that, once again, lower costs promote higher group achievements. Moreover, as we have $\eta_G(\delta^{[C]} = 0) \leq 0.5$ for all pure **SL** populations in this configuration, increasing the conformity probability will generally lead to an improvement on the group achievement, even though in some cases we may notice a slight decrease followed by a stronger increase of η_G.

Finally, the results for the **CRD** appear to be very similar to the ones obtained for the **NSH**. However, in this case, for most the pure **SL** populations the group achievement lays under the 0.5 threshold, meaning that, once again, regardless on the initial η_G, conformity will always become generally beneficial in terms of cooperation maximization. From sub-figure **(f)**, and specifically to **CRD**, one may perceive how sensible the system's dynamic is to the cost, as η_G rapidly decreases with a small increase of c, until reaching values nearly 0 for $c \approx 0.35$.

Generally, and in accordance with the previous insights, conformity promotes a fixed group achievement of

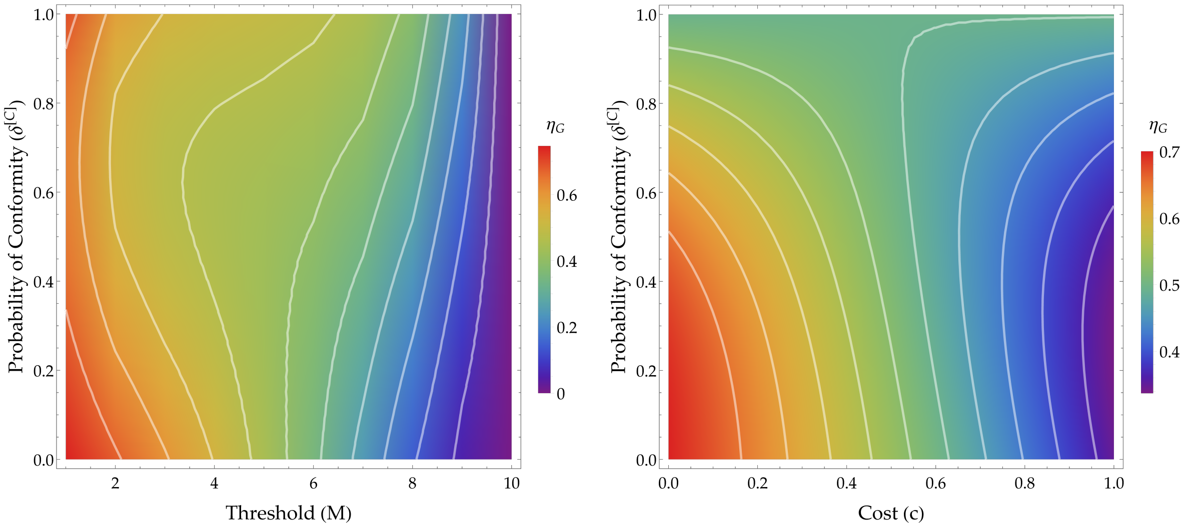

(a) **NSG**, with $(N, M, b, c) = (10, M, 1, 0.75)$.

(b) **NSG**, with $(N, M, b, c) = (10, 5, 1, c)$.

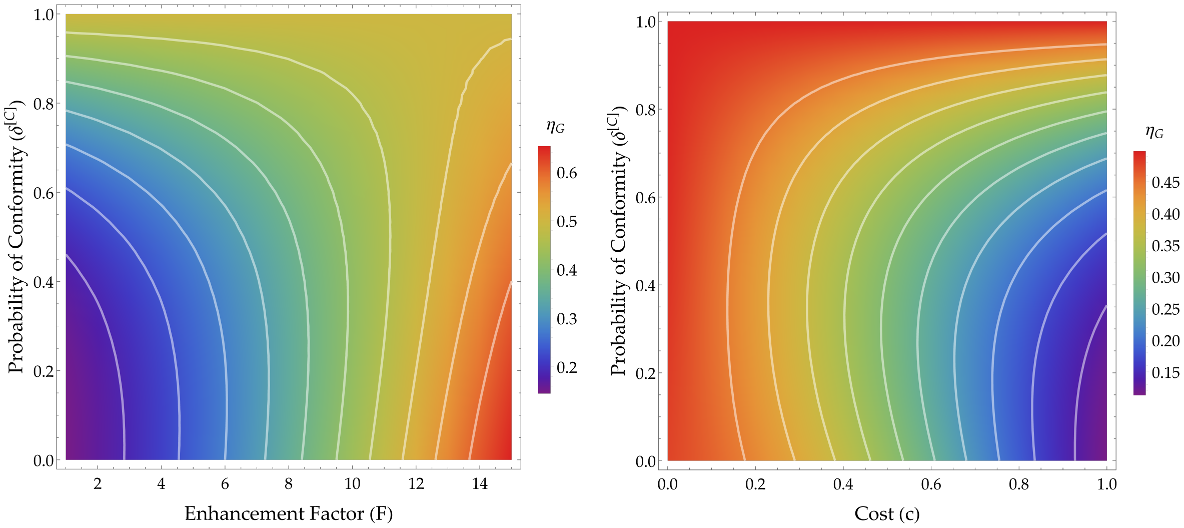

(c) **NSH**, with $(N, M, F, c) = (10, 5, F, 0.2)$.

(d) **NSH**, with $(N, M, F, c) = (10, 5, 10, c)$.

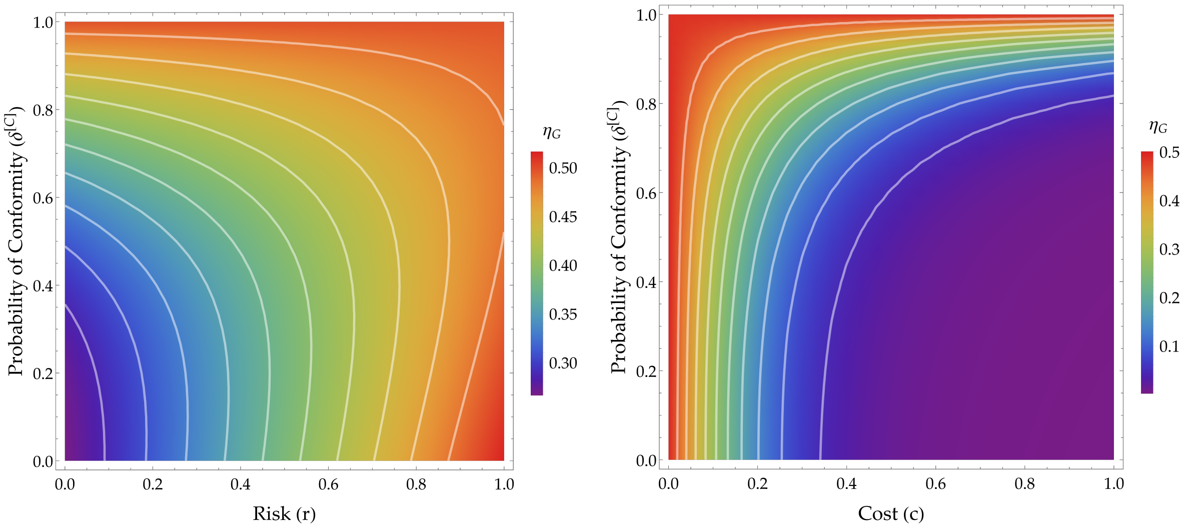

(e) **CRD**, with $(N, M, b, c, r) = (10, 5, 1, 0.1, r)$.

(f) **CRD**, with $(N, M, b, c, r) = (10, 5, 1, c, 0.1)$.

Figure 4.6: Group achievement for different N-person games under conformity, in well-mixed, homogeneous and finite populations sized $Z = 30$, $\mu = \frac{1}{Z}$, $\beta^{[SL]} = 1.0$, $\beta^{[C]} = 1.0$. For each graphic, we vary both the probability of conformity and one specific game's variable, and compute the η_G for each entry. For all the points we apply a 2$^{\text{nd}}$-order interpolation.

$\eta_G = 0.5$, correspondent to the unstable fix point characteristic of the conformity coordination dynamics. We showed that this result is independent on the game's configuration, with exception on both group size and threshold. This final result could be intriguing, since the group achievement should be maximum, as, in its formal definition, conformity-driven individuals are not engaged in groups. This brings up a whole new problematic that calls into question the results described above, urging the need for a new success measurement tool that takes into account all new learning rules, independently on how they are internally organized. However, we recall that we have been studying the effects on group achievement, specifically defined according to equation 2.35, that, even if not complete for the whole homogeneous dynamics, we may assume to be valid for all the learning rules displayed in groups.

4.2.2 Counterfactual Thinking in N-Person Games

In contrary to conformity, as counterfactual reasoning expressly depends on the game's configuration, we still have the possibility to let defectors exploit the common good. In accordance with the previous studies [13], we expect that even when individuals seldom resort to **CT**, highly cooperative standards are achieved. Although these insights were specifically applied for the **NSH**, we are also interested in analyzing how the presence of individuals with **CT**-enabled strategies affects the evolutionary dynamics under other collective action problems, namely, in the **NSG**, the **PGG** (in the form of **NPD**) and the **CRD**.

Once again, we start by investigating population dynamics in communities with different number of **CT**-driven agents, in a social learning environment. Attending to the multi-rule formulation, specifically for homogeneous populations, having $\mathcal{L} = \{SL, CT\}$, we may define the stochastic gradient of selection identically to equation 4.2. At this point, and recalling the previous insights about $T_{\pm}^{[CT]}$ value's magnitude relatively to $T_{\pm}^{[SL]}$, one must expect **CT** to have a very strong impact in a population full of social learners, an effect that can be countered by assuming an intensity of selection much stronger than the intensity of counterfactual reasoning, and so balance both learning rules relative strength, just like we previously explained in section 4.1.2. Like we did in the previous section, we compute the group achievement for each population, that is, for each value of $\delta^{[CT]}$. Recall that the results for the **PGG** are meaningless, standing at a constant value of $\eta_G = 1$, as we assume a null threshold for the **NPD**.

Once again, in a well-mixed, homogeneous and finite population of social learners and counterfactual thinkers, we will vary the probability of **CT** in the interval $\delta^{[CT]} = [0;1]$ and for each value we will compute the relative gradient of selection. For all the four N-person games previously described, more specifically, for **NSG** with $(N, M, b, c) = (10, 6, 1, 0.75)$, **NSH** with $(N, M, F, c) = (10, 5, 10, 0.2)$, **PGG** with $(N, F, c) = (10, 10, 0.5)$ and **CRD** with $(N, M, b, c, r) = (10, 6, 1, 0.1, 0.75)$, we take a population sized $Z = 50$, $\mu = \frac{1}{Z}$, $\beta^{[SL]} = 5.0$ and $\beta^{[CT]} = 1.0$, and we compute the relative gradient of selection for all $x \in [0; 1]$. The results are shown below in Figure 4.7.

With exception to the **PGG**, all the game dynamics are similar to each other. Having this, and taking into consideration the suggestions from [13], one would expect that a small prevalence of **CT**-driven agents is responsible for pushing the entire population to very high cooperative standards. In fact, our results go exactly in accordance with these insights: for all the **NSG**, **NSH** and **CRD**, a small increase on the probability of counterfactual thinking is responsible for an impressive improvement of the group achievement. However, there are some other things that we must be aware when analyzing these graphics.

Firstly, we may observe that, although a small incidence **CT** individuals is beneficial in terms of cooperation, after the reaching the maximum value for η_G, adding more and more **CT**-driven agents will progressively prejudice the cooperative standards. Furthermore, in some cases, like in **NSG**, from a certain value of $\delta^{[CT]}$, the group achievement gets even lower than on its initial value, on a pure **SL** population. Having this, we may complement the conclusions previously taken in [13] by stating that a small prevalence of **CT**-driven individuals promotes highly co-

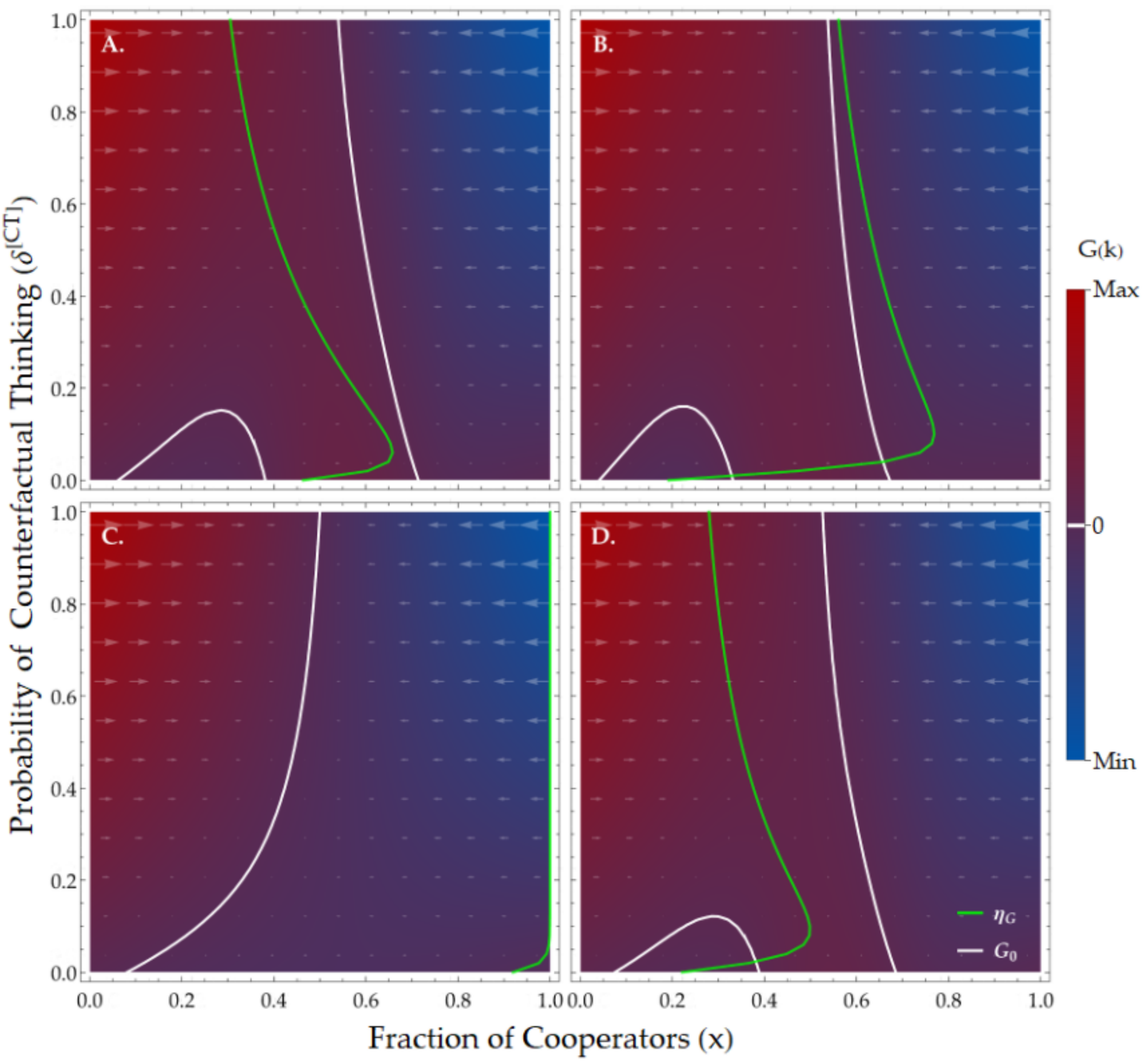

Figure 4.7: Relative gradient of selection in N-person games for populations of counterfactual thinkers and social learners, homogeneously well-mixed. We take a population sized $Z = 50$, with a mutation rate of $\mu = \frac{1}{Z}$, and with both intensities of social learning and counterfactual reasoning respectively as $\beta^{[SL]} = 5.0$ and $\beta^{[CT]} = 1.0$. Panels from **A** to **D** respectively show the results on the **NSG**, **NSH**, **PGG** and **CRD** games. The gradient of selection is given relatively through normalization, from its minimum to its maximum values. The line in white represent the points of null gradient, while the green line represents the evolution of the group achievement (η_G) as we increase the value of $\delta^{[CT]}$. Recall that the gradient of selection, being explicitly defined as a function of x for a fixed value of $\delta^{[CT]}$, evolves horizontally in the graphic, and not vertically. With exception to the **PGG**, the population dynamics are very similar to each other. In all cases, and as expected, we notice that a small prevalence of **CT**-driven individuals is responsible for nudging the entire population towards very high cooperative standards, although after a certain critical $\delta^{[CT]}$ the addition of more **CT** agents in the population becomes a disadvantage. Notice these results are only valid for this population configuration's in particular.

operative standards, but only until a certain point, from which adding more counterfactual thinkers to the population becomes a disadvantage to cooperative action.

Besides that, and like previously for conformity, notice that the results above shown are only valid for the specific game's configurations. For other different game's setup, very different dynamics may arise. This effect may be observed when, for one same N-person game, we vary one of the game's configuration variable and analyze how it impacts the group achievement. In Figure 4.8, we take the 3 most relevant N-person games and for each we take two (one at a time) of the game variables and vary them in a specific range. For each population, we finally compute the η_G, like we did previously, so we can analyze the dependency of η_G in the system's configurations.

In the Figure 4.8, there are a lot of many different insights that may be taken, depending on the social game. For instance, for the **NSG**, in sub-figure **(b)**, the group achievement is maximized for lower costs, especially whenever we have a lower value of $\delta^{[CT]}$. Besides that, from sub-figure **(a)**, while higher values for M affects η_G very negatively, lowering the threshold progressively favours η_G, although this only happens after reaching a certain critic probability of **CT**. Notice that this last insight corresponds exactly to the conclusions previously taken for Figure 4.7, where for all **NSG**, **NSH** and **CRD** we verified that a small portion of **CT**'s improves a lot the group achievement.

Regarding the **NSH**, from sub-figure **(c)**, while increasing the enhancement factor promotes higher values of η_G, for lower values of F raising the number of **CT** progressively leads to higher values for the group achievement. For higher values of F, in other hand, after a certain point increasing the number of **CT**'s does not have a great impact in the overall η_G, meaning that, while in some cases the amount of **CT**-driven individuals is linearly increasing the group achievement, in other cases having a small amount of counterfactual thinkers is enough to boost significantly η_G. Regarding the impact of varying the cost c, in sub-figure **(d)**, in a first analysis we notice it is completely different than the cost in the **NSG**, showing how different are the dynamics between each other. Furthermore, we may observe that $\delta^{[CT]}$ impact on η_G varies considerably with the cost, as we notice that increasing $\delta^{[CT]}$ does not have an impact at all, when c is very small, while for higher values of c rising the probability of **CT**'s leads to the massive growth of η_G, that we can observe.

Finally, for the **CRD**, from sub-figure **(e)**, we see that the risk follows approximately the same learning rule as the enhancement factor in the **NSH**, that is, higher values of r generally promotes higher η_G, independently on the probability of **CT**, while for lower risks we have lower values for the group achievement, that progressively increase as we raise $\delta^{[CT]}$. Regarding the costs, in a pure-**SL** population, $c = 0$ gives us the highest values for η_G in this setup, that rapidly decreases as we increase c, in such a way that, for approximately $c = 0.2$, we already reach a null group achievement regime. In this scenario, even though we observe that rising the number of **CT**-driven agents generally promotes an increase on η_G, for a very small values of c we notice that increasing $\delta^{[CT]}$ actually reduces the group achievement. This effect is easily noticeable for $c = 0$, where η_G is maximal when $\delta^{[CT]} = 0$ and gets progressively reduced as we increase the probability of counterfactual reasoning.

These are just some of the possible outcomes when studying the impact of different population's configurations, made specifically for the game settings above presented. If one intend to maximize the cooperative standards, for a certain game, many different studies of this kind should be performed, so by crossing all the information one would get the configuration that would maximize the group achievement.

4.3 Final Notes

For both 2-person and N-person framework, conformity shows to bring a very stable dynamic, being completely independent on the social game's configuration. Even though this dynamic strongly depends on the intensity of conformity, the formal definition of conformity states that it should promote coordination regardless on the system's configuration. In short, values of $\beta^{[C]}$ that promote co-existence rather than coordination are said to be invalid, as conformity would lose its physical meaning. This way, we may generally conclude that conformity will always promote a pure coordination dynamic, with its characteristic unstable fix point at $x = 0.5$. Furthermore, one may also conclude that it is required a considerable prevalence of conformity-driven agents to substantially change the social game dynamics, as the conformity gradient is dimensionally equivalent to the social learning gradient.

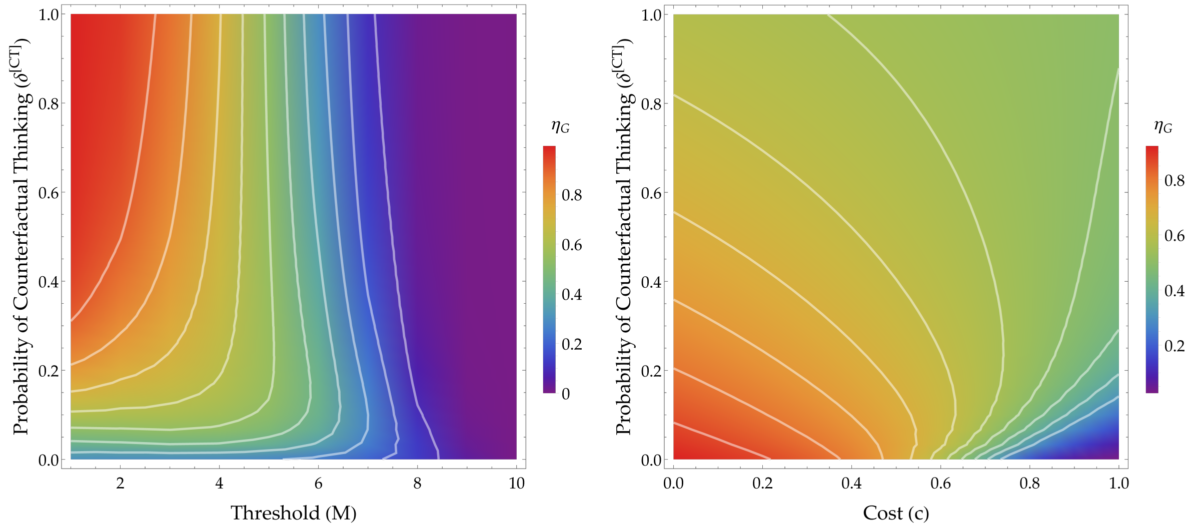

(a) **NSG**, with $(N, M, b, c) = (10, M, 1, 0.75)$.

(b) **NSG**, with $(N, M, b, c) = (10, 5, 1, c)$.

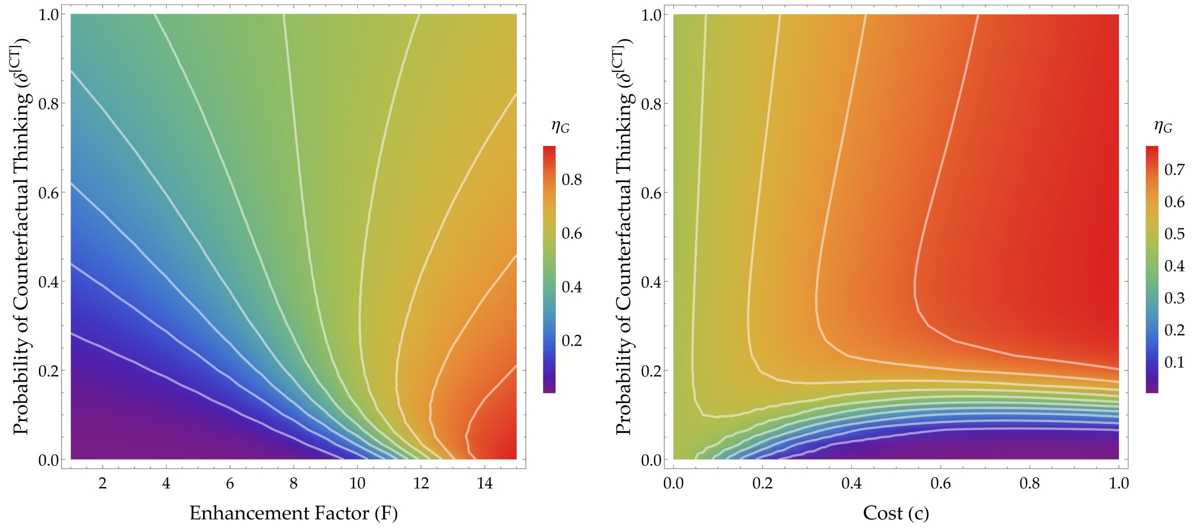

(c) **NSH**, with $(N, M, F, c) = (10, 5, F, 0.2)$.

(d) **NSH**, with $(N, M, F, c) = (10, 5, 10, c)$.

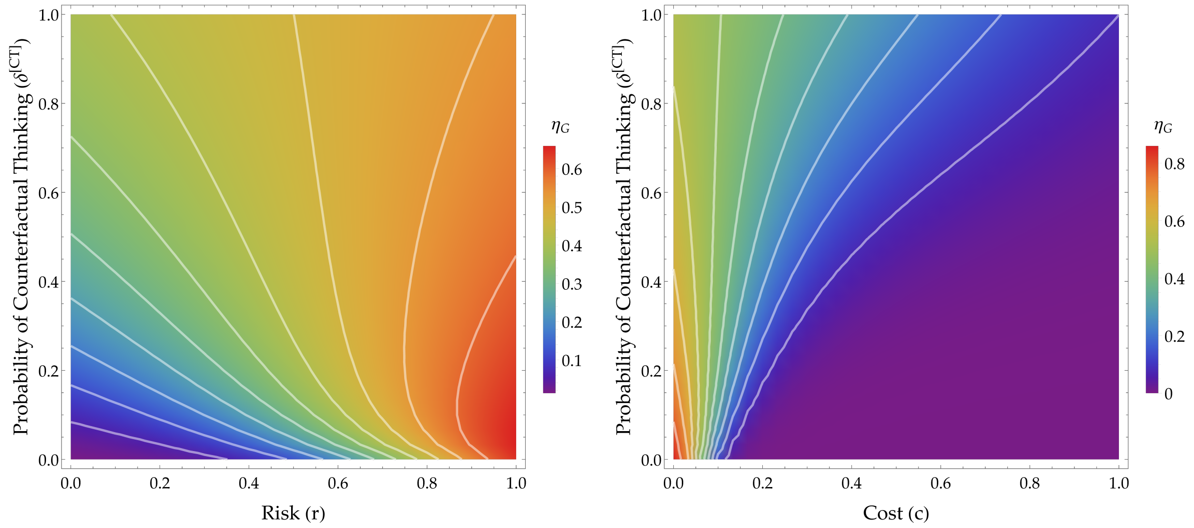

(e) **CRD**, with $(N, M, b, c, r) = (10, 5, 1, 0.1, r)$.

(f) **CRD**, with $(N, M, b, c, r) = (10, 5, 1, c, 0.5)$.

Figure 4.8: Group achievement for different N-person games, in well-mixed, homogeneous and finite populations sized $Z = 30$, $\mu = \frac{1}{Z}$, $\beta^{[SL]} = 5.0$, $\beta^{[CT]} = 1.0$. For each graphic, we vary one specific game's variable and the $\delta^{[CT]}$, and compute the η_G. For all the points we apply a 2nd-order interpolation.

Recall this modification on the dynamics may have either a positive or a negative impact regarding cooperation maximization, depending whether the **SL** dynamics provides, or not, a worst scenario in terms of cooperation, when compared to the conformity coordination dynamics.

Regarding counterfactual reasoning, things get more complex. We saw that, for populations in the exact same conditions, increasing the level of counterfactual thinking may lead to opposite dynamics, that highly depend on the intensity of **CT**. While for relatively lower values of $\beta^{[CT]}$ individuals resorting to **CT** promote a co-existence dynamic, for higher intensities a coordination dynamic is favoured. Moreover, we saw that **CT** is highly dependent on the game's configuration, although generally acts in favor of maximizing cooperation, especially in the N-person framework, were we saw that, in most cases, increasing $\delta^{[CT]}$ leads to higher η_G, until a certain critic point. We were able to complement the insights from [13], showing that, for some cases, regarding collective action, a small prevalence of **CT**-driven individuals is sufficient to foster highly cooperative standards, but only until a certain point, from which adding more **CT** agents becomes a disadvantage.

Despite the complexity on studying these population dynamics, it is common to reach the same results for different combinations of configurations. To reduce the dimensionality of the problem, it may be relevant to suppress some variables, by defining a new one as a function of other two, just like previously done in Figure 3.5. For this section, it would appropriate to compute the relation between $\beta^{[SL]}$ and $\beta^{[CT]}$, but however, it may not be trivial. Experimentally, one may verify that having $\beta^{[SL]} = 5$ and $\beta^{[CT]} = 1$ will produce very different results than $\beta^{[SL]} = 1$ and $\beta^{[CT]} = 0.2$. This may indicate that, when building these relations, one must be also aware of the magnitude of the values of the variables themselves. For further work, it would be very relevant to find any relations between certain combination of variables, that would allow a much simpler and direct evaluation of the system's dynamics.

Chapter 5

Population Dynamics in Heterogeneous Populations

In real world networks, for a same population, individuals may be organized heterogeneously according to their learning rules, that is, agents following different learning rules are commonly displayed in different sub-populations, rather than homogeneously mixed in one same population. In this chapter, we investigate the dynamics of different N-person games, in the case of well-mixed and finite populations, heterogeneously sub-divided according to the available learning rules. More specifically, we evaluate the multi-dimensional gradient of selection that will map out the system's fix points, eventually giving rise to a whole new dynamics, that one expects to be different from the results previously obtain for homogeneous populations.

5.1 Heterogeneous Populations

When exploring heterogeneous populations, a different approach must be taken. While in homogeneous populations the number of cooperators or defectors, or even the population size, is not discriminated for each learning rule, in heterogeneous populations one must track each of the variables individually. Roughly speaking, moving to heterogeneous populations, with l available learning rules, means we are dividing our main population into l sub-populations of individuals with the same learning rule. Each sub-population may be, then, evaluated singularly, just as if it were, by itself, an homogeneous well-mixed pure-learning rule population. However, its dynamics will always depend on all the other sub-populations, a dependency that will be weighted by the homophily, h, just as previously described in section 2.4.3: when $h = 0$ anyone in the population may influence and be influenced by anyone else, while when having $h = 1$ individuals are restricted to influence (and be influenced) by those of the same sub-population.

In the following studies, we ought to analyze the effect of homophily in the behavioral dynamics, from a completely homophilic relation between learning rules, with $h = 1$, to the absence of homophily, with $h = 0$. In the latter case, as individuals interact with one another regardless on their sub-population, we recover the essence of the homogeneous dynamics, now represented in the l-dimensional space. We perform a study similar to [36], but however, in our setup, the different learning rules take the role of the different social classes. This new dynamics may be escorted by different challenges, as not all learning rules regulate their strategic decisions based in strategy fitness, which is the case of conformity, for instance, that bases its strategic decision on the frequency strategies occur. In this sense, for each study we will explicitly present all the dynamics behind the results seen along the chapter.

More in concrete, we will be exploring the population dynamics for different heterogeneous populations, in scenarios with only two learning rules ($b = 2$), thus having $\mathcal{L} = \{L_1, L_2\}$, with $L_{1,2} \in \{SL, C, CT\}$. In this specific case, and for the sake of simplicity, we assume the homophily to be bidirectional, that is, we assume $h_{L_1 \to L_2} = h_{L_2 \to L_1} \equiv h$. Of course, for more complex dynamics, it would be interesting to analyze various population dynamics where this assumption is not valid, looking to find any relation between the distinct homophilies and cooperation optimization, but for now, we will stick to this simpler case.

All the following analysis will be performed under different N-person social games, due to their much more complex dynamics. Moreover, and as an evaluation tool for cooperation maximization, we may compute the average group achievement. For multiple learning rules, we make use of the multivariate hypergeometric sampling to compute the average fraction of groups that accomplish a total in contribution of $Mc\bar{b}$, corresponding to achieving the public good, previously designated as $a_G(\boldsymbol{i})$. In other words, and similarly to the previously explained in section 2.3.3, it may be obtained by replacing $\Pi_{S_k}(\boldsymbol{j})$ by $\Theta(\sum_{L \in \mathcal{L}} c^{[L]} j_C^{[L]} - Mc\bar{b})$ in Equation 2.10, where $c^{[L]}$ is defined as the contributions from cooperators resorting to learning rule $L \in \mathcal{L}$, and $\bar{b}$ the average endowment. Having $a_G(\boldsymbol{i})$, we may finally compute the average group achievement, η_G, again according to equation 2.35.

5.2 Conformity and Social Learning

We start by building a population configuration where we have both social learners and conformist, that is, having the set of available learning rules as $\mathcal{L} = \{SL, C\}$. In this setup, and following the previous descriptions for heterogeneous populations, from section 2.4.3, we consider a population of $Z = Z^{[SL]} + Z^{[C]}$ individuals, from where $Z^{[SL]}$ obey to social learning while $Z^{[C]}$ follow conformity. Individuals resorting each learning rule are given an initial endowment, $b^{[SL]}$ for **SL** and $b^{[C]}$ for conformity, that will remain fixed, and play the N-person game in study, thus engaging in groups sized N. Each type of cooperators will contribute for the public good with $c^{[SL]} = c \cdot b^{[SL]}$ and $c^{[C]} = c \cdot b^{[C]}$, respectively for **SL** and **C**. For each the collective social game, one must specify each the possible payoffs resulting from agent's interactions. Following each game's formulation from section 2.1.3, and attending to [36] formulation, the payoffs for each the N-person social games may be given according to:

- **NSG**, with the parameters $(N, M, \bar{b}, b^{[C]}, b^{[SL]}, c)$:

$$\Pi_C^{[SL]}(i_C^{[SL]}, i_C^{[C]}) = \Pi_D(i_C^{[SL]}, i_C^{[C]}) - \frac{c^{[SL]}}{i_C^{[SL]} + i_C^{[C]}}\Theta - \frac{c^{[SL]}}{M}(1 - \Theta) \tag{5.1}$$

$$\Pi_D^{[SL]}(i_C^{[SL]}, i_C^{[C]}) = b^{[SL]}\Theta \tag{5.2}$$

- **NSH**, with the parameters $(N, M, \bar{b}, b^{[C]}, b^{[SL]}, c, F)$:

$$\Pi_C^{[SL]}(i_C^{[SL]}, i_C^{[C]}) = \Pi_D(i_C^{[SL]}, i_C^{[C]}) - c^{[SL]} \tag{5.3}$$

$$\Pi_D^{[SL]}(i_C^{[SL]}, i_C^{[C]}) = (i_C^{[SL]} + i_C^{[C]})\frac{F\bar{c}}{N}\Theta \tag{5.4}$$

- **CRD**, with the parameters $(N, M, \bar{b}, b^{[C]}, b^{[SL]}, c, r)$:

$$\Pi_C^{[SL]}(i_C^{[SL]}, i_C^{[C]}) = \Pi_D(i_C^{[SL]}, i_C^{[C]}) - c^{[SL]} \tag{5.5}$$

$$\Pi_D^{[SL]}(i_C^{[SL]}, i_C^{[C]}) = b^{[SL]}(\Theta + (1 - r)(1 - \Theta)) \tag{5.6}$$

where for all cases we have $\Theta \equiv \Theta(c^{[SL]} i_C^{[SL]} + c^{[C]} i_C^{[C]} - \bar{c}M)$ as the Heaviside function, that is, $\Theta(k) = 1$ whenever $k \geq 0$ and $\Theta(k) = 0$ otherwise. We also have $\bar{c} = c\bar{b}$ where $Z\bar{b} = Z^{[SL]} b^{[SL]} + Z^{[C]} b^{[C]}$ is the average endowment. Notice that all quantities, c, $\bar{b}$, $b^{[SL]}$ and $b^{[C]}$ are all real positive numbers.

In contrary to **SL**, conformity does not rely on fitness in the strategic decision, rather depending in the number of individuals following each strategy. In this sense, one may generally define:

$$\Pi_C^{[C]} \equiv x_C^{(Z-1)} = \frac{i_C^{[C]} + i_C^{[SL]}}{Z-1} \qquad \Pi_D^{[C]} \equiv x_D^{(Z-1)} = \frac{i_D^{[C]} + i_D^{[SL]}}{Z-1} \tag{5.7}$$

From these payoffs, one may compute the fitness $f_S^{[L]}$ for any strategy $S \in \mathcal{S}$ and any learning rule $L \in \mathcal{L}$. As conformity populations are not engaged in groups of size N, like social learners, the conformity fitnesses are reduced to their respective payoffs. Regarding social learning, we may define the respective fitnesses naturally using the multivariate hypergeometric sampling without replacement, according to equation 2.10 as:

$$f_C^{[SL]}(\boldsymbol{i}) = \binom{Z-1}{N-1}^{-1} \sum_{j^{[SL]}=0}^{N-1} \sum_{j^{[C]}=0}^{N-1-j^{[SL]}} \binom{i^{[SL]}-1}{j^{[SL]}} \binom{i^{[C]}}{j^{[C]}} \binom{Z - i^{[SL]} - i^{[C]}}{N-1-j^{[SL]}-j^{[C]}} \Pi_C^{[SL]}(j^{[SL]}+1, j^{[C]}) \tag{5.8}$$

$$f_D^{[SL]}(\boldsymbol{i}) = \binom{Z-1}{N-1}^{-1} \sum_{j^{[SL]}=0}^{N-1} \sum_{j^{[C]}=0}^{N-1-j^{[SL]}} \binom{i^{[SL]}}{j^{[SL]}} \binom{i^{[C]}}{j^{[C]}} \binom{Z-1-i^{[SL]} - i^{[C]}}{N-1-j^{[SL]}-j^{[C]}} \Pi_D^{[SL]}(j^{[SL]}, j^{[C]}) \tag{5.9}$$

Assuming an asynchronous updating process in the evolutionary dynamics, from these fitnesses we may compute all the required transition probabilities, for both learning rules, directly derived from equation 2.51, as follows:

$$T_{C\to D \backslash D \to C}^{[SL]}(\boldsymbol{i}) \equiv T_{\mp}^{[SL]}(\boldsymbol{i}) = \frac{i_{C\backslash D}^{[SL]}}{Z} \left\{ \frac{i_{D\backslash C}^{[SL]} + (1-h) i_{D\backslash C}^{[C]}}{Z^{[SL]} - 1 + (1-h) Z^{[C]}} \left(1 + e^{\beta^{[SL]}(f_{C\backslash D}^{[SL]}(\boldsymbol{i}) - f_{D\backslash C}^{[SL]}(\boldsymbol{i}))^{-1}} \right) \right\} \tag{5.10}$$

$$T_{C\to D \backslash D \to C}^{[C]}(\boldsymbol{i}) \equiv T_{\mp}^{[C]}(\boldsymbol{i}) = \frac{i_{C\backslash D}^{[C]}}{Z} \left\{ \frac{i_{D\backslash C}^{[C]} + (1-h) i_{D\backslash C}^{[C]}}{Z^{[C]} - 1 + (1-h) Z^{[SL]}} \left(1 + e^{\beta^{[C]}(f_{C\backslash D}^{[C]}(\boldsymbol{i}) - f_{D\backslash C}^{[C]}(\boldsymbol{i}))^{-1}} \right) \right\} \tag{5.11}$$

where $f_S^{[C]}$ is reduced to $\Pi_S^{[C]}$, for $S \in \{C, D\}$, as previously stated. Recall that taking into account a certain mutation rate does not change in heterogeneous populations, and hence one may redefine the previous transition probabilities according to equations 2.23 and 2.24.

From these transition equations, we may compute the transition matrix, following the description from section 2.3.3, however it must be adapted to a multi-dimensional space. To do so, we start by indexing all the possible states, that is, all configurations $\boldsymbol{i} = \{i_C^{[SL]}, i_C^{[C]}\}$, with an integer number. For this conversion, we define a bijective function V such that $p = V(\boldsymbol{i})$ and $q = V(\boldsymbol{i'})$, and, consequently, $\boldsymbol{i} = V{-}1(p)$ and $\boldsymbol{i'} = V{-}1(q)$. Afterwards, we may write the transition matrix in such a way that $\mathcal{T}_{qp} = T_{\boldsymbol{i}\to\boldsymbol{i'}}$, where $T_{\boldsymbol{i}\to\boldsymbol{i'}}$ is the corresponding transition probability from configuration $\boldsymbol{i}$ to $\boldsymbol{i'}$, and, having computed $\mathcal{T}$, one may finally obtain the stationary distribution as usual, according to equation 2.33 [36]. To the obtained vector it is applied the inverse of V so one may finally obtain the stationary distribution directly as a function of $\boldsymbol{i}$, as $\bar{s} \equiv \bar{s}(\boldsymbol{i})$.

Lastly, from this transition probabilities, and following equation 2.52, we may generally define the 2-dimensional heterogeneous gradient of selection for social learning and conformity as follows:

$$\nabla(\boldsymbol{i}) = \{G^{[SL]}(\boldsymbol{i}), G^{[C]}(\boldsymbol{i})\} = \{T_+^{[SL]}(\boldsymbol{i}) - T_-^{[SL]}(\boldsymbol{i}), T_+^{[C]}(\boldsymbol{i}) - T_-^{[C]}(\boldsymbol{i})\} \tag{5.12}$$

In this N-person framework, specifically in a setup with two learning rules, we may evaluate the overall dynamics in terms of cooperation optimization by computing the group achievement as:

$$\eta_G(\boldsymbol{i}) = \sum_{j^{[SL]}=0}^{Z^{[SL]}} \sum_{j^{[C]}=0}^{Z^{[C]}} a_G(\{j^{[SL]}, j^{[C]}\}) \cdot \bar{s}(\{j^{[SL]}, j^{[C]}\}) \tag{5.13}$$

Having all this quantities, we are now in conditions to proceed to the gradient evaluation. For each the N-person games, previously defined in equations 5.1-5.6, we start by investigating the effects of homophily in evolutionary dynamics for populations with an equal amount of social learners and conformists, that is, having $Z^{[SL]} = Z^{[C]}$.

In the same way as in the homogeneous populations studies, we will evaluate the system's dynamics in both terms of the gradient of selection, $\nabla(\boldsymbol{i})$, and the stationary distribution, $\bar{s}(\boldsymbol{i})$, for every single possible configuration, which, in this case, corresponds to varying both $i_C^{[SL]} \in [0; Z^{[SL]}]$ and $i_C^{[C]} \in [0; Z^{[C]}]$. Taking a population size of $Z = 100$, hence having $Z^{[SL]} = Z^{[C]} = 50$, with a mutation rate of $\mu = \frac{1}{Z}$, and with both learning rules equally balanced with the intensities $\beta^{[SL]} = \beta^{[C]} = 1$, we start by investigating the homophily effects on the dynamics of both **NSG** and **NSH**. The obtained results are shown in the Figure 5.1 below.

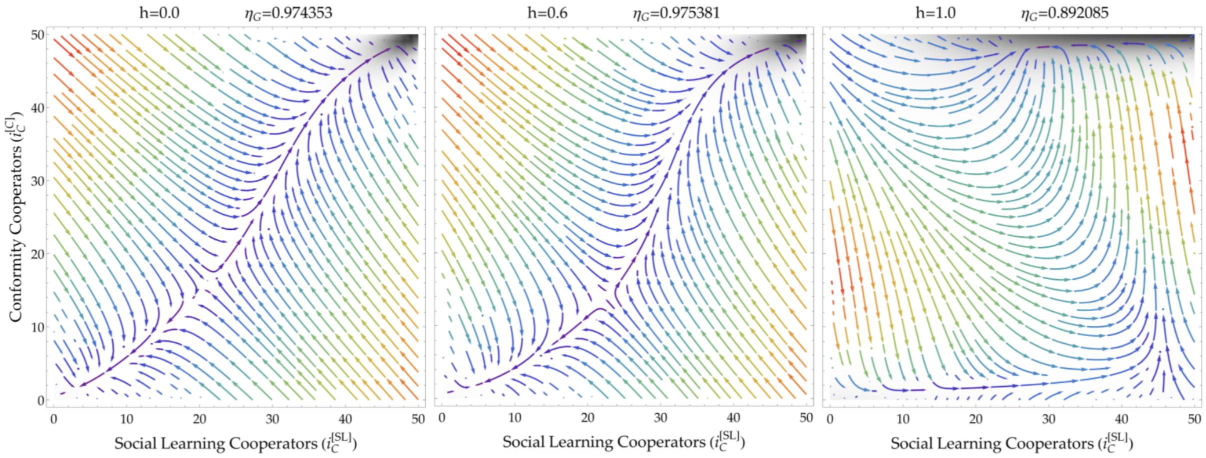

(a) **NSG**, with $(N, M, b^{[SL]}, b^{[C]}, c) = (10, 5, 1, 1, 0.1)$.

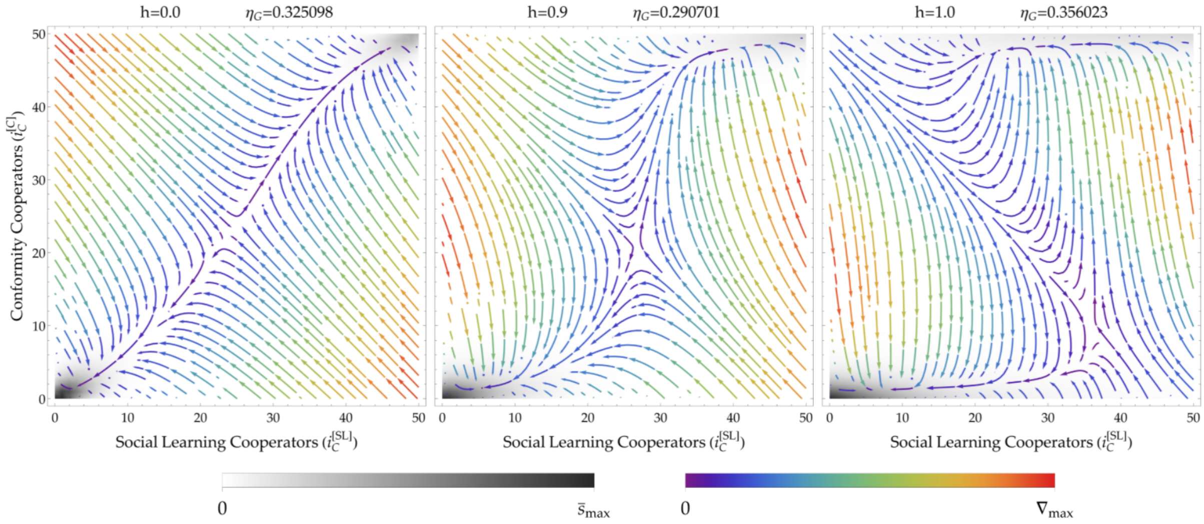

(b) **NSH**, with $(N, M, b^{[SL]}, b^{[C]}, c, F) = (10, 5, 1, 1, 0.1, 9)$.

Figure 5.1: Gradient of selection for the **NSG** and the **NSH** under conformity, in heterogeneous populations with $Z^{[SL]} = Z^{[C]} = 50$, $\mu = \frac{1}{Z}$, $\beta^{[SL]} = \beta^{[C]} = 1.0$. We investigate the effects of increasing homophily in the population dynamics, that is, on ∇ and $\bar{s}$ for each possible configuration.

A quick reminder that, along this chapter, most studies will be performed for a specific game setup, as we rather focus on the overall dynamics in heterogeneous populations than on its dynamics dependency on the game setup.

Regarding the figure above, for both **NSG** and **NSH**, we notice that, having null homophily, one can recover, in some way, the typical homogeneous conformity dynamics, characterized by the existence of three fix points, two of them being stable on the monomorphic states (they will be addressed as such), in this case, with $(i_C^{[SL]}, i_C^{[C]}) \approx (0,0)$ or $(i_C^{[SL]}, i_C^{[C]}) \approx (Z^{[SL]}, Z^{[C]})$, while the other is unstable at the center, at $(i_C^{[SL]}, i_C^{[C]}) \approx (0.5\, Z^{[SL]}, 0.5\, Z^{[C]})$. This insight comes more clear if we take into consideration the symmetry of the dynamics, which in this case may be considered practically symmetrical. In general, this dynamic seems to replicate with increasing homophily, but only until a certain point, from which the dynamics is highly modified.

For the **NSG** in this specific setup, from sub-figure **(a)**, and attending to the stationary distribution, the stable equilibrium relative to the cooperation monomorphic state is clearly much stronger than the other one, as the system spends much more time in the first case. Moreover, we notice that the population dynamics is not much sensitive to most lower homophily values, when, even having homophily at 60%, the population dynamics is practically the same as for $h = 0$, but however, if one keep increasing the homophily, we will eventually reach a threshold from which the system dynamics strongly changes, specially when h is maximum. In this latter case, as we can see from the graphic on the right, the cooperation monomorphic fixed point has moved to the left (lower $i_C^{[SL]}$), while the other two fix points, the other stable and the unstable one, have disappeared. This result may suggest that an increase of the homophily may lead a new dynamics where the only most probable outcome, after a sufficient amount of time, is a configuration that promotes highly cooperative standards. Even though the group achievement is lower than in the other cases with lower h, which could indicate a worst performance in terms of cooperation optimization, we no longer have the tendency to move towards the defection monomorphic state, having only one strong attraction point (in terms of evolutionary dynamics a stable fix point is an attraction point).

The same does not occur in the **NSH**, shown in sub-figure **(b)**. Firstly, we may observe that, contrary to the **NSG**, the stationary distribution has its maximum value for the defection monomorphic state, rather than for the cooperation one. Besides that, but now alike the previous case, the population dynamics is not sensitive to most lower values of homophily, although, keeping to increase the value of h will eventually lead to strong modifications in the population dynamics. However, in this case, instead of the fix points disappear, they progressively move away from their homophilic position. In specific, the cooperation monomorphic fix point moves the left (lower $i_C^{[SL]}$) and the defection monomorphic fix point, the stronger one, slightly moves to the right (higher $i_C^{[SL]}$), while the unstable equilibrium moves to a configuration with higher $i_C^{[SL]}$ but lower $i_C^{[C]}$. So, contrary to to the **NSG**, for this specific setup, increasing the homophily will not affect conceptually the dynamic of the population, where defection is favoured, although the equilibria, either stable or unstable, will change with increasing h.

Regarding the group achievement, we notice something particularly interesting: the relations between η_G and h are not linear, that is, the value for h for which the group achievement is maximum is not necessarily 1. For instance, from the available results for the **NSG**, we infer a very light increase of η_G from $h = 0$ to $h = 0.6$, whereas for the homophilic setup the group achievement reaches its lowest value. In opposition, for the **NSH**, the group achievement starts to decrease with increasing homophily, however it rapidly rises from the lowest value on $h = 0.9$ to its maximum at $h = 1$. Having such different learning rules for the relation between the homophily and the probability of success, that is, for $\eta_G(h)$, a more detailed study on this topic shall be addressed. But firstly, we will analyze the homophily effects on the **CRD** dynamics, just like previously done for both **NSG** and **NSH**.

The dynamic of the collective risk dilemma is usually known to be very sensitive to the risk, as one may infer from many different studies [33, 35–37]. In this reasoning, and like previously performed, for this game in specific, we will address the investigation of the effect of increasing homophily on the population dynamics for different values of the risk, specifically, for $r = \{0, 0.5, 1\}$. The results are shown below in Figure 5.2.

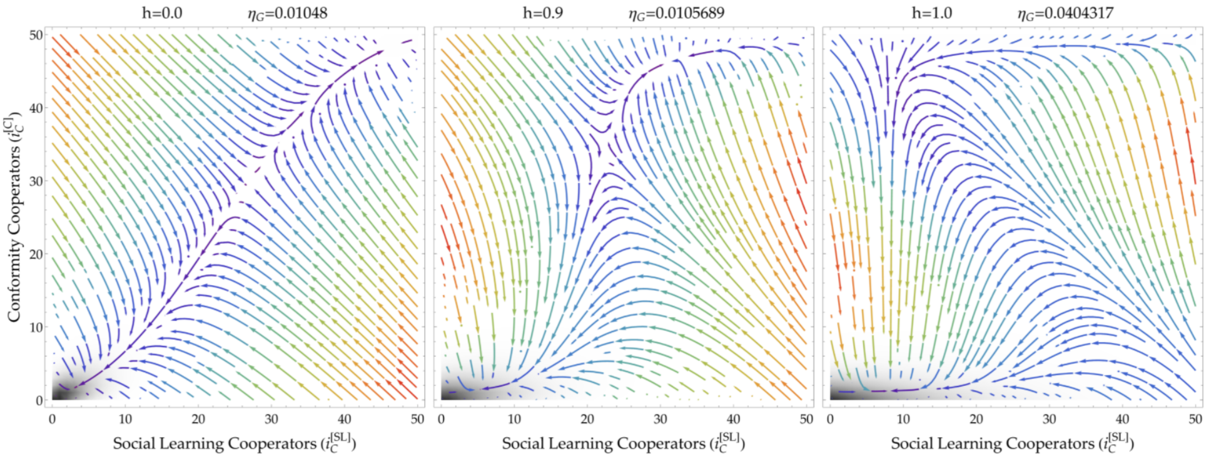

(a) **CRD**, with $(N, M, b^{[SL]}, b^{[C]}, c, r) = (10, 5, 1, 1, 0.1, 0)$.

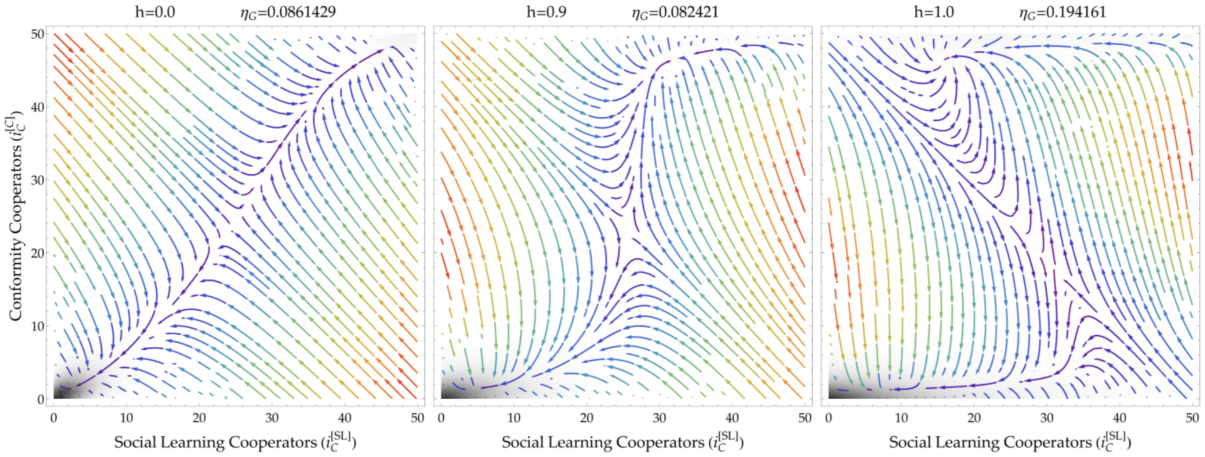

(b) **CRD**, with $(N, M, b^{[SL]}, b^{[C]}, c, r) = (10, 5, 1, 1, 0.1, 0.5)$.

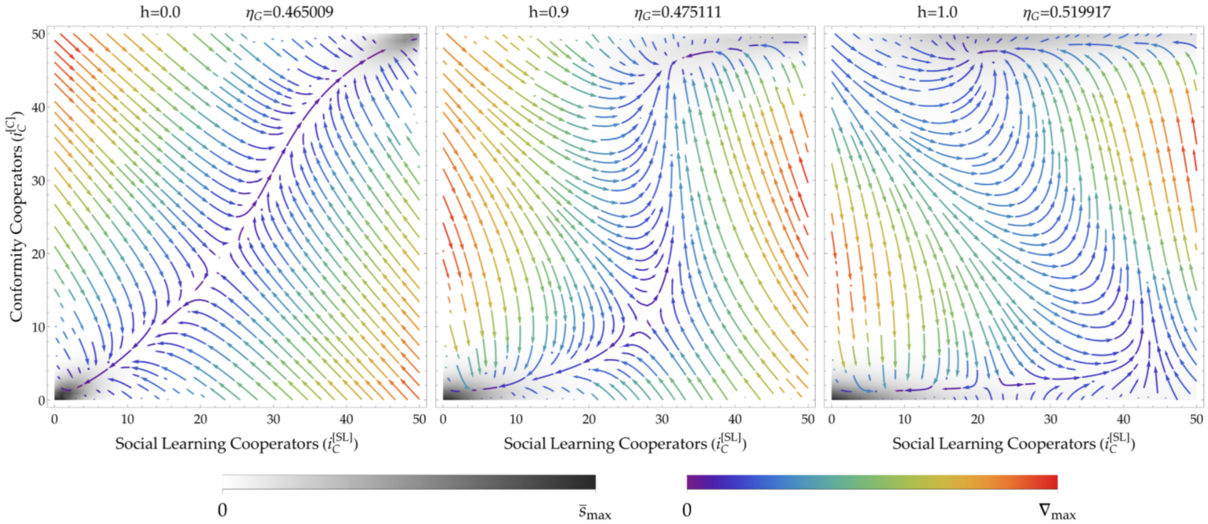

(c) **CRD**, with $(N, M, b^{[SL]}, b^{[C]}, c, r) = (10, 5, 1, 1, 0.1, 1)$.

Figure 5.2: Gradient of selection for different **CRD** games, with various r, under conformity, in heterogeneous populations with $Z^{[SL]} = Z^{[C]} = 50$, $\mu = \frac{1}{Z}$, $\beta^{[SL]} = \beta^{[C]} = 1.0$. We investigate the effects of increasing homophily in the population dynamics, that is, on ∇ and $\bar{s}$ for each possible configuration.

We start by ascertain that, when the homophily is null, regardless on the value of the risk, the dynamics are nearly the same, as we have recovered the homogeneous conformity dynamics. The only differences come from a very slight variation of the position of the unstable fix point, that progressively moves to the left as we increase the risk, and on the stationary distribution, where we observe the cooperation monomorphic state is also a viable outcome when the risk is maximum, while for the other cases only defection is expected. Like before, for both **NSG** and **NSH**, the dynamics maintains the same as we increase the homophily, until a certain point, from where it is highly modified. In fact, when we have $h = 0.9$, we may already notice that the fix points on the edges, for cooperation and defection monomorphic states, have, respectively, moved to the left (lower $i_C^{[SL]}$) and to the right (higher $i_C^{[SL]}$). Moreover, regarding the position of the internal equilibrium, it is interesting to notice the following: as we increase the risk, the fix point gradually moves down (lower $i_C^{[C]}$), a result that goes along with the first insight taken for $h = 0$. In fact, the overall dynamics appears to be the result of twisting the null homophily symmetry, in a circular motion, counter-clockwise, and hence slightly pushing the edge's fix points closer to the center. However, this insights are merely empirical speculations, from only a visual point of view, and hence they should not be taken as formally well-grounded.

For the maximum homophily regime, things get more exciting. Starting off with half risk, $r = 0.5$, and attending to the previous insights, the internal equilibrium stands approximately in the middle, regardless on the homophily, even though, when it is maximum ($h = 1$), it lightly deviates from the central position in a bottom-right direction. The stable fix points follow a learning rule very close to the one from **NSH**, where cooperation monomorphic equilibrium has moved to lower $i_C^{[SL]}$ and defection equilibrium has moved to higher $i_C^{[SL]}$. Conceptually, in this case, the dynamics keeps its original form, and hence we will take it as a comparison basis. When the risk is null, we notice that two equilibria, the unstable and one stable, have disappeared, just like for the **NSG**, but instead of the defection one, it is the cooperation monomorphic equilibrium that is gone. Furthermore, alike the **NSG**, the fix point associated with a stronger stationary distribution is the one that remains present in the dynamics. Finally, having the maximum possible risk, the dynamics seems to be the opposite of the previous study-case (for $r = 0$), however, no fix-points have vanished. Instead, the unstable equilibrium appears to move towards the defection monomorphic state, at very low levels of $i_C^{[C]}$, while both stable equilibria stay as expected, similarly as for $r = 0.5$.

Attending to the stationary distribution that, in this case, is significantly present for both the stable equilibria, whereas for null risk it is only strongly present for the defection monomorphic fix point, we can be led to think that, when trying to predict the effects of homophily, the stationary distribution in $h = 0$ may work as an anchor for the stable equilibria, as the fix points for which $\bar{s}$ is meaningful will remain present on the population dynamics as we increase the homophily, whereas the other fix points vanish. This insight may taken from both Figures 5.1-**(a)** and 5.2-**(a)**. Although in the **CRD** with $r = 0.5$ the same does not occur, we notice that, for this specific game, the unstable fix point is initially exactly at the middle, while in the other cases it is lightly deviated from the center of the configurations. However, these latter insights lack a formal foundation, being entirely empirical speculations. Furthermore, they are based only on the present studies, and hence, they are hardly generalizable. Nevertheless, it would be interesting to investigate more about these effects and if the stationary is really helpful in predicting the effects of homophily in the population dynamics.

Regarding the group achievement, independently on the value of the risk, we notice there are a tendency of an overall increase of η_G with increasing homophily. One may notice, however, in sub-figure **(b)**, the group achievement for a 90% homophilic population is (slightly) lower than for the not homophilic case, even though it generally increases from $h = 0$ to $h = 1$, that is, $\eta_G(h = 0) < \eta_G(h = 0)$, which suggest the first insight was incorrect. In this sense, and like previously mentioned for both **NSG** and **NSH**, one may wonder about the evolution of the relation $\eta_G(h)$. To conclude about any correlation, for each the games previously presented, we vary the homophily in small steps and compute the group achievement for those configurations. The result is presented below, in Figure 5.3.

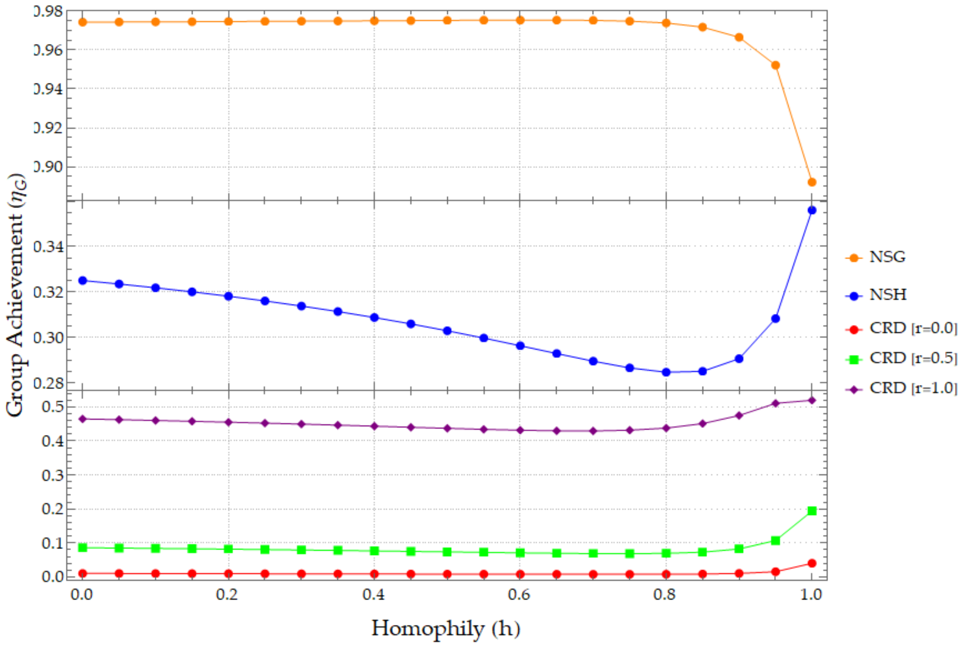

Figure 5.3: Group achievement for different N-person games, under conformity and social learning, in all the heterogeneous populations previously studied. The evolution of $\eta_G(h)$ is not regular and even for the same game it may change a lot. This may be indicative of a dependency on game's configurations.

For the **NSG**, the values of η_G appear to be constant with increasing h, although, attending to Figure 5.1-**(a)**, we know it actually lightly increases, but only until a certain point, from which it drops drastically. For the **NSH**, the opposite occurs, now much more clearly: η_G decreases with h until a critical homophily, from with it increases significantly. For the **CRD**, and contrary to the earlier insights, the group achievement shows a learning rule similar to the one taken for the **NSH**, that is, initially it decreases followed by an (in this case, not so) abrupt increase. From an overall point of view, whereas for the **NSG** the homophily seems to prejudice the probability of success, for both the **NSH** and **CRD** it seems to enhance that probability, being beneficial in terms of cooperation maximization. Attending to all these insights, we are led to suggest that the group achievement goes, not only as a function of the homophily, but also as a function of the game's configuration, that is, $\eta_G \equiv \eta_G(h, v)$ with v the set of variables that identify each game. This result would be expected if one take into consideration the previous chapter conclusions, where we proved the dependency $\eta_G \equiv \eta_G(v)$. As that, in order to maximize the group achievement, we suggest that different studies on the relation $\eta_G(v)$ or $\eta_G(h, v)$, respectively for homogeneous and heterogeneous populations, shall be performed. The resulting information shall then be crossed in order to obtain the desired maximum possible η_G.

The conformity's dynamics, alike we saw for homogeneous populations, is very specific and easily identifiable, generally not depending on the game. In its pure for, it is characterized by the coordination dynamic, with two stable equilibria on both the monomorphic states and one unstable internal fix point. Moving to heterogeneous populations, homophily shows itself as able to change the overall expected conformity dynamic, as it may either promote a C-dominance (in the case of **NSG**) and a D-dominance (for the **CRD**) dynamic, which would not happen in homogeneous populations. In this sense, conformity in heterogeneous populations brings up a whole new set of possible dynamics from which we may infer very interesting knowledge.

5.3 Counterfactual Thinking and Social Learning

Along this thesis, counterfactual thinking has shown to be a very interesting and complex learning rule, where, depending on the intensity $\beta^{[CT]}$, it may either foster coordination or co-existence, hence becoming a very flexible learning rule. In homogeneous populations we saw that, contrary to conformity, counterfactual reasoning in its pure form does depend on the played game, as it directly depend on agents' fitnesses on its updating process. This way, we expect to find a very rich and complex dynamics that may contrary any previous intuition.

Like before, we start by building a population sub-divided onto two sub-populations, one of social learners and the other constituted by counterfactual thinkers, thus having $\mathcal{L} = \{SL, CT\}$. Following the same reasoning as for conformity, we consider our population has a size of $Z = Z^{[SL]} + Z^{[CT]}$ individuals, from where $Z^{[SL]}$ are social learners and $Z^{[CT]}$ follow **CT**, that will play a given N-person game. Individuals resorting to either **SL** or **CT** are given an initial endowment $b^{[SL]}$ and $b^{[CT]}$, respectively, and, being cooperators, they are compelled to contribute, proportionally to their respective endowments, with $c^{[SL]} = c \cdot b^{[SL]}$ and $c^{[CT]} = c \cdot b^{[CT]}$. Having counterfactual thinking based on fitness, just as social learning, the payoffs relative to **SL** for each the N-person games, from equations 5.1-5.6, remain unchanged, now only substituting $[C]$ by $[CT]$ in the learning rules. The payoffs relative to **CT** are trivially obtained by replacing the **SL** characteristic variables, that is, both $b^{[SL]}$ and $c^{[SL]}$ by, respectively, $b^{[CT]}$ and $b^{[CT]}$ in equations 5.1-5.6.

From these payoffs, we may compute the fitness $f_S^{[L]}$ for any $S \in \mathcal{S}$ and $L \in \mathcal{L}$. Following the same approach as before, again taking the multivariate hypergeometric sampling without replacement, we obtain the fitness for **SL** similarly to equations 5.8 and 5.9, but substituting $[C]$ by $[CT]$. For **CT** the fitness may be obtained in the same way as before but swapping $[SL]$ with $[CT]$, however, taking into consideration the **CT** formulation, we have that:

$$f_C^{[CT]}(i_C^{[SL]}, i_C^{[CT]}) = \begin{cases} f_C^{[SL]}(i_C^{[SL]}, i_C^{[CT]}) & C \to D \\ f_C^{[SL]}(i_C^{[SL]}, i_C^{[CT]} + 1) & D \to C \end{cases} \tag{5.14}$$

$$f_D^{[CT]}(i_C^{[SL]}, i_C^{[CT]}) = \begin{cases} f_D^{[SL]}(i_C^{[SL]}, i_C^{[CT]} - 1) & C \to D \\ f_D^{[SL]}(i_C^{[SL]}, i_C^{[CT]}) & D \to C \end{cases} \tag{5.15}$$

Having this, and again considering an asynchronous updating process in the evolutionary dynamics, we may compute the required transition probabilities, for both learning rules, as follows:

$$T^{[SL]}_{C\to D\backslash D\to C}(\boldsymbol{i}) \equiv T^{[SL]}_{\mp}(\boldsymbol{i}) = \frac{i^{[SL]}_{C\backslash D}}{Z}\left\{\frac{i^{[SL]}_{D\backslash C} + (1-h)i^{[CT]}_{D\backslash C}}{Z^{[SL]} - 1 + (1-h)Z^{[CT]}}\left(1 + e^{\beta^{[SL]}(f^{[SL]}_{C\backslash D}(\boldsymbol{i}) - f^{[SL]}_{D\backslash C}(\boldsymbol{i}))^{-1}}\right)\right\} \tag{5.16}$$

$$T^{[CT]}_{C\to D\backslash D\to C}(\boldsymbol{i}) \equiv T^{[CT]}_{\mp}(\boldsymbol{i}) = \frac{i^{[CT]}_{C\backslash D}}{Z}\left\{\left(1 + e^{\beta^{[CT]}(f^{[CT]}_{C\backslash D}(\boldsymbol{i}) - f^{[CT]}_{D\backslash C}(\boldsymbol{i}))^{-1}}\right)\right\} \tag{5.17}$$

where for the **CT** we do not consider the second fraction of $C\backslash D$, attending to the fact counterfactual thinking follows a static update in its revision process, that is, it does not depend on one another to proceed to its revision. In the case of **SL**, in its formal definition, a social learner will only evaluate the fitness of a certain strategy, not considering the learning rule of the other interacting individual. In this reason, the second term (in equation 2.10) would be the same as the first one, and hence they may be condensed into a single term, just like previously formalized in the **SL-C** framework, once that both learning rules are based in different functions - fitness for social learning and fraction of S-individuals ($S \in \{C, D\}$) for conformity.

From this transition probabilities, like before, we are able to compute the major tools to evaluate a game's dynamics, such as the stationary distribution and the 2-dimensional gradient of selection. The first one will be calculated exactly as previously performed for conformity, whereas ∇ may generally be defined for social learning and counterfactual reasoning as follows:

$$\nabla(\boldsymbol{i}) = \{G^{[SL]}(\boldsymbol{i}), G^{[CT]}(\boldsymbol{i})\} = \{T_{+}^{[SL]}(\boldsymbol{i}) - T_{-}^{[SL]}(\boldsymbol{i}), T_{+}^{[CT]}(\boldsymbol{i}) - T_{-}^{[CT]}(\boldsymbol{i})\} \tag{5.18}$$

Finally, to evaluate the game dynamics, we may compute he group achievement similarly to equation 5.13 but, again, substituting $[C]$ by $[CT]$ in the learning rules' index. Another quantity of interest, which allow us, is the expected fraction of cooperators, EFC, that goes as previously defined in equation 2.34. Having different sub-populations, one may compute the EFC specifically for each sub-population, or for the population as a whole. In this case, we will define EFC_{SL} and EFC_{CT}, respectively, as the expected fraction of cooperators for the sub-populations of **SL** and **CT**, and EFC will refer to the whole population. Formally, we will have the following:

$$EFC = \frac{i_C^{[SL]} + i_C^{[CT]}}{Z^{[SL]} + Z^{[CT]}} \cdot \bar{s} \qquad EFC_{SL} = \frac{i_C^{[SL]}}{Z^{[SL]}} \cdot \bar{s} \qquad EFC_{CT} = \frac{i_C^{[CT]}}{Z^{[CT]}} \cdot \bar{s} \tag{5.19}$$

Attending to previous studies, as in [13], when having homogeneous populations, one would expect that a small prevalence of individuals resorting to **CT** strongly favours cooperation. In this sense, and before proceeding with our investigation on the effects of homophily in the evolutionary dynamics, it would be interesting to evaluate the overall dynamics of populations when varying the different sub-populations sizes. Specifically, we will take a population with a fixed size $Z = 100$, with $\mu = \frac{1}{Z}$, and we will vary the proportion $Z^{[SL]}/Z^{[CT]}$, where $Z = Z^{[SL]} + Z^{[CT]}$. For each population, we compute all the available evaluating tools, η_G, EFC, EFC_{SL} and EFC_{CT}, looking to find any correlation that would provide interesting conclusions. For two **CRD** with $(N, M, b^{[SL]}, b^{[CT]}, c, r) = (10, 5, 1, 1, 0.01, r)$, where $r = \{0.2, 1.0\}$, with an homophily of $h = 0.9$, and having both learning rules equally balanced with $\beta^{[SL]} = \beta^{[CT]} = 5$, we may obtain the results on the Figure 5.4, shown below.

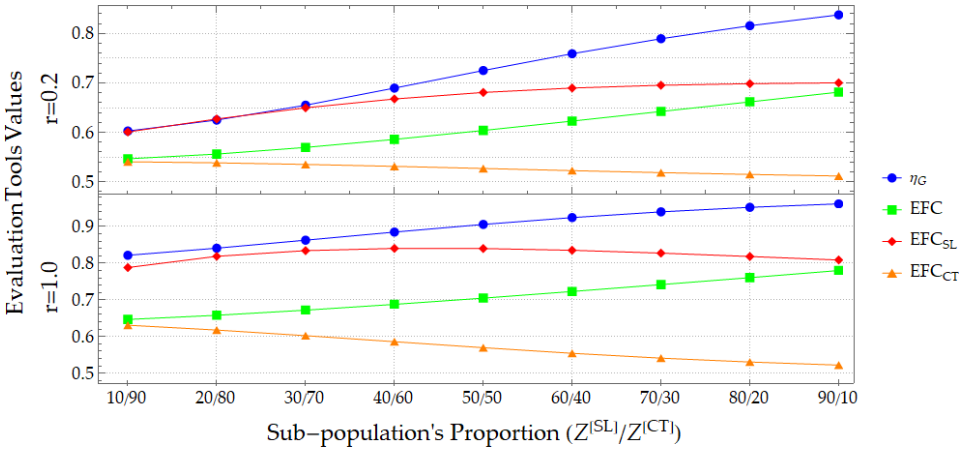

Figure 5.4: η_G, EFC, EFC_{SL} and EFC_{CT} versus the proportion between the sizes of the different sub-populations. For all the cases we have $Z = 100$, $\mu = \frac{1}{Z}$, $h = 0.9$ and $\beta^{[SL]} = \beta^{[CT]} = 5$, for the **CRD** with $(N, M, b^{[SL]}, b^{[CT]}, c, r) = (10, 5, 1, 1, 0.01, r)$, where $r = \{0.2, 1.0\}$.

In the case where $r = 0.2$, we notice that all quantities, with exception to the EFC_{CT}, progressively increase as we increase the proportion of $Z^{[SL]}/Z^{[CT]}$, reaching their maximum values for the highest proportion of $Z^{[SL]}/Z^{[CT]} = 90/10$. It will also be interesting to notice that it is exactly in this point where we find the minimum value for the EFC_{CT}, which reveals a very exciting result: counterfactual reasoning, while responsible for fostering the population dynamics towards much more cooperative standards, does not concerned about improving the cooperation standards of the ones of its kind. Moreover, it is to be noted that this results go along with the previously obtained insights for homogeneous populations, from Figure 4.7, where we saw that increasing the prevalence of **CT** agents is firstly responsible for strongly nudge the entire population towards highly cooperation standards, but only until a certain critical point, where η_G reaches its maximum value, that is followed by a progressive decrease of the group achievement. When setting apart the two learning rules onto two sub-populations, one may inspect specifically which type of individuals are being enhanced, in terms of cooperation, which in this case turns out to be the social learners, while cooperation is not fostered among **CT**'s.

Regarding the second case, with maximum risk, in contrary to the previous case, we may observe the EFC_{SL}, after reaching its maximum value, starts decreasing progressively as we increase the proportion of $Z^{[SL]}/Z^{[CT]}$. However, and attending that EFC_{CT} also decreases with increasing sub-populations' proportion, it is not intuitive that the overall EFC follows the opposite trend, being maximum for the minimum fraction of **CT** individuals. Although this seems contradictory, one must take into consideration the proportion of $Z^{[SL]}/Z^{[CT]}$ as a measure of the contribution of both EFC_{SL} and EFC_{CT} on the overall EFC. In fact, we may notice that, having $Z^{[SL]}/Z^{[CT]} = 10/90$, the EFC is much closer to EFC_{CT} than to EFC_{SL}, while in the opposite case $Z^{[SL]}/Z^{[CT]} = 90/10$, the EFC is much closer to EFC_{SL}. Nevertheless, and regardless on the curves for EFC_{SL} and EFC_{CT}, for the both graphics above, specifically for the **CRD**, we may infer that a lower fraction of **CT**, relatively to the fraction of **SL**, promotes higher group achievements and EFC, regardless of the risk.

As the above results were performed specifically for a fixed homophily of $h = 0.9$, one may now wonder if, besides the sub-populations' sizes, homophily also shows an impact on the overall cooperative quality of a certain population. In this sense, and alike in the previous conformity study, we may proceed to the study of the relation between the group achievement and the homophily, that is, the evolution of $\eta_G(h)$, for different populations. More specifically, and as a reference, we will focus on same-sized sub-populations. Taking a population size of $Z = 100$, with a mutation rate of $\mu = \frac{1}{Z}$, and with both learning rules equally balanced with $\beta^{[SL]} = \beta^{[CT]} = 5$, we investigate the evolution of η_G with the homophily for both the **NSG** with $(N, M, b^{[SL]}, b^{[CT]}, c) = (10, 7, 1, 1, 0.75)$, a **NSH** with $(N, M, b^{[SL]}, b^{[CT]}, c, F) = (10, 5, 1, 1, 0.5, 9.5)$ and for **CRD** with $(N, M, b^{[SL]}, b^{[CT]}, c, r) = (10, 5, 1, 1, 0.01, r)$, where we have $r = \{0, 0.5, 1\}$. The obtained results are shown below, on Figure 5.5.

From the figure above, we may be lead to suggest that an increase of the homophily is responsible for increasing the group achievement, regardless on the social game. Although this is true for most games, in some configurations the opposite occurs, as homophily progressively lowers the probability to achieve cooperative success. This is the case of the **CRD** that, having the same exact configurations, but changing the risk, may either lead to a cooperation enhancement, for higher risks, or to lowering of the overall cooperation standards. Again, as we saw for conformity, this strongly suggests that, regarding cooperation optimization, the overall quality of the evolutionary dynamics' outcome for a certain population is dependable on the social game's configuration, that is, not only we have $\eta_G \equiv \eta_G(h)$ but we also have $\eta_G(h, v)$, where v stands for the set of variables that define a certain social game. Once again, one may notice this conclusions are no different from the ones taken for homogeneous, just as previously discussed in the previous section 5.2.

Finally, one small note on the previous results: contrary to conformity, we may observe that either the minimum or maximum values of the group achievement, regardless on the game's configuration, occur the homophily extremes, that is, for either full homophilic sub-populations or for perfectly well-mixed sub-populations. In accordance with the upper conclusions, that is, attending higher η_G are more often reached for maximum homophily, one may be

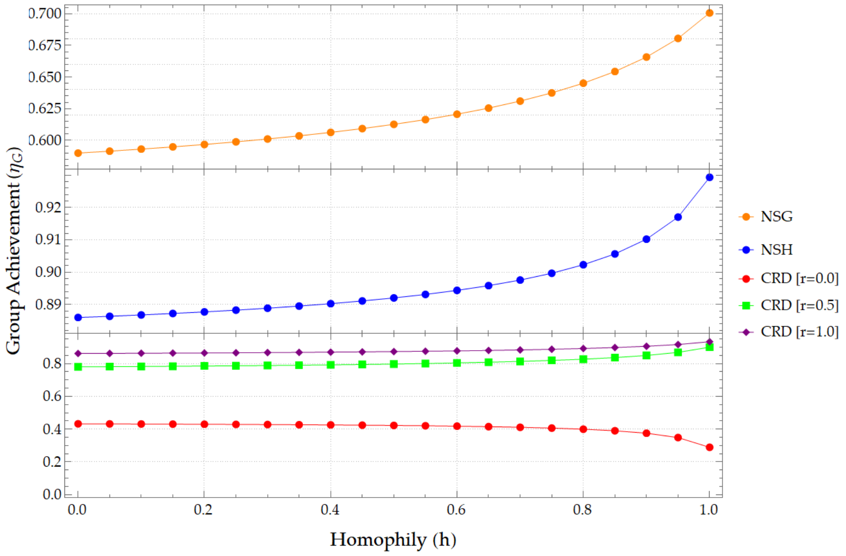

Figure 5.5: Group achievement for different N-person games, under counterfactual thinking and social learning, in the heterogeneous populations' framework. In most cases, the η_G grows up with increasing homophily, but for other cases the opposite occurs. In the **CRD**, for instance, we see that different risks may lead to different outcomes. This may be indicative of a dependency on game's configurations.

lead to suggest that, generally, heterogeneity promotes higher cooperative standards, or, in other words, well-mixed populations lead to worst performance in terms of cooperation maximization. Although these insights sound very exciting, they are devoid of a considerable amount of information, being based only on 5 results. In this sense, we suggest a more wide investigation on this subject would be required to verify these primordial insights, but nonetheless, it would be interesting to conclude pure heterogeneity fosters cooperation, at least generally.

Similarly to previous studies on the effects of homophily in the population dynamics, we will evaluate the system's dynamics, in both terms of the gradient of selection, $\nabla(\boldsymbol{i})$, and of the stationary distribution, $\bar{s}(\boldsymbol{i})$, for every single possible configuration, which, in this case, corresponds to varying both $i_C^{[SL]} \in [0; Z^{[SL]}]$ and $i_C^{[CT]} \in [0; Z^{[CT]}]$. Specifically, we take the same populations' configurations as for the previous study on Figure 5.5, that is, $Z^{[SL]} = Z^{[CT]} = 50$, $\mu = \frac{1}{Z}$, and $\beta^{[SL]} = \beta^{[CT]} = 5$, and we investigate the homophily effects on the population dynamics for all the **NSG**, the **NSH** and the **CRD**, above described. In this study, contrary to homogeneous populations, we will not focus on balancing the different learning rules through their respective intensities, as we intend to see how they react in their true form. The results are shown below in Figure 5.6.

Firstly we notice that, contrary to conformity dynamics, counterfactual thinking does not replicate the typical homogeneous dynamics for when the homophily is null. In fact, we notice that, regardless on the social game, there are not any signs of symmetry on the dynamics for $h = 0$. The results in the figure even suggest that increasing the homophily does not significantly affects the overall population dynamics. Attending to the definitions for the transition probabilities for **CT**, in equations 5.16 and 5.17, this latter insight could be justified if one takes into consideration that, not only counterfactual thinking has a much stronger dynamic, when compared to social learning, but also it is independent on the homophily. In this reasoning, the only changes on $\nabla(\boldsymbol{i})$ with homophily will come from the differences on the x-component, relative to $G^{[SL]}$.

Even though the overall dynamics in terms of the gradient of selection does not significantly change, the system internal equilibria does change with the homophily, and, with that, the stationary distribution. Starting with the **NSG**, when $h = 0$, one can identify three fix points, two stable, one more hidden on the left and a stronger one on the right, and one unstable, that is close to the weaker stable equilibrium. Recall in this analysis we weight the strength

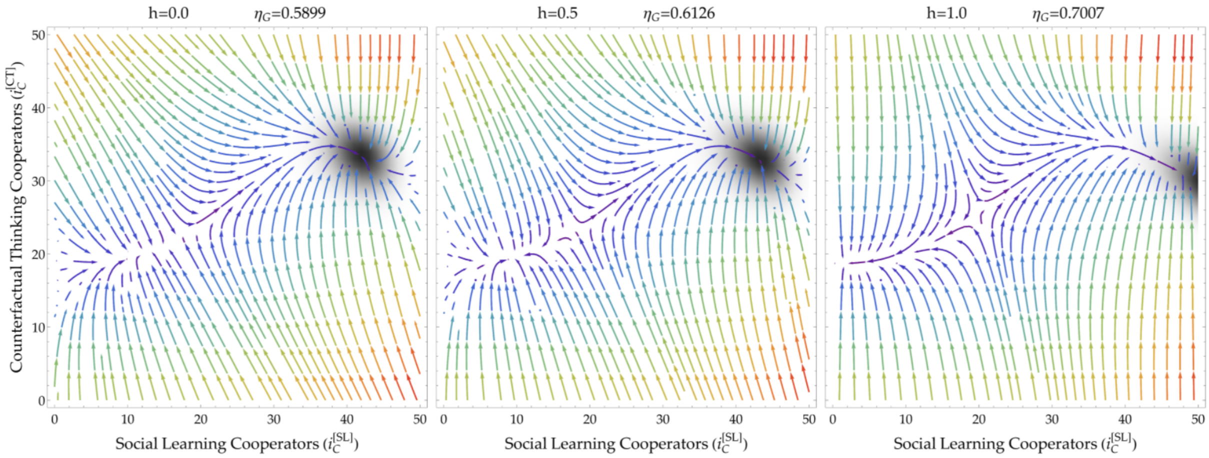

(a) **NSG**, with $(N, M, b^{[SL]}, b^{[CT]}, c) = (10, 7, 1, 1, 0.75)$.

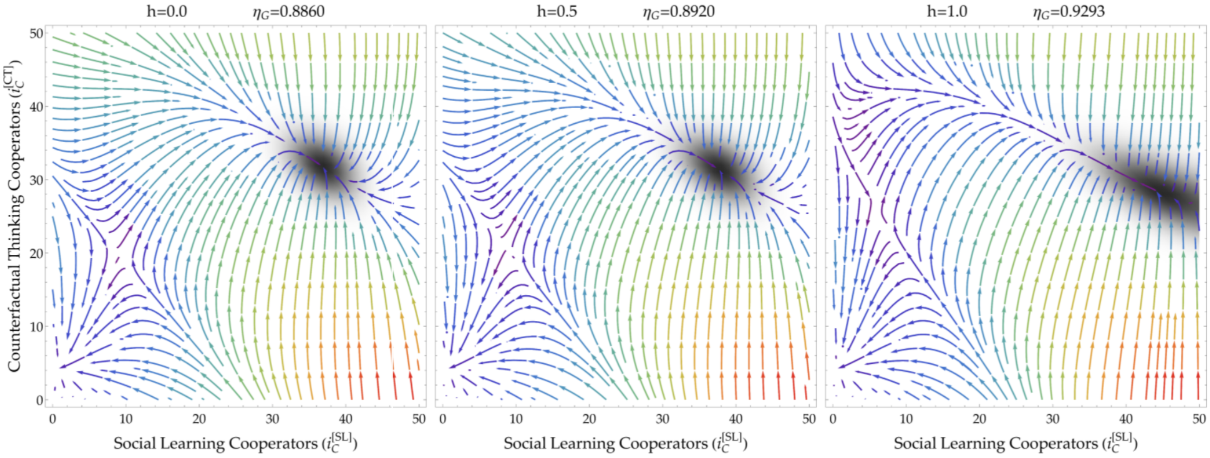

(b) **NSH**, with $(N, M, b^{[SL]}, b^{[CT]}, c, F) = (10, 5, 1, 1, 0.5, 9.5)$.

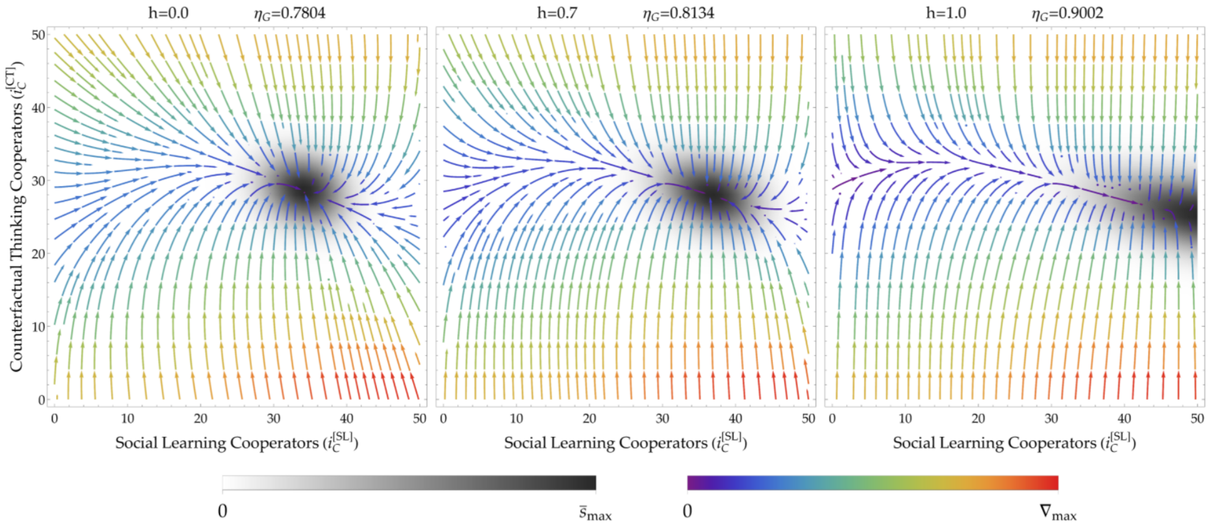

(c) **CRD**, with $(N, M, b^{[SL]}, b^{[CT]}, c, r) = (10, 5, 1, 1, 0.01, 0.5)$.

Figure 5.6: Gradient of selection for the **NSG** and the **NSH** under conformity, in heterogeneous populations with $Z^{[SL]} = Z^{[CT]} = 50$, $\mu = \frac{1}{Z}$, $\beta^{[SL]} = \beta^{[CT]} = 5.0$. We investigate the effects of increasing homophily in the population dynamics, that is, on ∇ and $\bar{s}$ for each possible configuration.

of the fix points in terms of the stationary distribution, being that it is on the stronger fix point that we may find $\bar{s}_{max}$. As we increase the homophily, for instance, at $h = 0.5$, both the unstable and the stable and weak fix points start to get more visible, while the stronger equilibria slightly moves to the right, corresponding to a better performance for the **SL** sub-population, in terms of cooperation. When finally reaching the maximum homophily, besides the unstable fix point being now much more clear, we also notice the weaker stable equilibria has moved entirely to the left, whereas the stronger fix point is now very close to $i_C^{[SL]} \approx Z^{[SL]}$. This means that, in this specific case, even though we do not have any improve on the cooperative dynamics of **CT**, the presence of **CT**'s, in a full homophilic scenario, nudges specifically the entire sub-population of **SL** towards extremely high cooperative standards, a result that matches the previous insights from Figure 5.4.

For the other two social games, and focusing on the stationary distribution over the stronger stable fix point, very similar results may be achieved: increasing the homophily progressively pushes this stronger stable equilibrium towards high **SL** cooperative standards, that is, $i_C^{[SL]} \approx Z^{[SL]}$, even though cooperation in the **CT** sub-population is not only not favoured, but even harmed. As this result is transverse to all the presented social games, we are willing to suggest a possible generalization of this conclusion. It is interesting to notice that, even when expecting a decrease on η_G for the **CRD** for a null risk, we may notice a considerable increase of the group achievement for $r = 0.1$. This insight may indicates that the exception cases on the previous conclusions, regarding homophily being responsible for an increase of the η_G, occur only for very small risks, enhancing the generality of those conclusions.

5.4 Final Notes

When compared to the homogeneous case, the evolutionary dynamics of heterogeneously organized populations brings a whole new range of possible outcomes, depending on the degree of heterogeneity, that could be measured according to the homophily. In the conformity on social learning framework, the increasing homophily is responsible for twisting the typical coordination dynamics, characteristic of conformity in well-mixed populations, onto a wide variety of completely different scenarios, such as C-dominance or D-dominance, depending on the game's configuration. Consequently, the group achievement reveals itself as dependent, not only on the game's variables, as we saw in homogeneous populations, but also on the homophily. It should be noted that, in some cases, the maximum or minimum group achievements occur in non extreme homophilies, that is, not in either $h = 0$ or $h = 1$, which suggest a non-linear relation for $\eta_G(h)$.

Regarding the framework with counterfactual thinkers on social learning, a completely different dynamic may be achieved. For one same level of heterogeneity, we have concluded that one may obtain the highest cooperation standards, evaluated either by the η_G and the **EFC**, for the smallest prevalence of **CT**-driven agents. More specifically, we suggested that **CT** individuals, while responsible for fostering the population dynamics towards much more cooperative standards, does not concerned about improving the cooperation standards of the ones of its kind, a result achievable when analyzing the evolution of both EFC_{SL} and EFC_{CT}. Furthermore, although the results on the relation $\eta_G(h)$ go in agreement with the conformity results, contrary to this framework, higher heterogeneous levels generally promote higher cooperative outcomes, or, in other words, well-mixed populations lead to worst performance in terms of cooperation maximization. Nevertheless, take into consideration this result lacks of a significant amount of information, most likely not having enough evidence to support, thus should be taken solely as a primordial, and possibly premature, insight. Finally, having the **CT** formulation independent on the homophily, the level of heterogeneity does not highly influence the overall social dynamics, but however, regardless on the social game, it does push the entire population towards specifically highly **SL** cooperative standards.

Chapter 6

Conclusions

Earlier in Chapter 1 we have defined our main objectives for this thesis. In a general way, along this thesis, we saw that very different configurations may lead to very distinct dynamics, from which we generally concluded that cooperation is highly dependent on most (or even, all) of the variables that characterize a certain population. We stand now at a position to evaluate the our results relative to each one of these goals, individually.

6.1 Achievements

Synchronism and Asynchronism

Starting off with Chapter 3, we saw that the effects of increasing the synchronism level, along the spectrum of synchrony, are in general nearly negligible, not only for a pure social learning population, but also for homogeneously well-mixed populations of social learners and conformists, and regardless on the social game. Thereby, also the cooperation evaluation tools, such as the group achievement and the expected fraction of cooperators, suffered negligible modifications with increasing synchronism.

However, we found out those changes are not generic as there's a dependency on the set of game's configuration, that is, while for some games these slight changes may act in order to increase η_G, in other cases the opposite occurs. Formally speaking, we have concluded that $\eta_G \equiv \eta_G(v, n_r)$, where we define v as the set of the game's configuration variables. Regarding convergence, although synchronism generally accelerates the system's convergence for either one of the absorption states, approximately linearly with n_r, also the average fixation time increases, suggesting the total number of revisions increase with increasing synchronism level.

In opposition to the previous insights, counterfactual thinking shows to be much sensitive to synchronous updates, generally suggesting a progressive increase of the group achievement as we increase the number of revisions in the updating process, which, contrary to conformity or social learning, are no longer so small to be negligible.

Population Dynamics in Homogeneous Populations

Moving on to homogeneous populations, and now fixing the updating process on the birth-death process, in Chapter 4 we saw that depending on the learning rule, conformity or counterfactual thinking, many different conclusions may be taken. In general, we saw that cooperative action is highly dependent on, not only the game's configuration variables, but also on the populations composition, in terms of learning rules. Formally, we found that $\eta_G \equiv \eta_G(v, \boldsymbol{\delta})$, where here we define $\boldsymbol{\delta} = \{\delta^{[SL]}, \delta^{[C]}, \delta^{[CT]}\}$.

Firstly, conformity shows to bring a very stable dynamic, being, on its pure form, completely independent on the social game's configuration, either in the 2-person or the N-person framework. In this sense, even though this dynamic strongly depends on the intensity of conformity, the formal definition of conformity states that it should always promote coordination. Regarding cooperation maximization, conformity may have either a positive or a negative impact on the overall group achievement, depending on **SL**'s characteristic η_G position relatively to the unstable equilibria. Furthermore, one may also conclude that, contrary to **CT**, it is required a considerable prevalence of conformity-driven agents to substantially change the social game dynamics.

In the counterfactual reasoning case, however, the dynamic does depend on the game's configuration. Firstly, we saw that **CT** is very versatile, as while for relatively lower values of the $\beta^{[CT]}$ individuals resorting to **CT** promote a co-existence dynamic, for higher intensities a coordination dynamic is favoured. Moreover, we saw that **CT** is highly dependent on the game's configuration, although generally acts in favor of maximizing cooperation. To complement the insights from [13], we showed that, for some cases, regarding collective action, a small prevalence of **CT**-driven individuals is sufficient to foster highly cooperative standards, but only until a certain critical point, from which adding more **CT** agents becomes a disadvantage for cooperative action.

Population Dynamics in Heterogeneous Populations

Finally, on the heterogeneous populations framework, in Chapter 5 we concluded that the cooperative action is highly dependent, not only on the game's configuration variables, but also on the level of heterogeneity, measured according to the homophily. For the conformity on social learning framework, the increasing homophily is responsible for progressively twisting the typical coordination dynamics, characteristic of conformity in well-mixed populations, onto a wide variety of completely different scenarios, depending on the social game. Results also suggest that there is not a direct relation between the group achievement and the homophily, hence meaning the probability to achieve success, not only depends on the game, but also on the level of heterogeneity.

For the counterfactual thinking, on the other hand, very different results were achieved. Firstly, for one same level of heterogeneity, the highest cooperation standards may be obtained for the smallest prevalence of **CT**-driven individuals, meaning the best cooperative performance is achieved only for a small fraction of **CT**'s. Results also suggest that **CT** individuals, while responsible for fostering the population dynamics towards much more cooperative standards, does not concerned about improving the co-operation standards of the ones of its kind. Moreover, in contrary to conformity's framework, higher heterogeneous levels generally promote higher cooperative outcomes, or, in the other hand, well-mixed populations lead to worst performance in terms of cooperation maximization.

6.2 Future Work

Generally, our model looks very complete and easily generalizable, although it lacks on simplicity. In fact, we saw on Chapter 3 the formulation for the general transition matrix is quite complex, as computing $\mathcal{T}^n$ quickly becomes computationally extremely extensive, and hence we find ourselves in a very limiting situation. In this sense, it would be extremely helpful to find a new formulation that accomplishes the results from equation 2.17 in a much more simple and elegant way. If such would be achieved, much more detailed studies on the effects of synchronism could be performed, with special interest on how these synchronism processes may enhance the performance of **CT**-driven individuals, regarding cooperative action. More over, having this new formulation, we would have more evidence that would strongly support our previously mentioned insights.

Regarding population dynamic, more profound studies may be performed, similarly to the ones performed along this thesis, that look to find the group of conditions that allow us to maximize cooperative action. The more information we have, the more aware of all the possible outcomes we will be. Besides that, as mentioned, it would be very relevant to find new ways to study the system's dynamics, for instance, by looking for any relations between certain combination of variables that would allow us to reduce the problem dimensionality a much simpler and direct evaluation of the system's dynamics. Moreover, it could be interesting to construct a new formulation for conformity when considering group action, just like in the case of **SL**. Along that, we have also discussed an urging need for a new success measurement tool that takes into account all new learning rules, independently on how they are internally organized.

In our heterogeneous populations' framework, we have introduced a whole new dynamics so far never seen before. From this, we have produced some results that we find out to be interesting, however this study is far from being complete. As one may understand, these new dynamics are very complex are allow a really wide set of possible outcomes. In this sense, for further work, we suggest the need of more studies under this framework, and even adding other different learning rules, in order to increase our knowledge on this topic of cooperative action on heterogeneous populations. Furthermore, and as previously mentioned, it would also be interesting to study what happen when having non bi-directive homophilies, that is, having $h_{L_A \to L_B} \neq h_{L_B \to L_A}$, for any two sub-populations of individuals respectively resorting to L_A and L_B, with $L_A, L_B \in \mathcal{L}$.

Still regarding this population's dynamics topic, it would also be interesting to focus our study not much on the evolution of strategies by itself, but on the evolution of all the different learning rules. Instead of taking them as fixed parameters, one could let it go freely, probably bring into the system a completely new dynamic. Moreover, differnet studies on boundaries of the used mathematical framework should be performed. For instance, the inverse of temperature (β), as seen, show that different characteristic dynamics are possible depending on its values, so it could be interesting to evalutate what actually happens in the trannsition point between the different dynamic scenarios.

Finally, it would be remarkable to take some of the insights previously taken, regarding counterfactual reasoning, and wonder about higher levels of counterfactual thinking, that is, one may wonder what happens as we increase in level depth in Theory of Mind for (at least some) individuals in a population. We hope to find very interesting results that could give us many different and interesting insights about this new dynamic.

Regardless on the kind of study, one shall always take into its mind that we aim to explain the emergence of cooperation in human communities.

Bibliography

[1] R. Axelrod. *The Evolution Of Cooperation*. Basic Books, Inc., Publishers, 1984. ISBN 9780465021215.

[2] E. Pennisi. How did cooperative behavior evolve? *Science*, 309(5731):93–93, 2005. doi: 10.1126/science.309.5731.93.

[3] D. D. Kennedy and C. Norman. What don't we know? *Science*, 309(5731):75–75, 2005. doi: 10.1126/science.309.5731.75.

[4] M. Perc, J. Jordan, D. Rand, Z. Wang, S. Boccaletti, and A. Szolnoki. Statistical physics of human cooperation. *Physics Reports*, 687:1–51, 2017. doi: https://doi.org/10.1016/j.physrep.2017.05.004.

[5] M. Nowak. Five rules for the evolution of cooperation. *Science (New York, N.Y.)*, 314:1560–3, 2007. doi: 10.1126/science.1133755.

[6] M. A. Nowak. *Evolutionary Dynamics: Exploring the Equations of Life*. Harvard University Press, 2006. ISBN 9780674023383.

[7] J. Maynard-Smith and G. R. Price. The logic of animal conflict. *Nature*, 246 (5427):15–18, 1973.

[8] A. Traulsen, M. Nowak, and J. Pacheco. Stochastic dynamics of invasion and fixation. *Physical review. E, Statistical, nonlinear, and soft matter physics*, 74:011909, 2006. doi: 10.1103/PhysRevE.74.011909.

[9] C. P. Roca, J. A. Cuesta, and A. Sánchez. Evolutionary game theory: Temporal and spatial effects beyond replicator dynamics. *Physics of Life Reviews*, 6(4):208–249, 2009. ISSN 1571-0645.

[10] M. Nowak, A. Sasaki, C. Taylor, and D. Fudenberg. Emergence of cooperation and evolutionary stability in finite populations. *Nature*, 428:646–50, 05 2004.

[11] A. Szolnoki and M. Perc. Conformity enhances network reciprocity in evolutionary social dilemmas. *Journal of The Royal Society Interface*, 12(103):20141299, 2015. doi: 10.1098/rsif.2014.1299.

[12] A. Szolnoki and M. Perc. Leaders should not be conformists in evolutionary social dilemmas. *Scientific Reports*, 6:23633, 03 2016. doi: 10.1038/srep23633.

[13] L. M. Pereira and F. C. Santos. Counterfactual thinking in cooperation dynamics. *Studies in Applied Philosophy, Epistemology and Rational Ethics*, page 69–82, 2019.

[14] R. B. Myerson. *Game Theory: Analysis of Conflict*. Harvard University Press, 1991. ISBN 9780674341166.

[15] J. von Neumann. Zur theorie der gesellschaftsspiele. *Mathematische Annalen*, 100:295–320, 1928.

[16] M. Mccubbins, M. Turner, and N. Weller. The theory of minds within the theory of games. *Proceedings of the 2012 International Conference on Artificial Intelligence, ICAI 2012*, 1, 2012.

[17] W. Yoshida, R. J. Dolan, and K. J. Friston. Game theory of mind. *PLOS Computational Biology*, 4(12):1–14, 2008. doi: 10.1371/journal.pcbi.1000254.

[18] J. Nash. Non-cooperative games. *Annals of Mathematics*, 54(2):286–295, 1951.

[19] M. D. de Almeida Santos. *Evolutionary dynamics of collective action in structured populations*. PhD thesis, Universidade de Lisboa, 2012.

[20] M. Perc and A. Szolnoki. Coevolutionary games—a mini review. *Biosystems*, 99(2):109–125, 2010. doi: https://doi.org/10.1016/j.biosystems.2009.10.003.

[21] K. Holzinger. Common goods, matrix games and institutional response. *European Journal of International Relations*, 9(2):173–212, 2003.

[22] D. G. Rand and M. A. Nowak. Human cooperation. *Trends in Cognitive Sciences*, 17(8):413–425, 2013. ISSN 1364-6613. doi: https://doi.org/10.1016/j.tics.2013.06.003.

[23] M. O. Souza, J. M. Pacheco, and F. C. Santos. Evolution of cooperation under n-person snowdrift games. *Journal of Theoretical Biology*, 260(4):581 – 588, 2009.

[24] T. Siegfried, editor. *A Beautiful Math: John Nash, Game Theory, and the Modern Quest for a Code of Nature*. The National Academies Press, Washington, DC, 2006.

[25] J. M. Pacheco, F. C. Santos, M. O. Souza, and B. Skyrms. Evolutionary dynamics of collective action in ¡i¿n¡/i¿-person stag hunt dilemmas. *Proceedings of the Royal Society B: Biological Sciences*, 276(1655): 315–321, 2009. doi: 10.1098/rspb.2008.1126.

[26] M. A. Javarone, A. Antonioni, and F. Caravelli. Conformity-driven agents support ordered phases in the spatial public goods game. *EPL (Europhysics Letters)*, 114(3):38001, 2016. doi: 10.1209/0295-5075/114/38001.

[27] C. S. Gokhale and A. Traulsen. Evolutionary games in the multiverse. *Proceedings of the National Academy of Sciences*, 107(12):5500–5504, 2010. doi: 10.1073/pnas.0912214107.

[28] S. V. Segbroeck, F. C. Santos, T. Lenaerts, and J. M. Pacheco. Selection pressure transforms the nature of social dilemmas in adaptive networks. *New Journal of Physics*, 13(1):013007, 2011. doi: 10.1088/1367-2630/13/1/013007.

[29] G. Hardin. The tragedy of the commons. *Science*, 162(3859):1243–1248, 1968. doi: 10.1126/science.162.3859.1243.

[30] D. T. Bishop and C. Cannings. Models of animal conflict. *Advances in Applied Probability*, 8, 1976. doi: 10.2307/1425917.

[31] M. O. Souza, J. M. Pacheco, and F. C. Santos. Evolution of cooperation under n-person snowdrift games. *Journal of Theoretical Biology*, 260(4):581–588, 2009. ISSN 0022-5193. doi: https://doi.org/10.1016/j.jtbi.2009.07.010.

[32] T. Pfeiffer and M. Nowak. All in the game. *Nature*, 441:583–584, 2006. doi: https://doi.org/10.1038/441583a.

[33] M. Milinski, R. D. Sommerfeld, H.-J. Krambeck, F. A. Reed, and J. Marotzke. The collective-risk social dilemma and the prevention of simulated dangerous climate change. *Proceedings of the National Academy of Sciences*, 105(7):2291–2294, 2008. ISSN 0027-8424. doi: 10.1073/pnas.0709546105.

[34] A. Góis, F. Santos, J. Pacheco, and F. Santos. Reward and punishment in climate change dilemmas. *Scientific Reports*, 9:16193, 11 2019. doi: 10.1038/s41598-019-52524-8.

[35] F. C. Santos, V. V. Vasconcelos, M. D. Santos, P. N. B. Neves, and J. M. Pacheco. Evolutionary dynamics of climate change under collective-risk dilemma. *Mathematical Models and Methods in Applied Sciences*, 22 (supp01):1140004, 2012. doi: 10.1142/S0218202511400045.

[36] V. Vasconcelos, F. Santos, J. Pacheco, and S. Levin. Climate policies under wealth inequality. *Proceedings of the National Academy of Sciences of the United States of America*, 111, 01 2014. doi: 10.1073/pnas.1323479111.

[37] F. Santos and J. Pacheco. Risk of collective failure provides an escape from the tragedy of the commons. *Proceedings of the National Academy of Sciences*, 108:10421 – 10425, 2011.

[38] M. Redei. *John von Neumann: Selected Letters*. American Mathematical Society, Providence, Rhode Island, 2005.

[39] H. W. Kuhn and A. W. Tucker. John von neumann's work in the theory of games and mathematical economics. *Bull. Amer. Math. Soc.*, 64:100–122, 1958.

[40] W. Chen, C. Gracia-Lázaro, and Z. L. et al. Evolutionary dynamics of n-person hawk-dove games. *Scientific Reports*, 7:4800, 2017.

[41] V. Vasconcelos, F. Santos, and J. Pacheco. A bottom-up institutional approach to cooperative governance of risky commons. *Nature Clim. Change*, 3:797–801, 09 2013. doi: 10.1038/nclimate1927.

[42] V. V. L. de Vasconcelos. *Emergence and Self-organization of Cooperation*. PhD thesis, Universidade do Minho, 2016.

[43] L. J. S. Allen. *An Introduction to Stochastic Processes with Applications to Biology*. Chapman and Hall/CRC, 2010. ISBN 1439818827.

[44] L. Hindersin and A. Traulsen. Counterintuitive properties of the fixation time in network-structured populations. *Journal of The Royal Society Interface*, 11(99):20140606, 2014. doi: 10.1098/rsif.2014.0606.

[45] A. Traulsen and C. Hauert. Stochastic evolutionary game dynamics, 2008.

[46] C. Grilo and L. Correia. Effects of asynchronism on evolutionary games. *Journal of theoretical biology*, 269: 109–22, 10 2010. doi: 10.1016/j.jtbi.2010.10.022.